EXPLORING NUCLEAR MATTER, RADIATION, ATOMS, THIN FILMS, AND SYMMETRY THROUGH PHYSICAL APPROACHES

Editor
HASAN BİRCAN

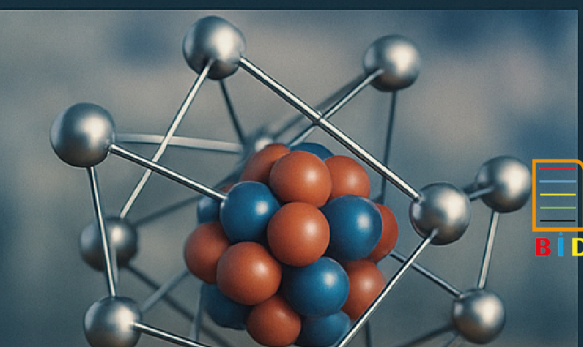

BİDGE

BİDGE Yayınları

Exploring Nuclear Matter, Radiation, Atoms, Thin Films, and Symmetry Through Physical Approaches

Editor: HASAN BİRCAN

ISBN: 978-625-6645-86-8

1st Edition
Page Layout By: Gözde YÜCEL
Publication Date: 2025-06-25
BİDGE Yayınları

Certificate No: 71374

www.bidgeyayinlari.com.tr - bidgeyayinlari@gmail.com
Krc Bilişim Ticaret ve Organizasyon Ltd. Şti.
Güzeltepe Mahallesi Abidin Daver Sokak Sefer Apartmanı No: 7/9 Çankaya / Ankara

PREFACE

*"**Physics is the soul of science.**"*
— Hasan Bircan[1]

The foundation of scientific progress lies in a deep curiosity—to understand nature and to transform that knowledge into technologies that make life easier and better. This book presents a multifaceted scientific journey that begins with nuclear matter and atomic structures, continues through crystalline systems, and culminates in the exploration of physical symmetry—including its manifestations in both nature and cultural patterns.

Created with the contributions of esteemed scientists from various universities, this work reflects an interdisciplinary perspective. It covers fundamental topics such as symmetric nuclear matter, Monte Carlo simulation, chemical bonding, mass and linear attenuation coefficients, properties of biomaterials, thin-film production techniques, crystallography, and symmetry.

One of the unique features of the book is its exploration of how the concept of physical symmetry resonates in cultural forms.

This work aims to show that physics exists not only in laboratories, but also in the structure of matter, the behavior of materials, and the patterns that shape our cultural identity. It seeks to highlight the meaningful journey of science— from nuclear matter to atom, from atoms to crystals, from symmetry to motifs.

We dedicate this book to all researchers, students, and curious minds who believe in the power of interdisciplinary science.

---

[1] Assoc. Prof. Dr. Kütahya Dumlupınar University Faculty of Arts And Sciences Physics Department Kütahya/Türkiye, Orcid: 0000-0003-2067-7855, hasan.bircan@dpu.edu.tr

İÇİNDEKİLER

CHAPTER 1

SYMMETRIC NUCLEAR MATTER: EXTENDED LIQID-DROP MODEL

Hasan BİRCAN[1]
Kaan MANİSA[2]
Mehmet ERDOĞAN[3]

1. NUCLEAR MATTER

Nuclear matter is an idealized system composed of interacting nucleons protons and neutrons in the absence of Coulomb forces. This system is defined to be translationally invariant and to possess a fixed neutron-to-proton ratio, typically corresponding to symmetric nuclear matter. The theoretical modeling of nuclear matter begins with the nucleon-nucleon (NN) interaction, often represented by a two-body potential. However, it

[1] Assoc. Prof. Dr. Kütahya Dumlupınar University Faculty of Arts And Sciences Physics Department Kütahya/Türkiye, Orcid: 0000-0003-2067-7855, hasan.bircan@dpu.edu.tr
[2] Prof. Dr. Kütahya Dumlupınar University Faculty of Arts And Sciences Physics Department Kütahya/Türkiye, Orcid: 0000-0002-4063-277X, kaan.manisa@dpu.edu.tr
[3] Prof. Dr. Selçuk University, Physics Department, Konya/Türkiye, Orcid: 0000-0003-1879-8500, merdogan@selcuk.edu.tr

is well established that no realistic two-body NN interaction alone can adequately reproduce the empirical bulk properties of nuclear matter, such as the binding energy per nucleon and the saturation density [1, 2].

As a result, it becomes essential to incorporate three-body and higher-order many-body forces to achieve a realistic description of nuclear matter. These many-body contributions play a crucial role in determining the saturation mechanism and other key characteristics of nuclear systems.

The study of nuclear matter not only provides insights into the properties of infinite nuclear systems but also serves as a valuable tool for examining the validity and limitations of different nuclear interaction models. Through systematic many-body calculations, one can investigate how various components of the nuclear force such as tensor, spin-orbit, and short-range correlations affect the macroscopic properties of matter. Moreover, nuclear matter studies can help determine whether a given potential model is fundamentally viable or inadequate for describing the nuclear force [1].

Ultimately, one of the central goals of nuclear matter theory is to derive the empirical properties of nuclear systems such as the binding energy, saturation density, incompressibility modulus, and symmetry energy from microscopic NN interactions. Achieving this would represent a significant step toward a unified and predictive theory of nuclear forces and structure [2].

2. THE NUCLEAR MATTER EQUATION OF STATE (EOS)

The dependence of the total energy per nucleon on the density of nuclear matter is known as the nuclear matter equation of state (EOS). As previously discussed, nuclear matter refers to a hypothetical system of nucleons distributed uniformly in space and interacting via the strong nuclear force. In this framework, the energy per particle is a function of the nuclear density, or equivalently, of the Fermi momentum kF. The minimum of the energy-density curve defines the saturation point of nuclear matter.

Empirically, the saturation density lies within the range of approximately 0,145 fm^{-3} 0,20 fm^{-3}, corresponding to a Fermi momentum k_F between 1,29 – 1,44 fm^{-1}, and an energy per particle ranging from about -15 to -17 MeV [3]. Any assumed two-body nucleon-nucleon interaction yields a specific EOS, that is, a curve representing the energy per particle as a function of density. Detailed calculations and information regarding the equation of state of nuclear matter, as well as its empirical properties such as saturation density, binding energy, symmetry energy, and incompressibility, can be found in references [2, 4-11].

A physically realistic two-body potential must predict an EOS whose saturation point agrees with the empirical data. Therefore, it is crucial to employ a reliable theoretical framework capable of accurately computing the binding energy of nuclear matter across a range of densities. Only when such calculations reproduce the empirical saturation properties with sufficient precision can the underlying interaction potential be considered acceptable [3].

3. EXTENDED LIQUID-DROP MODEL (ELDM)

The Extended Liquid-Drop Model (ELDM) represents a significant refinement of the classical Liquid-Drop Model (LDM), developed to achieve a more precise and comprehensive description of nuclear properties such as binding energies, shape deformations, and fission dynamics. While the traditional LDM conceptualizes the nucleus as a homogeneous, incompressible droplet of nuclear matter capturing only the bulk macroscopic features of the nucleus, the ELDM introduces additional correction terms that allow it to reflect more subtle and complex physical phenomena. These enhancements include contributions from surface curvature, higher-order deformation effects, and, in many formulations, phenomenological microscopic corrections such as shell and pairing effects. By extending the basic LDM framework, the ELDM enables a more realistic modeling of finite nuclei, especially in regions far from stability or for heavy and super heavy elements, where shell effects and deformation energies play a critical role in determining nuclear structure and decay behavior.

The extended liquid drop model, two parametrizations of the EOS was proposed [12, 13]. The first parametrization is commonly referred to as the linear Equation of State (EOS), as it predicts a linear increase in energy with density at high-density regimes (Fig.1):

Figure 2 shows that the obtained pressure of nuclear matter for the expanded liquid drop model.

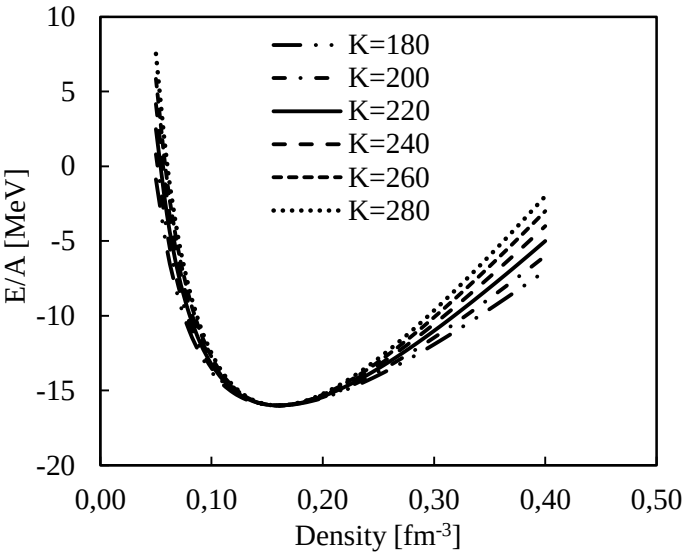

Figure 1. The extended liquid drop model the linear Nuclear Equation of State (EOS) at high-density regimes.

Formulations: [13]

$$\frac{E}{A}(\rho) = \begin{cases} \frac{K(\rho-\rho_0)^2}{18\rho\rho_0} + \frac{E}{A}(\rho_0), & \rho \geq \rho_c \\ -a\rho, & \rho < \rho_c \end{cases} \quad (1)$$

where

$$\rho_c = \frac{\rho_0}{1-\frac{q}{K}\frac{E}{A}} \quad (2)$$

and

$$a = K\frac{1-\rho^2/\rho_c^2}{18\rho_0} \quad (3)$$

The corresponding pressure is

$$p(\rho) = \rho^2\frac{\partial\frac{E}{A}(\rho)}{\partial\rho} = \begin{cases} \frac{K\left(\rho^2-{\rho_0}^2\right)}{18\rho_0}, & \rho \geq \rho_c \\ -\left(a + K\frac{\rho^2/{\rho_c}^2}{9\rho_o}\right)\rho^2, \rho < \rho_c \end{cases} \quad (4)$$

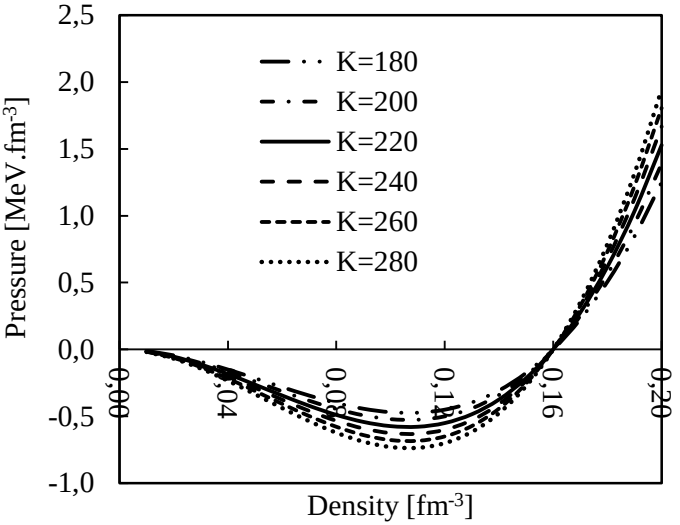

Figure 2. Pressure of nuclear matter.

The quadratic EOS (see Fig. 3)

$$\frac{E}{A}(\rho) = \frac{K(\rho-\rho_0)^2}{18{\rho_0}^2} + \frac{E}{A}(\rho_0), \quad (5)$$

and pressure

$$p(\rho) = \rho^2 \frac{\partial \frac{E}{A}(\rho)}{\partial \rho} = \frac{K(\rho-\rho_0)}{9}\left(\frac{\rho}{\rho_0}\right)^2 \quad (6)$$

are obtained.

In this case the requirement E/A(0)=0 and E/A(ρ_0)= -16,5±0,5 MeV at ρ_0= 0,166 fm^{-3} fixes the nuclear incompressibility at K≈ 283 MeV. Thus,

$$\frac{E}{A}(\rho) = A\rho^2 + B\rho + C \quad (7)$$

where A = 571 MeV.fm^6 , B = -194 MeV.fm^3 and C=0 [13].

4. RESULTS OF SYMMETRIC NUCLEAR MATTER CALCULATIONS

It can be seen from various studies in found the literatüre that the nuclear matter saturation density is in the range of 0,145 – 0,20 and the binding energy at the saturation density is E/A -16 MeV [2, 3, 5, 11].

In the present work, the parameters of extended liquid drop model A, B, and C were calibrated to reproduce the empirical saturation condition of nuclear matter, namely an energy per nucleon E/A=−16 MeV at the saturation density, as described by Equation (7). In this study the parameter sets are found given in Table 1.

Table 1. Parameter sets for different saturation densities.

ρ_0	A	B	C
0,145	783,2897	-224,1310	0,030292
0,150	737,0050	-217,4166	0,029869
0,155	662,7761	-206,1488	0,029875
0,160	621,2470	-199,5862	0,029870
0,165	595,7422	-195,4482	0,029880
0,170	565,7113	-190,4643	0,029882
0,175	537,1628	-185,6028	0,029886
0,180	483,1775	-176,0269	0,029890

When the pressure value at the equilibrium density is set to zero, the parameter sets are calculated as follows given Table 2.

Table 2. Parameter sets for zero pressure at different saturation density.

ρ_0	A	B	C
0,145	762,4396	-221,1075	0,030294
0,150	712,4386	-213,7316	0,029869
0,155	667,2164	-206,8371	0,029874
0,160	626,1668	-200,3734	0,029869
0,165	588,7927	-194,3016	0,029880
0,170	554,6672	-188,5869	0,029883
0,175	523,4249	-183,1987	0,029886
0,180	494,7497	-178,1099	0,029889

The EOS results calculated with different parameter sets for different saturation densities are shown in Figure 3.

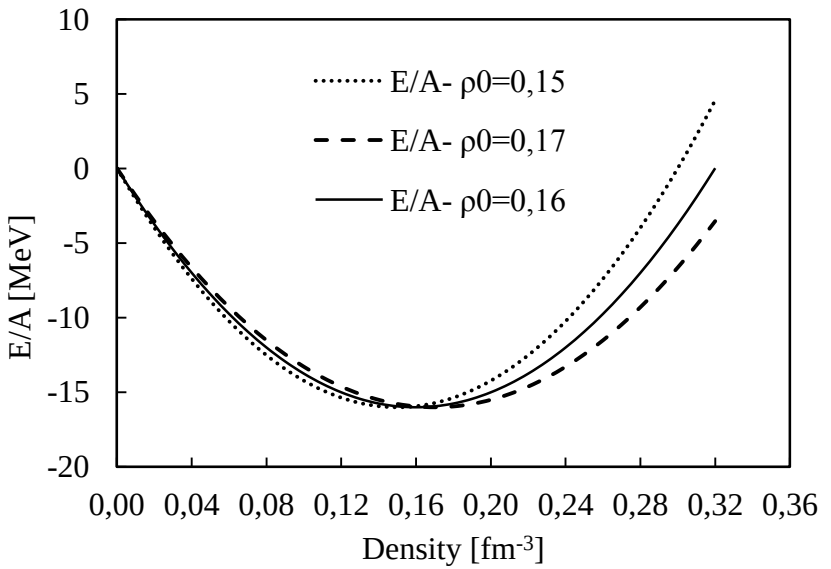

Figure 3. The obtained for nuclear matter EOS by using new parameter set for ELDM.

The pressure (P) and incompressibility (K) values calculated using the parameter sets are shown in Table 3.

Table 3. Pressure (P) and Incompressibility K values calculated using parameter sets.

ρ_0	E/A	Pressure	Incompressibility
0,145	-16,00	0	288,54528
0,150	-16,00	0	288,53765
0,155	-16,00	0	288,53773
0,160	-16,00	0	288,53765
0,165	-16,00	0	288,53785
0,170	-16,00	0	288,53790
0,175	-16,00	0	288,53795
0,180	-16,00	0	288,53800

The obtained pressure and incompressibility of nuclear matter by using new parameter set are given Table 3. It can be seen from Table 3 that at a saturation density ρ_0 value of 0,16 the energy per nucleon E/A = -16,00 MeV, pressure P = 0 and incompressibility K = 286,5 MeV were calculated.

Incompressibility was calculated using different parameter sets, results were found to be compatible with the literature value of 283 MeV [13].

The change of E/A values with density for saturation points 0,16 and 0,17 are given in Table 4.

In this study, we demonstrated a simple model for calculating some properties of nuclear matter. Numerous models and studies examining the properties of nuclear matter exist in the

literature. Researchers can use these parameters to calculate other properties of nuclear matter.

Table 4. E/A [MeV] values calculated using the new parameter sets.

ρ (fm^{-3})	**E/A (for ρ_0=0,16)**	**E/A (for ρ_0=0,17)**
0,02	-3,72713	-3,51999
0,03	-5,41778	-5,12852
0,04	-6,9832	-6,62612
0,05	-8,42338	-8,01279
0,06	-9,73833	-9,28853
0,07	-10,928	-10,4533
0,08	-11,9925	-11,5072
0,09	-12,9318	-12,4501
0,10	-13,7458	-13,2821
0,11	-14,4346	-14,0032
0,12	-14,9981	-14,6133
0,13	-15,4364	-15,1125
0,14	-15,7495	-15,5008
0,15	-15,9374	-15,7781
0,16	**-16,0000**	-15,9445
0,17	-15,9374	**-16,0000**
0,18	-15,7495	-15,9445
0,19	-15,4364	-15,7781
0,20	-14,9981	-15,5008
0,21	-14,4346	-15,1125
0,22	-13,7458	-14,6133
0,23	-12,9318	-14,0032
0,24	-11,9925	-13,2821
0,25	-10,928	-12,4501
0,26	-9,73833	-11,5072
0,27	-8,42338	-10,4533
0,28	-6,9832	-9,28853
0,29	-5,41778	-8,01279
0,30	-3,72713	-6,62612

REFERENCES

[1]. V. R. Pandharipande and R. B. Wiringa, 1979. *Rev. Mod. Phys*. **51**, 821.

[2]. K. Manisa, Ü. Atav, R. Oğul, 2005. *International Journal of Modern Physics E (IJMPE)*, **14**, 255–267.

[3]. B. D. Day, *Reviews of Modern Physics*, July 1978, 50(**3**).

[4]. K. Manisa, Ü. Atav, S. Sarıaydın, 2010. *Central. European. Journal of Physics*, 8(**4**), 587–595.

[5]. K. Manisa, *Physics of Atomic Nuclei*, 2011. 74(**7**), 958–970.

[6]. F. Manisa, A. Küçükbursa, K. Manisa, and T. Babacan, 2011. *Mathematical δ Computational. Applications*, **16**, 414.

[7]. K. Manisa, S*cience China Physics, Mechanics & Astronomy*, (2012) **55**, 443.

[8]. K. Manisa, M. Erdoğan and S. Bostan, *Romanian Journal of Physics*, 2015. 60(**3-4**), 429–443.

[9]. K. Manisa, *Romanian. Reports. In Physics*, 2016. **68**, 582.

[10]. K. Manisa, M. Erdoğan, H. Bircan and N. Z. Erdoğan, 2017. *Acta Physica Polonica B*, 48(2), , 183-194.

[11]. H. Bircan, 2020. *Physics of Atomic Nuclei*, 83(**2**), 351–367.

[12]. W. Scheid, R. Ligensa, W. Greiner, 1968. *Phys. Rev. Lett*., **21**, 1479.

[13] S. Misicu, 2007. *Romanian Reports in Physics*, 59(**4**) P. 11271167.

CHAPTER 2

MONTE CARLO SIMULATION OF PHOTON RADIATION TRANSFER

Hasan BİRCAN[1]
Kaan MANİSA[2]
Mehmet ERDOĞAN[3]
A. Engin ÇALIK[4]

1. INTRODUCTION

The Monte Carlo method is a powerful technique used across many fields. Its use has been expanding with advances in computational power, as it involves multiple approaches and makes use of random numbers. [1, 2, 3]

[1] Assoc. Prof. Dr. Kütahya Dumlupınar University Faculty of Arts And Sciences Physics Department Kütahya/Türkiye, Orcid: 0000-0003-2067-7855, hasan.bircan@dpu.edu.tr
[2] Prof. Dr. Kütahya Dumlupınar University Faculty of Arts And Sciences Physics Department Kütahya/Türkiye, Orcid: 0000-0002-4063-277X, kaan.manisa@dpu.edu.tr
[3] Prof. Dr. Selçuk University, Physics Department, Konya/Türkiye, Orcid: 0000-0003-1879-8500, merdogan@selcuk.edu.tr
[4] Assoc. Prof. Dr. Ege University, Physics Department, İzmir/Türkiye, Orcid: 0000-0003-3441-6496 engin.calik@ege.edu.tr

In this section, an Excel program has been developed that uses two different Monte Carlo (MC) methods (probability and inverse transform) to allow 1D visualization of photon transport and simulation and calculation of photon flux passing through a planar surface. The program also makes it easy to change certain parameters like mass attenuation coefficient through a graphical user interface.

Our goal is to provide workable tools for computing light distributions such as the amount and distribution of photochemical reactions in experimental solutions, films and biological tissues.

Photon absorption theory is compared with Monte Carlo simulation.

In this study, we used various some parameters, which mass attenuation coefficient and photon numbers, and investigate the effects of these changes on flux, as well as on the qualitative nature of the transport.

2. PHOTON RADIATION TRANSFER AND ABSORPTION

The mass attenuation coefficients for materials can be determined by radiation transmission method

$$I = I_o e^{-\mu_m x} \quad (1)$$

where

- μ_m is the total mass attenuation coefficient (cm^2/g), which total interaction (Rayleight, Photoelectric, Compton, Pair Production, …)
- I_o is incident photon intensity,
- I is photon intensity on x coordinate

- x is the mass thickness of the material.

The theoretical μ_m values for the present alloys were obtained by the WinXCom code [4]. This program depends on the use of the mixture rule to calculate the partial and total mass attenuation coecients for all elements, compounds, and mixtures at standard as well as selected energies.

There are many programs about to radiation absorption, photon transfer. MCNP [5, 6], Fluka [7], Geant [8], EGS [9], Phenelope [10], MCX [11], etc. Some of them not free, practical and difficult user interface.

In this study, we focused on Monte Carlo simulation for one-dimensional absorption. Two methods were implemented: the probability method and the inverse transform method. Due to the difficulty of implementing the probability method in Excel, it was necessary to use Visual Basic for coding.

3. METHODS

3.1. Probability Method (Probability-Based Event Simulation)

Probability-based event simulation is a Monte Carlo technique where the occurrence of events is determined by comparing random numbers to predefined probabilities. This method is commonly used to simulate systems with stochastic (random) behavior, such as particle transport, radioactive decay. Number of particles passing through layer x are given Eq.1.

Mean Free Path, (MFP) λ = average distance to collision

Macroscopic Cross-section, $\mu_m = \Sigma = 1/\lambda = N.\sigma$ Probability of interaction with a material, per unit distance traveled

N = number of target nuclei per cm^3 (nuclear number density) [$atoms/cm^3$]

σ = microscopic cross-section, target area per nuclide units: barns, 1 barn = 10^{-24} cm^2

μ_m or Σ = [nuclide/(barn.cm)] . [barn/nuclide] = 1 / cm

If a beam of particles is directed at a purely-absorbing infinite slab, what is the beam strength at penetration x?

Probability of traveling distance x without collision is $e^{-\mu_m x}$

Probability of colliding at distance x is $p(x) = \mu_m e^{-\mu_m x}$

MC codes use this relation to sample the distance to the next collision probability of colliding at x per-unit-distribution] x [probability of reaching x without collision]

MC codes use this relation to sample the distance to the next collision

$$\xi = \int_0^{x_1} p(x)dx = 1 - e^{-\mu_m x_1} \qquad (2)$$

The absorption of light of intensity I_o or N_o particle numbers in matter is shown in Fig.1.

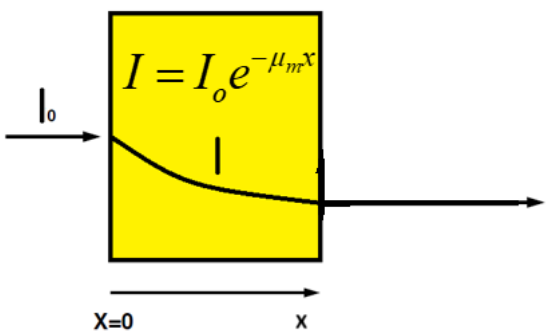

Figure 1. The absorption of light of intensity I_o in a material.

Algorithm for Monte Carlo Possibility Calculation Visual Basic or Another Compiler

1) Declaration of particle number, mass attenuation coefficient … etc.
2) Loop for particle number
3) increase the position of photon in material x = x + dx (Where dx is a bin.)
4) Possibility calculation at x from theory
5) Loop for non absorbed particle
6) r=Rnd() to create a random number for Monte Carlo simulation
7) If Condition for the possibility of absorp or pass
8) Count a pass and absorbed particle
9) End if
10) End Loop
11) Print a result (x thickness of material, absorbed particle and passed from x)
12) End Loop & End Program

3.2. Inverse Transform Method

The Inverse Transform Method is a technique used in Monte Carlo simulations to generate random samples from a given probability distribution.

Use the inverse of the cumulative distribution function (CDF), F^{-1} , to transform U into a sample X from the target distribution:

$$X = F^{-1}(U) \tag{3}$$

The method is generally applied when the cumulative distribution function (CDF) has a known analytical inverse. If the

function F does not have an inverse, the method cannot be used directly; instead, alternative indirect sampling techniques are employed.

Let's see how it is done in Photon absorption, which is an exponential distribution:

- One consider the sampling of the step size for photon movement, x, The probability density function is given: [1, 2]

$$P(x) = \mu_m e^{-\mu_m x}$$

where interaction coefficient μ_m, total mass attenuation coefficient.

- Using this function

$$\xi = \int_0^{x_1} p(x)dx = \int_0^{x_1} \mu_m e^{-\mu_m x} dx = 1 - e^{-\mu_m x_1}$$

expression for a sampled value, x_1, based on the random number ξ:

- Solving for the value x_1:

$$x_1 = -\ln(1 - \xi)/\ \mu_m$$

the above expression is equivalent to:

$$x_1 = -\ln(\xi)/\ \mu_m$$

  - ξ is a random number uniformly chosen in range [0,1]
  - This is the fundamental principle behind Monte Carlo techniques and is used to sample randomly from Probability Density Function (PDF)
  - Code is given below for Turkish and English version Excel
  - =SIKLIK($I$3:$I$402;E4)
  - =Frequency($I$3:$I$402;E4)

Where ($I$3:$I$402) is array form exponential distribution.

- E4 is a bin for calculation frequency.
- The calculations have been made for each bin.
- =-mu*ln(x_random) for I Column

Excel formul is =S_SAYI_ÜRET() or =RAND() for producing uniform a random number.

4. RESULTS AND COMPARISONS

Figure 2 illustrates 400 random points representing simulated particle impacts on the material surface.

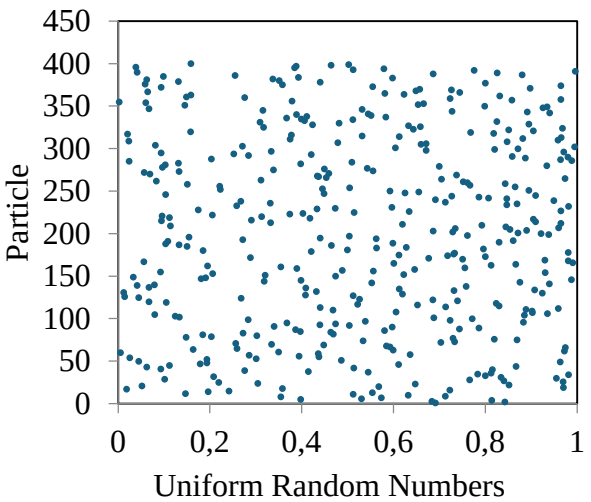

Figure 2. Simulated particles impacts on the material surface.

There are 31 random points generated at 6 cm represent the particles and are given in Table 1. These particles do not yet interact with matter. Sample calculation parameters are given in Table 2.

Table 1. random numbers

x (cm)	i	uniform random numbers
0	1	0,624162512
0,2	2	0,87978933
0,4	3	0,132880402
0,6	4	0,356238418
0,8	5	0,897790731
1	6	0,256865204
1,2	7	0,339754176
1,4	8	0,239430962
1,6	9	0,65215377
1,8	10	0,391693092
2	11	0,318267221
2,2	12	0,460105486
2,4	13	0,315039255
2,6	14	0,72375685
2,8	15	0,762207802
3	16	0,080281588
3,2	17	0,274231413
3,4	18	0,715456522
3,6	19	0,685004357
3,8	20	0,2657904
4	21	0,788598252
4,2	22	0,532674359
4,4	23	0,183864097
4,6	24	0,021751922
4,8	25	0,365191307
5	26	0,155034616

Table 2. Example of Calculation Parameters

MFP=lamda=1/ μ_m = Mean Free Path	15
μ_m= Total Mass Attenuation Coefficient	0,066666667
Monte Carlo Result MFP	14,85
Total passed MFP	256
Total no passed MFP	144
Total Particle	400

Where μ_m =Total Mass Attenuation Coefficient or Mean Free Path and Total particle number are changeable parameters. Table 2 also presents a MC results: the number of particles, out of 400, that passed through (256) or were absorbed (144) after traveling a mean free path (MFP) length.

Monte Carlo simulation results for probability method for N=800 and μ_m =1/15 are given Table 3.

The Monte Carlo simulation results for the probability method, the inverse transformation method and theory calculation results are given in Table 4 and Figure 3.

Table 3. Monte Carlo simulation results for probability (possibility) method

x (cm)	N	N Passed
0	800	0
0,2	789	11
0,4	786	14
0,6	774	26
0,8	761	39
1,0	752	48
1,2	736	64
1,4	723	77
1,6	715	85
1,8	706	94
2,0	695	105
2,2	688	112
2,4	677	123
2,6	670	130
2,8	665	135
3,0	657	143
3,2	648	152
3,4	644	156
3,6	638	162
3,8	627	173
4,0	620	180
5,0	578	222
6,0	541	259
7,0	507	293

Table 4. Monte Carlo simulation results for inverse transform, probability (possibility) method and theory.

x (cm)	Inverse Transform Method	Probability (Possibility) Method	Theory
0	400	400	400,00
1	381	378	374,20
2	357	354	350,07
3	339	322	327,49
4	321	304	306,37
5	298	283	286,61
6	282	267	268,13
7	260	254	250,84
8	246	243	234,66
9	229	226	219,52
10	214	211	205,37
11	202	198	192,12
12	188	185	179,73
13	178	172	168,14
14	170	164	157,30
15	162	148	147,15
16	159	141	137,66
18	139	124	120,48
19	131	114	112,71
20	120	109	105,44

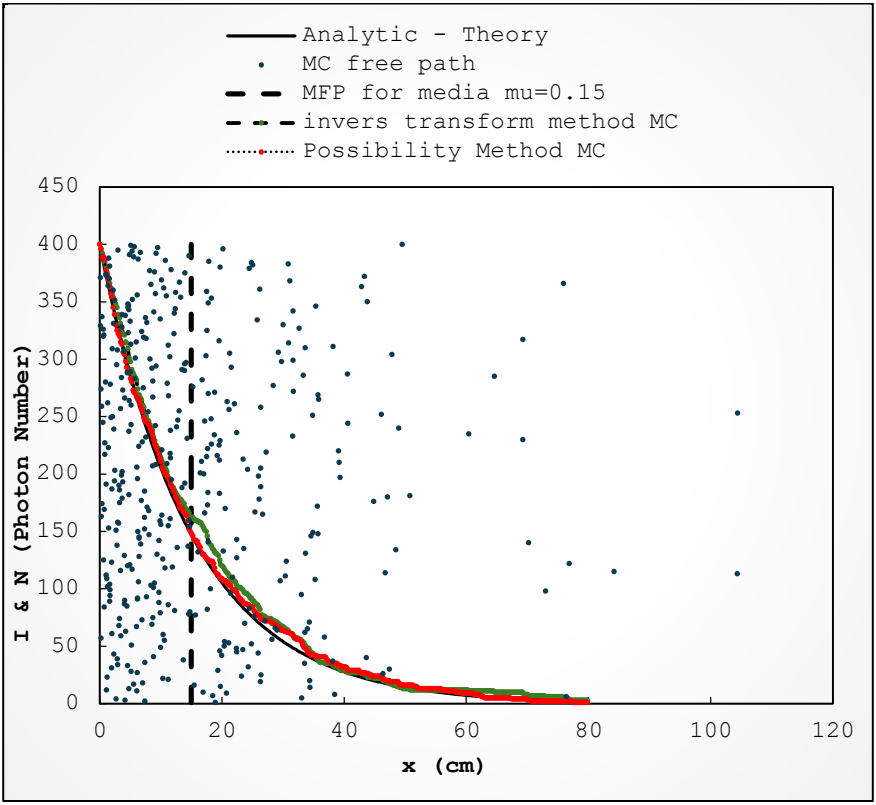

Figure 3. Monte Carlo simulation of photon radiation results for inverse transform, probability (possibility) method and analytic-theory.

Table 5 compares the Monte Carlo simulation results with reported mean free path (MFP) values from references [4, 12, 13] for B-100 bone-equivalent plastic, demonstrating strong consistency with the literature.

Figure 4 shows screenshot from the simulation program interface.

Table 5 compares the Monte Carlo simulation results Comparison of Monte Carlo Simulated Mean Free Path (MFP) Values with Calculated from Literature Data [3, 13, 14] for B-100 Bone-Equivalent Plastic.

Energy	**μ/ρ**	**μ**	**MFP**	**MFP MC Results [This Study]**
(MeV)	(cm^2/g)	(1/cm)	(cm)	(cm)
0,200	0,132500	0,192125	5,20	4,99
1,000	0,067230	0,097484	10,26	10,12
2,000	0,047050	0,068223	14,68	14,97

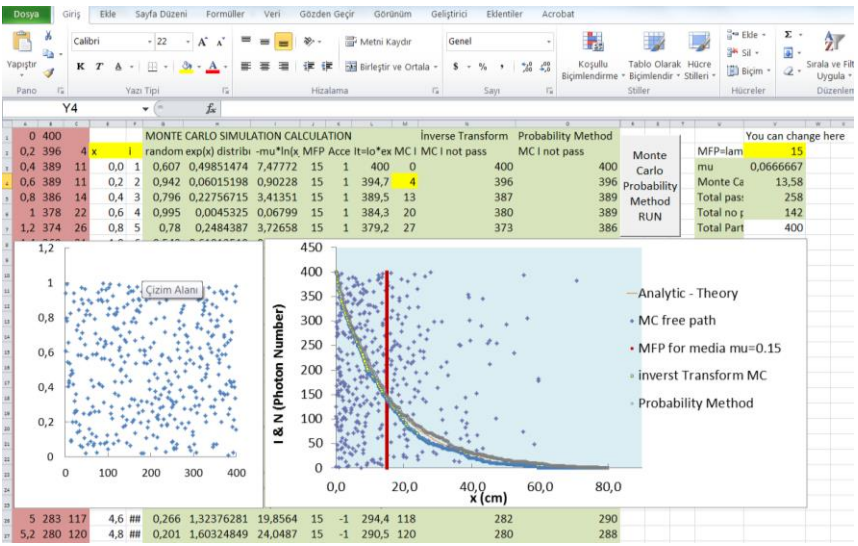

Figure 4. A screenshot from the simulation program interface.

The results confirm the reliability of the Monte Carlo method for simulating photon interactions in matter. The study demonstrates accurate modeling of absorption behavior using Monte Carlo techniques.

REFERENCES

[1]. Introduction to Monte Carlo Radiation Transfer, 2013. Kenneth Wood, Barbara Whitney, Jon Bjorkman, & Michael Wolff.

[2]. Monte Carlo Techniques for Nuclear Systems, 2025 – Theory Lectures Forrest Brown, National Laboratory Professor, NE Dept., UNM Senior Research Scientist, XCP-3, LANL.

[3]. Monte Carlo Modeling of Light Transport in Multi-layered Tissues in Standard C, 1992. Lihong Wang, Ph. D. Steven L. Jacques, Ph. D. Laser Biology Research Laboratory University of Texas M. D. Anderson Cancer Center.

[4]. Hubbell, J.H. and Seltzer, S.M. 2004. Tables of X-Ray Mass Attenuation Coefficients and Mass Energy-Absorption Coefficients (version 1.4). [Online] Available: http://physics.nist.gov/xaamdi [16.09.2021]. National Institute of Standards and Technology, Gaithersburg, MD.

[5]. https://mcnp.lanl.gov/ (access date: 28.05.2025)

[6]. Tekin, Huseyin Ozan & Manici, Tuğba, 2017. Simulations of mass attenuation coefficients for shielding materials using the MCNP-X code. *Nuclear Science and Techniques*. **28**, 10.1007/s41365-017-0253-4.

[7]. http://www.fluka.org/fluka.php (access date: 28.05.2025)

[8]. https://geant4.web.cern.ch/support/download (access date: 28.05.2025)

[9]. http://rcwww.kek.jp/research/egs/ (access date: 28.05.2025)

[10]. https://www.oecd-nea.org/tools/abstract/detail/nea-1525 (access date: 28.05.2025)

[11]. http://mcx.space (access date: 07.05.2025)

[12]. https://physics.nist.gov/PhysRefData/XrayMassCoef/tab2.html (access date: 07.05.2025)

[13]. https://physics.nist.gov/PhysRefData/XrayMassCoef/tab4.html (access date: 07.05.2025)

CHAPTER 3

TEKNESYUM (Tc) ELEMENTİNİN KÜTLE SOĞURMA KATSAYILARININ Phy-X PROGRAMI İLE İNCELENMESİ

Saniye TEKEREK[1]

1. Giriş

Enerji üretimi ve depolama, günümüzün en kritik bilimsel ve teknolojik sorunları arasında yer almakta; artan küresel enerji ihtiyacı, fosil yakıt rezervlerinin azalması ve çevresel sürdürülebilirlik kaygıları, daha verimli ve uzun ömürlü enerji çözümleri geliştirilmesini zorunlu kılmaktadır. Bu doğrultuda, özellikle yenilenebilir enerji kaynaklarının (güneş, rüzgâr vb.) süreksiz doğası, enerji arz-talep dengesini sağlayacak yüksek kapasiteli ve kararlı depolama sistemlerine olan gereksinimi artırmaktadır. Geleneksel enerji depolama teknolojileri (örneğin lityum-iyon piller, süperkapasitörler ve hidrojen depolama sistemleri) bu ihtiyacın belirli bir kısmını karşılayabilmekteyse de, özellikle uzay görevleri, askeri uygulamalar, nükleer santraller ve ulaşılması zor bölgeler için daha gelişmiş ve güvenilir alternatif sistemlere ihtiyaç duyulmaktadır (Hubbel 1999).

[1] Doç.Dr., Kahramanmaraş Sütçü İmam Üniversitesi, Sağlık Hizmetleri MYO, Tıbbi Hizmetler ve Teknikler Bölümü, Kahramanmaraş/TÜRKİYE, Orcid: 0000-0003-3326-358X, saniyetekerek@ksu.edu.tr

Bu çerçevede, nükleer özellikleri ile öne çıkan bazı radyoaktif elementler, özellikle yüksek enerji yoğunluğu, uzun yarı ömür ve kararlı enerji salımı gibi avantajları sayesinde alternatif enerji depolama çözümlerinde umut vadetmektedir. Bu elementler arasında yer alan teknesyum (Tc), atom numarası 43 olan, doğada serbest halde bulunmayan ve nükleer reaktörlerde uranyumun fisyonu sonucunda elde edilen ilk sentetik elementtir. Teknesyumun özellikle Tc-99m izotopu, nükleer tıpta tanı amaçlı görüntüleme tekniklerinde yaygın olarak kullanılmakta olup, kısa yarı ömrü ve gama ışını salımı sayesinde vücut içi dağılımı kolaylıkla izlenebilmektedir.

Teknesyumun yalnızca tıbbi değil, enerji teknolojileri açısından da dikkate değer potansiyeli bulunmaktadır. Radyoaktif bozunma sürecinde ortaya çıkan enerji, termoelektrik jeneratörler ve termo-fotovoltaik sistemler gibi düşük güçlü, uzun ömürlü enerji dönüşüm teknolojilerinde değerlendirilebilmektedir. Bu tür sistemlerde, özellikle yüksek özgül enerjiye ve kontrollü bozunma karakteristiğine sahip izotopların kullanılması, enerji dönüşüm verimliliğini artırmak açısından önemlidir. Bu bağlamda teknesyum, sahip olduğu özgül aktivite, uygun yarı ömrü ve radyasyon salımı özellikleriyle potansiyel bir aday olarak değerlendirilmektedir.

Bununla birlikte, radyoaktif izotopların enerji sistemlerinde etkin şekilde kullanılabilmesi için, elektromanyetik radyasyonla olan etkileşimlerinin ayrıntılı şekilde analiz edilmesi gerekmektedir. Bu etkileşimin nicel bir göstergesi olan kütle soğurma katsayısı (μ/ρ), bir maddenin birim kütlesinin radyasyonu ne oranda soğurabildiğini ifade eder ve özellikle foton enerjisine bağlı olarak değişkenlik göstermektedir (Bertin, 1975). Enerjiye bağımlı bu değişim, materyalin spesifik enerji aralıklarında daha etkin kullanımı açısından belirleyici olup, malzeme seçimi ve sistem tasarımı üzerinde doğrudan etkilidir. Bu bağlamda, söz

konusu çalışmada, teknesyumun elektromanyetik radyasyonla etkileşim özellikleri Phy-X/PSD programı kullanılarak değerlendirilmiş ve çeşitli enerji seviyelerinde kütle soğurma katsayısı değerleri elde edilmiştir. Phy-X, farklı enerjilerdeki foton-malzeme etkileşimlerini analiz etmek üzere geliştirilmiş açık erişimli bir yazılım olup, kullanıcılara kütle ve lineer soğurma katsayısı gibi parametreleri sunmaktadır.

Elde edilen veriler üzerinden teknesyumun enerji depolama sistemlerine uygunluğu değerlendirilmiş olup, elektromanyetik radyasyonla çalışan sistemlerde malzeme mühendisliğine dair öneriler geliştirilmiştir. Özellikle foton soğurma temelli enerji dönüşüm teknolojilerinde, teknesyumun uygulanabilirliği analiz edilerek, nükleer tabanlı enerji sistemleri için ileri düzey malzeme seçiminde bilimsel bir temel sunmuştur.

2. Phy-X Programı ve Yöntem

Phy-X/PSD (Photon Shielding and Dosimetry), X-ışınları ve gama ışınlarının maddeyle etkileşimini hesaplamak için geliştirilen, çevrimiçi erişilebilir bir yazılımdır. Belirli element, alaşım veya bileşiklerin foton enerjilerine bağlı olarak temel radyasyon parametreleri olan kütle soğurma katsayısı, lineer soğurma katsayısı, yarım değer tabakası ve etkili atom numarası gibi bilgiler sağlar. Phy-X/PSD programı, radyasyon güvenlik uygulamaları için yeni ve alternatif malzemelerin tasarımında kritik öneme sahip parametreleri hesaplar. Bu parametreler arasında doğrusal ve kütle zayıflatma katsayıları (LAC, MAC), yarı ve onda değer kalınlıkları (HVL, TVL), ortalama serbest yol (MFP), etkin atom numarası ve elektron yoğunluğu (Zeff, Neff), enerji absorpsiyonu ve maruz kalma birikim faktörleri (EABF, EBF) ve hızlı nötron kaldırma kesiti (FNRCS) bulunur. Phy-X, 1 keV'den 100 GeV'ye kadar sürekli enerji bölgesinde veri üretebilir. Ayrıca, Na-22, Co-60, Cs-137 gibi bilinen radyoaktif kaynakların ve bazı karakteristik X-ışını enerjilerinin (Cu, Mo, Ag gibi elementlere ait)

verilerini de içerir. Bu sayede kullanıcılar, önceden tanımlanmış enerji aralıklarında zırhlama parametrelerini kolayca elde edebilirler (Şakar ve ark., 2020; Özpolat ve ark., 2020).

Programın kullanım alanları oldukça geniştir; nükleer güvenlik uygulamalarından radyasyondan korunma malzemelerinin geliştirilmesine, tıbbi görüntülemede (tanısal görüntüleme) doz tahmininden radyoterapide kullanılacak malzemelerin değerlendirilmesine kadar birçok alanda fayda sağlar. Özellikle yeni nesil radyasyon zırhlama malzemelerinin tasarımında ve değerlendirilmesinde kritik bir rol oynar.

Kısacası Phy-X Programı, radyasyonun madde ile etkileşimini anlamak ve radyasyondan korunma için etkili malzemeler geliştirmek isteyen araştırmacılar ve mühendisler için değerli, çevrimiçi erişilebilir bir araçtır.

Bu çalışmada, Tc elementinin 10^{-3} MeV ile 10^{5} MeV arası enerji aralığında μ/ρ verileri elde edilmiştir. Hesaplamalar sırasında Tc'nin yoğunluğu 11,5 g/cm^3 olarak alınmıştır.

Enerji depolama sistemleri, özellikle yenilenebilir kaynakların süreksiz doğası nedeniyle büyük önem kazanmıştır. Radyoaktif izotopların, kararlı bir şekilde enerji salabilmeleri ve bu enerjinin elektrik enerjisine dönüştürülebilir olması, onları uzun ömürlü ve güvenilir güç kaynakları haline getirebilir. Tc'nin bazı izotopları (örneğin Tc-99m), belirli kontrollü ortamlarda enerji üretebilecek kapasiteye sahiptir. Teknesyum, uzun süreli güç kaynağına ihtiyaç duyulan uzay görevlerinde kullanılabilecek nitelikte bir malzemedir. Ayrıca geleneksel enerji kaynaklarına erişimin sınırlı olduğu bölgelerde ya da şebekeden bağımsız çalışan sistemlerde, düşük güçlü ve uzun ömürlü enerji çözümleri sunabilir. Bu özellikleri sayesinde, Tc temelli mikro bataryaların geliştirilmesi mümkündür. Termofotovoltaik sistemlerde ise foton

bazlı enerji dönüşüm süreçlerinde etkili bir radyasyon soğurucu olarak değerlendirilme potansiyeline sahiptir.

Phy-X programı ile elde edilen kütle ve lineer soğurma katsayı verileri düşük enerji aralığında Tc elementi için oldukça yüksek değerler göstermektedir. Örneğin 0,001 MeV için bu değer 5356,5 cm^2/g seviyelerine ulaşmaktadır. Bu durum, fotoelektrik etki mekanizmasının bu enerji düzeylerinde baskın olmasıyla açıklanabilir. Dolayısıyla, Tc düşük enerjili X-ışını ve gama ışınlarına karşı yüksek bir soğurma kapasitesine sahiptir.

Orta enerji seviyelerinde kütle soğurma katsayısı belirgin biçimde azalmakta ve yaklaşık 0,059–0,080 cm^2/g arasında sabitlenmektedir. Bu enerji aralığında, Compton saçılması etkileşimin baskın hale geldiği gözlemlenmektedir. Tc bu enerji düzeylerinde daha kararlı ve öngörülebilir bir radyasyon soğurma performansı sunmaktadır.

Yüksek enerji aralığında ise kütle soğurma katsayısı genellikle sabit kalmakta ve belirgin bir azalma ya da artış göstermemektedir. Bu durum, çift üretimi gibi mekanizmaların etkili olduğu, daha yüksek enerjili radyasyonlarla karşılaşılan durumlarda Tc'nin absorpsiyon kapasitesinin istikrarını koruduğunu ortaya koymaktadır.

Kütle soğurma katsayısı, denklem (1) kullanılarak hesaplanan kütle soğurma katsayısı enerjiye bağlı bir parametredir (Hubbell, 1999).

$$\mathrm{MAC} = \left(\frac{\mu}{\rho}\right)_{\mathrm{nanokompozit}} = \left(\frac{\mathrm{LAC}}{\rho}\right)_{\mathrm{nanokompozit}} \quad (1)$$

Denklem (1)'de ρ yoğunluk, (μ/ρ) elementin kütle soğurma katsayısıdır.

Radyasyona maruz kalan malzemenin HVL'si, malzemeye gelen radyasyon şiddetini yarıya indiren kalınlık olarak ifade edilir (Agar ve ark., 2019; Sayyed ve ark., 2018). HVL ve TVL değerleri Denklem (2) ve (3) kullanılarak program tarafından hesaplanmıştır.

$$\mathrm{HVL} = \frac{\mathrm{In2}}{LAC} \tag{2}$$

$$\mathrm{TVL} = \frac{\mathrm{In10}}{LAC} \tag{3}$$

3. Sonuç ve Öneriler

Bu kitap bölümünde, Technetium elementinin farklı enerji seviyelerinde gösterdiği kütle ve lineer soğurma katsayıları, Phy-X yazılımı kullanılarak elde edilmiş olup Tablo 1'de listelenmiştir. Elde edilen bulgular, Tc'nin (140 keV, yarı ömrü $t_{1/2}$=6saat) özellikle düşük ve orta enerji seviyelerinde yüksek soğurma kapasitesi sunduğunu ve bu nedenle enerji depolama sistemlerinde potansiyel bir malzeme olduğunu ortaya koymaktadır.

Teknesyumun radyoaktif özellikleri ile birlikte yüksek kütle soğurma katsayısı, onu nükleer mikro batarya, radyasyon temelli enerji üretim sistemleri ve uzay görevleri gibi özel alanlarda cazip bir malzeme haline getirmektedir.

Tablo 1. Teknesyum (Tc) radyoaktif elementinin Phy-X programından elde edilen Yarı değer katman kalınlığı, onda bir değer katman kalınlığı, kütle ve lineer soğurma katsayıları

Enerji [MeV]	Radyaktif İzotop Kaynak	Kütle Soğurma Katsayısı (μ/ρ) [cm^2/g]	Lineer Soğurma Katsayısı (μ) [cm^{-1}]	HVL [cm]	TVL [cm]
5,89E-03	Fe (55)	380,156	4394,604	0,0002	0,0005
5,90E-03	Fe (55)	378,302	4373,171	0,0002	0,0005
6,49E-03	Fe (55)	293,535	3393,266	0,0002	0,0006
6,54E-03	Fe (55)	288,064	3330,025	0,0002	0,0007
8,00E-03		168,299	1945,535	0,0004	0,0012
8,91E-03	Cu (29)	125,893	1455,327	0,0005	0,0016
1,00E-02		92,320	1067,216	0,0006	0,0022
1,34E-02	Rb (37)	41,958	485,037	0,0014	0,0047
1,38E-02	Am (241)	38,445	444,419	0,0016	0,0052
1,50E-02	Rb (37)	30,932	357,577	0,0019	0,0064
1,96E-02	Mo (42)	14,825	171,381	0,0040	0,0134
2,00E-02		14,099	162,980	0,0043	0,0141
2,21E-02	Ag (47)	66,003	762,991	0,0009	0,0030
2,21E-02	Ag (47)	66,003	762,991	0,0009	0,0030

Tablo 1 devamı. Teknesyum (Tc) radyoaktif elementinin Phy-X programından elde edilen Yarı değer katman kalınlığı, onda bir değer katman kalınlığı, kütle ve lineer soğurma katsayıları

Enerji [MeV]	Radyaktif İzotop Kaynak	Kütle Soğurma Katsayısı (μ/ρ) [cm^2/g]	Lineer Soğurma Katsayısı (μ) [cm^{-1}]	HVL [cm]	TVL [cm]
2,31E-02	Cd (109)	58,938	681,318	0,0010	0,0034
2,49E-02	Ag (47)	48,614	561,981	0,0012	0,0041
2,50E-02	Cd (109)	48,115	556,213	0,0012	0,0041
2,55E-02	Cd (109)	45,722	528,541	0,0013	0,0044
2,63E-02	Am (241)	42,048	486,079	0,0014	0,0047
3,00E-02		29,928	345,965	0,0020	0,0067
3,08E-02	Ba (133)	27,865	322,116	0,0022	0,0071
3,22E-02	Am (241)	24,837	287,111	0,0024	0,0080
3,32E-02	Am (241)	22,845	264,088	0,0026	0,0087
3,50E-02	Ba (133)	19,818	229,101	0,0030	0,0101
3,54E-02	Ba (133)	19,220	222,179	0,0031	0,0104
3,58E-02	Ba (133)	18,645	215,534	0,0032	0,0107
3,64E-02	Ba (56)	17,838	206,212	0,0034	0,0112
3,95E-02	Eu (152)	14,282	165,103	0,0042	0,0139
4,00E-02		13,803	159,562	0,0043	0,0144
4,01E-02	Eu (152)	13,691	158,270	0,0044	0,0145
4,45E-02	Tb (65)	10,346	119,603	0,0058	0,0193
4,59E-02	Eu (152)	9,499	109,809	0,0063	0,0210
4,70E-02	Eu (152)	8,886	102,718	0,0067	0,0224

Tablo 1 devamı. Teknesyum (Tc) radyoaktif elementinin Phy-X programından elde edilen Yarı değer katman kalınlığı, onda bir değer katman kalınlığı, kütle ve lineer soğurma katsayıları

Enerji [MeV]	Radyaktif İzotop Kaynak	Kütle Soğurma Katsayısı (μ/ρ) [cm^2/g]	Lineer Soğurma Katsayısı (μ) [cm^{-1}]	HVL [cm]	TVL [cm]
4,96E-02	Ba (133)	7,683	88,810	0,0078	0,0259
5,00E-02		7,524	86,981	0,0080	0,0265
5,04E-02	Tb (65)	7,370	85,202	0,0081	0,0270
5,32E-02	Ba (133)	6,364	73,573	0,0094	0,0313
5,95E-02	Am (241)	4,669	53,970	0,0128	0,0427
6,00E-02		4,572	52,847	0,0131	0,0436
8,00E-02		2,099	24,263	0,0286	0,0949
8,10E-02	Ba (133)	2,030	23,471	0,0295	0,0981
8,80E-02	Cd (109)	1,628	18,818	0,0368	0,1224
9,90E-02	Am (241)	1,200	13,876	0,0500	0,1659
1,00E-01		1,169	13,513	0,0513	0,1704
1,03E-01	Am (241)	1,084	12,531	0,0553	0,1837
1,22E-01	Eu (152)	0,716	8,278	0,0837	0,2782
1,50E-01		0,445	5,144	0,1348	0,4477
1,61E-01	Ba (133)	0,385	4,452	0,1557	0,5172
2,00E-01		0,253	2,929	0,2366	0,7861
2,23E-01	Ba (133)	0,211	2,439	0,2842	0,9440
2,45E-01	Eu (152)	0,184	2,128	0,3257	1,0819
2,76E-01	Ba (133)	0,156	1,808	0,3834	1,2736
2,84E-01	Cs (137)	0,152	1,752	0,3956	1,3142
2,84E-01	I (131)	0,151	1,748	0,3965	1,3170
2,96E-01	Eu (152)	0,144	1,665	0,4163	1,3830
3,00E-01		0,142	1,639	0,4230	1,4052
3,03E-01	Ba (133)	0,140	1,621	0,4277	1,4207

Tablo 1 devamı. Teknesyum (Tc) radyoaktif elementinin Phy-X programından elde edilen Yarı değer katman kalınlığı, onda bir değer katman kalınlığı, kütle ve lineer soğurma katsayıları

Enerji [MeV]	Radyaktif İzotop Kaynak	Kütle Soğurma Katsayısı (μ/ρ) [cm^2/g]	Lineer Soğurma Katsayısı (μ) [cm^{-1}]	HVL [cm]	TVL [cm]
3,44E-01	Eu (152)	0,122	1,415	0,4899	1,6274
3,47E-01	Co (60)	0,121	1,404	0,4938	1,6405
3,56E-01	Ba (133)	0,118	1,370	0,5061	1,6813
3,65E-01	I (131)	0,116	1,339	0,5175	1,7192
3,84E-01	Ba (133)	0,111	1,278	0,5426	1,8023
4,00E-01		0,107	1,233	0,5623	1,8680
4,11E-01	Eu (152)	0,104	1,205	0,5754	1,9115
4,44E-01	Eu (152)	0,098	1,132	0,6122	2,0337
5,00E-01		0,090	1,037	0,6686	2,2212
5,11E-01	Na (22)	0,088	1,021	0,6790	2,2555
6,00E-01		0,079	0,917	0,7557	2,5102
6,37E-01	I (131)	0,076	0,883	0,7846	2,6064
6,62E-01	Cs (137)	0,075	0,863	0,8032	2,6681
6,78E-01	Eu (152)	0,074	0,850	0,8151	2,7078
6,89E-01	Eu (152)	0,073	0,842	0,8229	2,7335
7,23E-01	I (131)	0,071	0,818	0,8470	2,8137
7,79E-01	Eu (152)	0,068	0,784	0,8847	2,9388
8,00E-01		0,067	0,772	0,8984	2,9845
8,26E-01	Co (60)	0,066	0,757	0,9151	3,0399
8,67E-01	Eu (152)	0,064	0,737	0,9409	3,1257
9,64E-01	Eu (152)	0,060	0,694	0,9993	3,3196
1,00E+00		0,059	0,679	1,0204	3,3896
1,01E+00	Eu (152)	0,059	0,677	1,0233	3,3993
1,09E+00	Eu (152)	0,056	0,648	1,0692	3,5517
1,09E+00	Eu (152)	0,056	0,647	1,0714	3,5590

Tablo 1 devamı. Teknesyum (Tc) radyoaktif elementinin Phy-X programından elde edilen Yarı değer katman kalınlığı, onda bir değer katman kalınlığı, kütle ve lineer soğurma katsayıları

Enerji [MeV]	Radyaktif İzotop Kaynak	Kütle Soğurma Katsayısı (μ/ρ) [cm^2/g]	Lineer Soğurma Katsayısı (μ) [cm^{-1}]	HVL [cm]	TVL [cm]
1,11E+00	Eu (152)	0,055	0,640	1,0833	3,5987
1,17E+00	Co (60)	0,054	0,621	1,1154	3,7053
1,28E+00	Na (22)	0,051	0,594	1,1659	3,8732
1,30E+00	Eu (152)	0,051	0,589	1,1773	3,9109
1,33E+00	Co (60)	0,050	0,581	1,1930	3,9632
1,41E+00	Eu (152)	0,049	0,565	1,2264	4,0741
1,46E+00	Eu (152)	0,048	0,556	1,2477	4,1447
1,50E+00		0,047	0,548	1,2649	4,2020
2,00E+00		0,042	0,484	1,4315	4,7552
2,51E+00	Co (60)	0,039	0,449	1,5443	5,1302

Şekil 1'de verilen grafikler incelendiğinde çok düşük enerjilerde (örn. 1,00E-03 MeV=1 keV), kütle soğurma katsayıları oldukça yüksek olup, bu enerjilerde fotoelektrik etkinin baskın olduğunu gösterir. Fotoelektrik etki, düşük enerjili fotonların madde tarafından güçlü bir şekilde soğurulmasına neden olur. Enerji arttıkça (örn. 2 keV, 3 keV, 4 keV), katsayılar düşüş göstermektedir. Orta enerjiler için belirli enerji eşiklerinde (örneğin, 8,91E-03 MeV'de Cu(29) için 125,893'ten 1,00E-02 MeV'de 92,320'ye düşüş), absorpsiyon kenarları (K, L kenarları) görülebilir. Bu, malzemeyi oluşturan elementlerin atomlarının iç yörünge elektronlarını iyonlaştırmak için gerekli enerji eşiklerinde soğurma katsayısında ani artışlar veya azalmalar anlamına gelir. Örneğin, 1,96E-02 MeV'de Mo(42) için 14,825 ve hemen ardından 2,21E-02 MeV'de Ag(47) için 66,003'e ani sıçrama, farklı elementlerin K-kenarlarının farklı enerjilerde olduğunu

göstermektedir. Yüksek Enerjiler için enerji arttıkça (örneğin 1 MeV ve üzeri), soğurma katsayıları belirgin şekilde düşer ve daha stabil hale gelir. Bu bölgede Compton saçılması ve çok yüksek enerjilerde çift oluşumu gibi etkileşimler baskın hale gelir. Özellikle 10 MeV'den sonra katsayıların tekrar hafifçe yükseldiği görülmektedir. Bu olayda çift oluşumu etkileşiminin artan enerjilerle daha belirgin hale gelmeye başladığını gösterebilir (Teli ve ark., 2001).

Şekil 2'de verilen grafik incelendiğinde, verilerin, başlangıçta enerji seviyesinin çok düşük olduğu 1,00 E-03 MeV gibi küçük enerjilerde soğurma katsayısının oldukça yüksek (61921,466) olduğunu ve enerji arttıkça bu değerin önemli bir şekilde azaldığını göstermektedir. Örneğin, enerji 5 MeV'ye ulaştığında soğurma katsayısı yalnızca 0,402 cm^{-1}'e düştüğü görülmektedir. Bu düşüş, maddenin ışığı emme kapasitesinin, özellikle yüksek enerjilerde önemli ölçüde azaldığını gösterir. Enerjinin arttığı aralıkta, soğurma katsayısının daha istikrarlı bir hal aldığını görmek mümkündür. 1 MeV civarındaki enerjilerde, lineer soğurma katsayısı hızla azalırken, daha yüksek enerjilerde (100 MeV gibi) bu azalma daha düz bir eğilim izler. Örneğin, 1 MeV ile 100 MeV arasında soğurma katsayısının sadece 0,679 ile 0,721 cm^{-1} arasında değişmesi, madde ile etkileşimlerin daha az belirginleştiği bir durumu yansıtır. Bu değişim, fotonların enerji seviyesinin arttıkça maddenin daha az etkileşime girmesi ve daha derine nüfuz etmesiyle açıklanabilir (Sitamahalakshmi ve ark., 2015).

Bu eğilim, daha yüksek enerjili parçacıkların maddede daha az soğurulmasını sağlayan fiziksel prensiplere dayanır. İleri düzeyde, yüksek enerji fotonlarının daha derinlere nüfuz edebilmesi, tıbbi radyasyon tedavisi ve nükleer endüstrilerdeki güvenlik protokollerinin tasarımında önemli bir rol oynar. Aynı şekilde, bu tür veriler, malzeme biliminde, özellikle zayıf soğurucu

özelliklere sahip yeni malzemelerin tasarımı ve geliştirilmesinde de kullanılır (Prasad ve ark., 1998; Hubbel 1999).

Bununla birlikte, enerjinin arttığı her bölgede kütle ve lineer soğurma katsayısındaki değişim, maddenin atomik yapısına, yoğunluğuna ve kimyasal bileşimine bağlı olarak farklılık gösterebilir. Bu bağlamda, enerji ve soğurma katsayısı verilerinin her bir spesifik uygulama için dikkatlice incelenmesi, doğru tasarımlar ve güvenlik önlemleri için kritik öneme sahiptir.

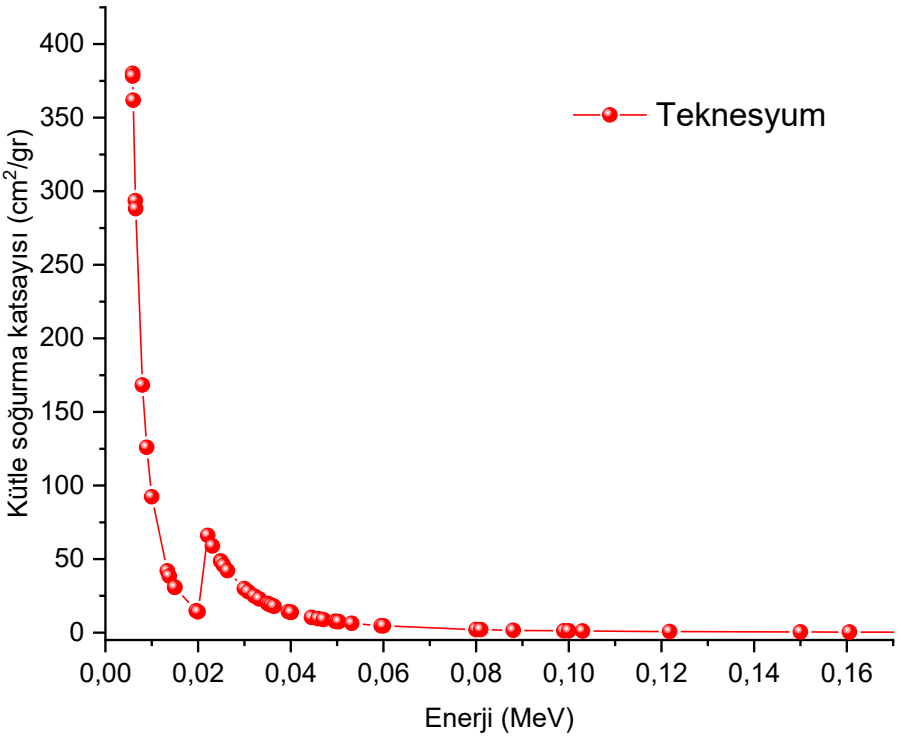

Şekil1. Teknesyuma ait kütle soğurma katsayının enerjiye göre değişim grafiği

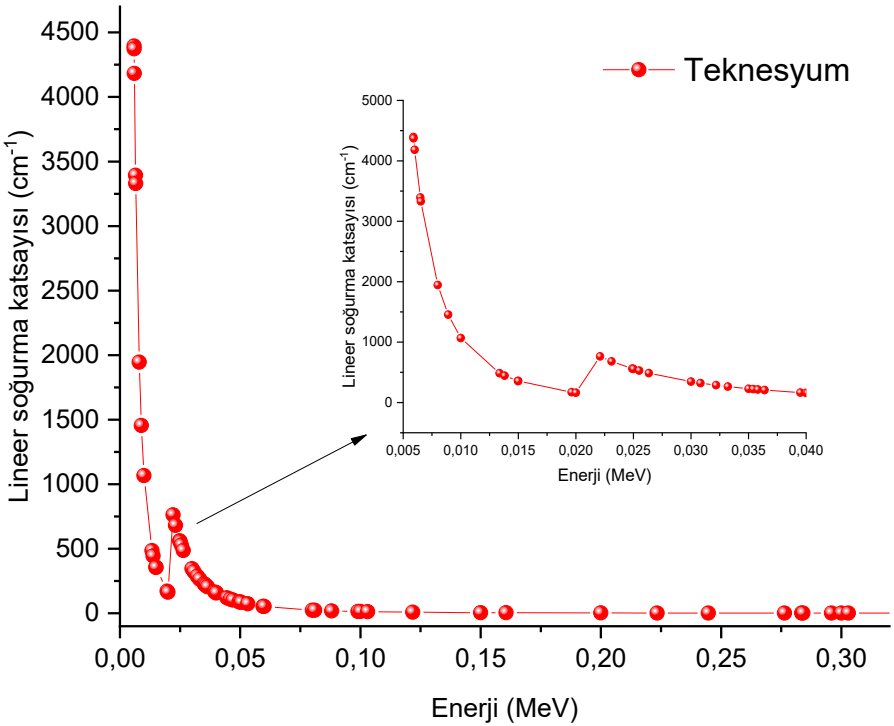

Şekil2. Teknesyuma ait lineer soğurma katsayının enerjiye göre değişim grafiği

Enerji ve lineer soğurma katsayısı arasındaki ilişki, özellikle fiziksel ve mühendislik bilimlerinde önemli bir yer tutar. Bu ilişki, ışığın ya da diğer elektromanyetik dalgaların bir madde içindeki zayıflama sürecini açıklamak için kullanılır. Soğurma katsayısı, bir ışın veya parçacığın maddeden geçerken ne kadar zayıfladığını belirler ve bu zayıflama, genellikle enerji seviyesinin bir fonksiyonu olarak incelenir.

Belirli enerji seviyelerine karşılık gelen kütle ve lineer soğurma katsayısı veri analizleri, çeşitli uygulamalarda, örneğin tıbbi görüntüleme, nükleer santrallerde güvenlik analizi ve

malzeme bilimi gibi alanlarda büyük önem taşır. Mevcut veriler, enerjinin artmasıyla birlikte soğurma katsayısının nasıl değiştiğini gözler önüne serer. Enerji seviyesinin düşük olduğu bölgelerde (1 keV civarında), soğurma katsayısı çok yüksek değerler gösterirken, enerji arttıkça bu katsayının düşme eğiliminde olduğu gözlemlenmektedir.

Elde edilen veriler ışığında Tc elementinin Phy-X verilerine dayanan kütle soğurma özellikleri dikkate alındığında, çeşitli enerji depolama sistemleri için uygunluk gösterdiği söylenebilir. Düşük enerji aralığında yüksek fotoelektrik etkileşim kapasitesine sahip olan Tc, özellikle Am-241 gibi izotoplarla çalışan termoelektrik jeneratörlerde radyasyon kaynaklı enerji depolama amacıyla kullanılabilir. Compton saçılmasının baskın olduğu orta enerji aralığında ise Tc, kararlı performansı sayesinde uzun ömürlü nükleer batarya teknolojileri için uygun bir malzeme adayıdır. Yoğun radyasyon içeren ortamlar için tasarlanan uzay ve savunma sanayi uygulamalarında, Tc'nin sabit soğurma karakteri sayesinde hem gelişmiş radyasyon koruması sağlanabilir hem de radyasyonun kontrollü biçimde enerjiye dönüştürülmesi mümkün olabilir.

Sonuç olarak, enerji ve kütle ve lineer soğurma katsayısı arasındaki ilişki, ışığın ya da diğer elektromanyetik dalgaların bir madde ile etkileşiminde önemli bir rol oynar. Bu ilişkinin doğru anlaşılması, bilimsel ve mühendislik alanlarında uygulama yaparken daha verimli ve güvenli çözümler sunmak adına büyük bir avantaj sağlar. Gelecekte yapılacak çalışmalarda, Tc izotoplarının farklı kimyasal bileşenler içinde kullanımı, nanoyapılarla etkileşimi ve biyouyumlu sistemlerle entegrasyonu gibi araştırma alanlarına odaklanılmasına ve bu sayede, daha verimli ve uzun ömürlü enerji depolama teknolojilerinin geliştirilmesine katkı sağlanabilir.

KAYNAKLAR

Agar, O., Sayyed, M. I., Akman, F., Tekin, H. O., & Kaçal, M. R. (2019). An extensive investigation on gamma ray shielding features of Pd/Ag-based alloys. Nuclear Engineering and Technology, 51(3), 853–859. https://doi.org/10.1016/j.net.2018.12.014

Bertin, E.P. (1975). Principles and Practice of X-Ray Spectrometric Analysis. 2nd Edition, Plenum Pres, New York, 1079s.

Hubbell, J. H. (1999). Review of photon interaction cross section data in the medical and biological context. Physics in Medicine and Biology, 44(1). https://doi.org/10.1088/0031-9155/44/1/001

İçelli, O. (2002). "Bazı Bileşik ve Kristallerde Lineer Diferansiyel Saçılma Katsayılarının Açısal dağılımının Ölçülmesi ve Etkin Atom numarasına Göre Değişiminin İncelenmesi", Yüksek Lisans Tezi, Fen Bilimleri Enstitüsü, Atatürk Üniversitesi, Erzurum, Türkiye.

Teli, M.T., Mahajan C.S. and Nathuram, R. (2001). Measurement of mass and linear attenuation coefficients of gamma-rays for various elements through aqueous solution of salts. *Indian J. Pure Appl. Phys*., 39(12), 816–824.

Sitamahalakshmi N.V., Kareem, M.A. and Premachand, K. (2015). Total photon attenuation coefficients in some rare earth elements using selective excitation method. *Radiat. Phys. Chem*., 106, 160– 164.

Prasad, S.G. Parthasaradhi, K. and Bloomer, W.D. (1998). Effective atomic numbers for photoabsorption in alloys in the energy region of absorption edges Radiation Physics and Chemistry Pergamon.

Hubbell, J.H. (1999). Review of photon interaction cross section data in the medical and biological context. *Phys. Med. Biol*., 44(1).

Özpolat, F., Alım, B., Şakar, E., Büyükyıldız, M. and Kurudirek, M. (2020). Phy-X/ZeXTRa: a software for robust calculation of effective atomic numbers for photon, electron, proton, alpha particle, and carbon ion interactions," Radiat. Environ. Biophys., vol. 59, no. 2, pp. 321–329.

Sayyed, M. I., Lakshminarayana, G., Dong, M. G., Ersundu, M. Ç., Ersundu, A. E., & Kityk, I. V. (2018). Investigation on gamma and neutron radiation shielding parameters for BaO/SrO–Bi2O3–B2O3 glasses. Radiation Physics and Chemistry, 145, 26–33.

https://doi.org/10.1016/j.radphyschem.2017.12.010

Şakar, E., Özpolat, Ö.F., Alım, B. Sayyed, M.I. and Kurudirek, M. (2020). Phy-X/ PSD: Development of a user friendly online software for calculation of parameters relevant to radiation shielding and dosimetry. *Radiat. Phys. Chem*., 166.

ODYOMETRİ CİHAZLARINDA KULLANILAN CoCrMo, CoNiCrMo ve TiNi BİYOMALZEMELERİN KÜTLE VE LİNEER SOĞURMA KATSAYILARININ HESAPLANMASI

Şeyma BİBER TEMİRCİK[1]

1. Giriş

Odyometri; işitme sisteminin hassasiyetini, sesleri algılama eşiğini ve frekanslara karşı yanıtını ölçen bir tanı yöntemidir. Odyometrik testlerde elde edilen veriler, işitme kaybının derecesi, tipi ve tedaviye uygunluğunu belirlemede kullanılır. Bu bağlamda, işitme cihazları ve koklear implant gibi yardımcı teknolojiler, odyometrik değerlendirme sonucunda bireye özgü olarak seçilen ve vücuda kısmen ya da tamamen entegre edilen biyomedikal cihazlardır.

Bu cihazlarda kullanılan biyomalzemeler, sadece mekanik dayanım ve biyouyumluluk açısından değil; aynı zamanda akustik performans, elektriksel iletkenlik, mikroelektronikle uyum ve son dönemde önemi artan radyasyon etkileşimi gibi kriterler bakımından da titizlikle seçilmektedir.

Biyomedikal alanındaki ilerlemelerle birlikte, canlı organizmalarla etkileşime giren malzemelerin biyolojik sistemlerle tam bir uyum içinde çalışması gerekliliği daha da ön plana

[1] Dr.,Kahramanmaraş Sütçü İmam Üniversitesi, Fen-Edebiyat Fakültesi, Fizik Bölümü, Kahramanmaraş/Türkiye, Orcid: 0000-0003-1650-6666, seymabiber@hotmail.com

çıkmıştır. Biyolojik ortama yerleştirilen bir malzemenin güvenilir, etkili ve biyouyumlu olması; hem hasta sağlığı hem de tedavi başarısı açısından kritik öneme sahiptir. Bu nedenle, biyomalzemelerin geliştirilmesi sürecinde biyolojik sistemlerle uyumlu çalışmaları ve olası yan etkilerin en aza indirilmesi amacıyla yoğun araştırma ve geliştirme faaliyetleri yürütülmektedir.

Biyomalzemeler; insan vücudundaki bozulmuş ya da işlevini yitirmiş dokuların ve organların yerine geçmek, bu yapıları desteklemek veya vücut fonksiyonlarını restore etmek amacıyla kullanılan özel malzemelerdir. Bu malzemeler, çoğu zaman uzun süreli ya da kesintili olarak vücut sıvılarıyla doğrudan temas hâlindedir. Gelişen teknoloji ve artan sağlık ihtiyaçları doğrultusunda, biyomalzemelerin kullanım alanları da her geçen gün genişlemekte; yalnızca protez uygulamalarıyla sınırlı kalmayıp, ekstrakorporeal cihazlardan (vücut dışında yer alan fakat vücutla etkileşim hâlinde çalışan sistemler) eczacılık ürünlerine ve tanı kitlerine kadar geniş bir yelpazeye yayılmaktadır (Gümüşderelioğlu, 2002). Bununla birlikte, biyomalzemelerle ilgili halen çözüm bekleyen önemli sorunlar da mevcuttur. Bu sorunlar arasında düşük biyouyumluluk, metal iyonu salımı kaynaklı alerjik reaksiyonlar, korozyon, yüksek yoğunluk, dokulara kıyasla yüksek sertlik gibi dezavantajlar öne çıkmaktadır. Söz konusu problemlerin üstesinden gelebilmek için doku mühendisliği, gen tedavisi gibi yenilikçi yöntemlerin yanı sıra, nanoteknoloji, bilişim teknolojileri ve ileri imalat tekniklerindeki gelişmeler, yeni nesil biyomalzemelerin geliştirilmesine olanak tanımaktadır.

Bu zorluklara rağmen, üstün mekanik özellikleri, kristal yapıları ve güçlü metalik bağları sayesinde metal ve alaşım temelli biyomalzemeler, biyomedikal uygulamalarda önemli bir yer tutmaktadır. Özellikle titanyum ve titanyum alaşımları, paslanmaz

çelikler, kobalt, altın gibi metaller ve bunların kombinasyonları; hem dayanıklılık hem de işlenebilirlik açısından avantaj sağlamaktadır. Bu malzemeler; ortopedik cerrahide eklem protezlerinden kemik yenileme sistemlerine, yüz ve çene cerrahisinden diş implantlarına, kalp kapakçıkları, yapay damarlar ve kateterler gibi kardiyovasküler uygulamalara kadar birçok farklı alanda yaygın şekilde kullanılmaktadır. Ayrıca, tanı ve tedaviye yönelik biyomedikal cihazların üretiminde de bu metalik biyomalzemeler sıklıkla tercih edilmektedir.

Odyolojik cihazlar, özellikle koklear implantlar gibi vücut içine yerleştirilen sistemler olduğunda, iyonlaştırıcı radyasyonla etkileşime girebilir. Örneğin, Bilgisayarlı Tomografide bulunan X-ışını kaynağı 40 keV ile 140 keV arasında geniş bir enerji spektrumuna sahip foton yaydığı belirtilmiştir (Demir, 2024). Radyoterapi gibi durumlarda hasta baş-boyun bölgesinden ışınlanıyorsa bu implantlar doğrudan doz absorpsiyonuna maruz kalabilir. Yüksek enerjili radyasyon, implantın içindeki entegre devrelerde bozulmalara yol açabilir. Bu nedenle cihazlar genellikle radyasyon koruyucu olarak tasarlanmalıdır. Örneğin, titanyum gibi yüksek atom numaralı metalik malzemeler, çevre dokuya göre daha fazla radyasyon soğurabilir (yüksek lineer soğurma katsayısına sahiptir). Bu durum radyasyon doz soğurumuna yol oluşturabilir. Ayrıca radyasyonun neden olduğu malzeme içi mikrohasarlar, özellikle polimerlerde ses iletimini bozabilir. Bu durum cihazın iletim performansını düşürebilir.

Sonuç olarak, biyomalzemelerin gelişimi, biyomedikal mühendislik ile malzeme biliminin kesişiminde yer alan disiplinlerarası bir alandır. Bu alandaki ilerlemeler, yalnızca tıbbi başarıyı değil, hastaların yaşam kalitesini de doğrudan etkilemektedir. Bu nedenle, biyomalzeme araştırmaları, gelecekte

daha güvenli, etkili ve kişiye özel sağlık çözümlerinin önünü açma potansiyeline sahiptir.

İşitme cihazlarında yaygın olarak kullanılan CoCrMo, CoNiCrMo ve TiNi alaşımlarının elektromanyetik radyasyonla etkileşim özelliklerini değerlendirmek amacıyla, fotonların bu biyomalzemeler içerisindeki zayıflatılma düzeyleri, kütle soğurma katsayısı (μ/ρ) ve lineer soğurma katsayısı (μ) cinsinden incelenmiştir. XCOM veritabanı kullanılarak, 5,9 keV, 17 keV, 26 keV, 40 keV ve 59,543 keV'lik enerji seviyeleri için teorik μ/ρ değerleri elde edilmiş ve bu değerler ilgili alaşımların gerçek yoğunlukları (sırasıyla 8,3 g/cm³, 9,2 g/cm³ ve 6,7 g/cm³) ile çarpılarak lineer soğurma katsayıları hesaplanmıştır. Bulgular, bu malzemelerin ışın geçirgenlik özelliklerini ve işitme cihazlarındaki uygulama potansiyellerini ortaya koymaktadır.

İşitme cihazlarında kullanılan biyomalzemeler, elektromanyetik radyasyonla etkileşim düzeylerine göre hem biyolojik güvenlik hem de cihaz performansı açısından değerlendirilmelidir. Bu etkileşim, özellikle X-ışınları gibi iyonlaştırıcı radyasyon altında, materyalin elektromanyetik enerjiyi ne ölçüde soğurduğu ile ilişkilidir. Bu bağlamda, kütle soğurma katsayısı (μ/ρ) ve lineer soğurma katsayısı (μ), fotonların materyal içindeki sönümlenme derecesini ifade eden kritik parametrelerdir. İşitme cihazlarında yapısal veya destekleyici bileşenlerde tercih edilen üç temel alaşımın bu parametreleri detaylı şekilde hesaplanmıştır.

1.1. Biyomalzemelerin Radyasyon Soğurma Özellikleri

Biyomalzemelerin biyouyumluluk, mekanik dayanıklılık ve korozyon direncinin yanı sıra, özellikle tanı ve tedavi amaçlı kullanılan radyasyon temelli biyomedikal uygulamalarda

radyasyonla etkileşim özellikleri de büyük önem taşımaktadır. Gelişen nükleer tıp, radyoterapi ve tıbbi görüntüleme tekniklerinde (özellikle X-ışını, gama ışını ve proton tedavisi gibi uygulamalarda), kullanılan implantların ve cihaz malzemelerinin radyasyonu nasıl soğurduğu, hem tedavi etkinliği hem de hasta güvenliği açısından belirleyici rol oynar.

Radyasyonun bir malzeme içerisindeki zayıflama miktarı, genellikle kütle soğurma katsayısı (μ/ρ) ve lineer soğurma katsayısı (μ) gibi parametrelerle ifade edilir. Bu parametreler, biyomalzemenin yapısal bileşimi (atom numarası, yoğunluk, bağ yapısı) ile doğrudan ilişkilidir. Yüksek atom numaralı elementler içeren metalik biyomalzemeler, özellikle düşük enerjili fotonlara karşı daha yüksek soğurma eğilimi gösterirler. Bu özellik, Tanısal Görüntüleme (Röntgen, BT) için yüksek radyasyon soğuruculuğa sahip malzemeler, görüntüleme sırasında artefakt oluşturabilir. Bu nedenle kullanılan biyomalzemenin, tanı kalitesini düşürmeyecek şekilde seçilmesi gerekir. Ayrıca Radyoterapi esnasında radyasyonla tedavi edilen kanser vakalarında, vücutta bulunan bir implantın radyasyon doz dağılımını değiştirmesi, tedavi başarısını etkileyebilir. Bu etkileşim malzemenin doz modülasyonu yapmasına neden olabilir. Nükleer tıp uygulamalarında ise radyoizotopların kullanıldığı teşhis ve tedavi prosedürlerinde, biyomalzemelerin bu radyonüklitlerle etkileşimi, doz dağılımı ve etkililik açısından değerlendirilmelidir.

2. Yöntem

2.1. Biyomalzeme Bileşimleri

Biyomalzemelerde sık kullanılan alaşımlar arasından CoCrMo (%60 Co, %30 Cr, %10 Mo) yoğunluk değeri 8,3 g/cm^3, CoNiCrMo (%40 Co, %20 Ni, %20 Cr, %20 Mo) 9,2 g/cm^3, TiNi (%55 Ti, %45 Ni) 6,7 g/cm^3'tür (Pasinli, 2004)

2.2. Soğurma Katsayılarının Hesaplanması

XCOM (NIST) veri tabanından alınan μ/ρ (cm^2/g) değerleri kullanılarak her bir alaşım için lineer soğurma katsayısı (μ) formül 4 ve 5 ile hesaplanmıştır. Gama ışınları alfa ve beta parçacıklarından farklı olarak, bir tek elementer olayda enerjilerine ve düştüğü maddenin özelliğine göre enerjisinin büyük bir kısmını, çoğu zaman tamamını kaybeder. İçinden geçtiği maddenin hangi atomunun civarında bu kaybın olacağı tamamen ihtimale bağlıdır. Bu sebeple gama ışınlarının madde tarafından soğurulmasında radyoaktif bozunma kanunlarına benzer bir kanun geçerlidir. Maddenin küçük bir dx kalınlığında absorblanan dI ışın şiddeti, bu kalınlığa giren I şiddeti ile orantılıdır.

I_o şiddetinde paralel bir γ-ışını demeti t (cm) kalınlığında, ρ (gr/cm^3) yoğunluğunda homojen bir soğurucu üzerine gönderildiğinde soğurucudan geçen γ-ışını demetinin şiddeti I olur, her zaman I_0'dan küçüktür. Bu da γ-ışınlarının maddeden geçerken güç yitirdiğini ya da soğrulmaya maruz kaldığını gösterir. Şekil 1 Burada γ-ışını şiddetindeki azalma dI ise,

$$\frac{dI}{I} = -\mu dt \qquad [1]$$

eşitliği ile verilir. Burada μ lineer soğurma katsayısı ve birimi cm^{-1}'dir. Negatif işaret, γ-ışının maddeyi geçerken şiddetinde azalma olduğunu gösterir. Eşitlik 1 ifadesi düzenlenerek;

$$I = I_0 \, exp\,(-\mu t) \qquad [2]$$

olur. Bu ifade "Lambert Kanunu" olarak bilinmektedir (Bertin, 1975).

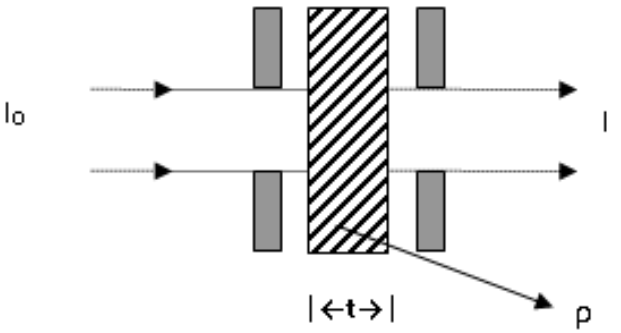

Şekil 1. γ-ışının Soğrulması (Bertin, 1975)

Soğurma katsayılarını eşitlik 2'ye göre ifade edilecek olunursa; Lineer soğurma katsayısı birim kalınlık başına birim alanda belirlenen soğrulmadır. μ ile gösterilir ve birim 1/cm'dir. Eşitlik 2'nin, logaritması alınırsa,

$$\mu = \frac{ln\frac{I_0}{I}}{t} \qquad [3]$$

olur.

Kütle soğurma katsayısı, birim kütlede birim alanda belirlenen soğrulmadır. μ_m ile gösterilir (Hubbell, 1999).

$$\mu_m = \frac{\mu}{\rho} \qquad [4]$$

Denklem (4)'de ρ yoğunluk(g/cm^3), μ_m elementin kütle soğurma katsayısıdır, birim cm^2/g'dir.

Geçirme katsayılarının hesaplanması soğurma deneylerinde

soğurucu materyalin belli bir kalınlıktan daha ince olması ki bu durumda bütün parçacıklar soğurucu materyali geçer ve belli bir kalınlıktan daha kalın ise parçacıklar bütün enerjisini kaybeder ve soğurucu materyalden çıkamaz (İçelli, 2002).

Radyasyona maruz kalan malzemenin yarı değer katman kalınlığı (HVL), malzemeye gelen radyasyon şiddetini yarıya indiren kalınlık, ondabir değer katman kalınlığı (TVL) ise 1/10 oranında azaltan kalınlık olarak ifade edilir (Agar ve ark., 2019; Sayyed ve ark., 2018). HVL ve TVL değerleri Denklem (5) ve (6) kullanılarak program tarafından hesaplanmıştır.

$$\mathrm{HVL} = \frac{\mathrm{In2}}{Lineer\ soğurma\ katsayısı} \quad [5]$$

$$\mathrm{TVL} = \frac{\mathrm{In10}}{Lineer\ soğurma\ katsayısı} \quad [6]$$

3. Bulgular ve Tartışma

Odyometri cihazlarında kullanılan CoCrMr, CrNiCrMo VE TiNi biyomalzemelerin kütle soğurma katsayısı, lineer soğurma katsayısı, HVL ve TVL değerleri farklı foton enerjileri kullanılarak 5,9 keV,17 keV, 26 keV, 40 keV ve 59,543 keV enerjilerde hesaplanmış ve Tablo 1'de listelenmiştir. Bu enerjiler seçilerken medikal öneme sahip özellikle Bilgisayarlı Tomografi cihazlarında kullanılan 40 keV civarı enerjiler olmasına odaklanılmıştır.

Tablo 1. *CoCrMo, CoNiCrMo ve TiNi biyomalzemelere ait HVL, TVL kütle soğurma ve lineer soğurma katsayıları*

Enerji [keV]	Alaşım	Kütle Soğurma Katsayısı [cm^2/g]	Lineer Soğurma Katsayısı [cm^{-1}]	HVL [cm]	TVL [cm]
5,9	CoCrMo	208,6	1731	0,0004	0,00133
	CoNiCrMo	187,7	1726	0,000402	0,001334
	TiNi	267,5	1792	0,000387	0,001285
17	CoCrMo	29,99	248,917	0,002785	0,00925
	CoNiCrMo	34,48	317,216	0,002185	0,007259
	TiNi	39,03	261,501	0,002651	0,008805
26	CoCrMo	27,51	228,333	0,003036	0,010084
	CoNiCrMo	24,85	228,621	0,003032	0,010072
	TiNi	11,89	79,663	0,008701	0,028904
40	CoCrMo	7,852	65,171	0,010636	0,035331
	CoNiCrMo	7,134	65,632	0,010561	0,035083
	TiNi	3,528	23,637	0,029325	0,097414
59,543	CoCrMo	2,6	21,224	0,032659	0,10849
	CoNiCrMo	2,4	22,144	0,031302	0,103982
	TiNi	1,2	8,04	0,086212	0,286391

CoCrMo, CoNiCrMo ve TiNi alaşımlarının 5,9 keV ile 59,543 keV arasındaki enerji seviyelerinde kütle ve lineer soğurma katsayısı (μ) Şekil 2 ve Şekil 3'de verilmiştir. CoNiCrMo alaşımı tüm enerji seviyelerinde en yüksek soğurma kapasitesine sahiptir. TiNi, özellikle yüksek enerjilerde en düşük soğurma katsayısı ile en geçirgen yapıyı sergilemektedir.

Enerji arttıkça tüm malzemelerin soğurma katsayısında belirgin bir azalma görülmekte, bu da fotonların malzeme içinde daha fazla nüfuz ettiğini göstermektedir. CoNiCrMo alaşımı tüm enerji seviyelerinde en yüksek soğurma kapasitesine sahiptir. TiNi,

özellikle yüksek enerjilerde en düşük soğurma katsayısı ile en geçirgen yapıyı sergilemektedir.

Enerji arttıkça tüm malzemelerin soğurma katsayısında belirgin bir azalma görülmekte, bu da fotonların malzeme içinde daha fazla nüfuz ettiğini göstermektedir.

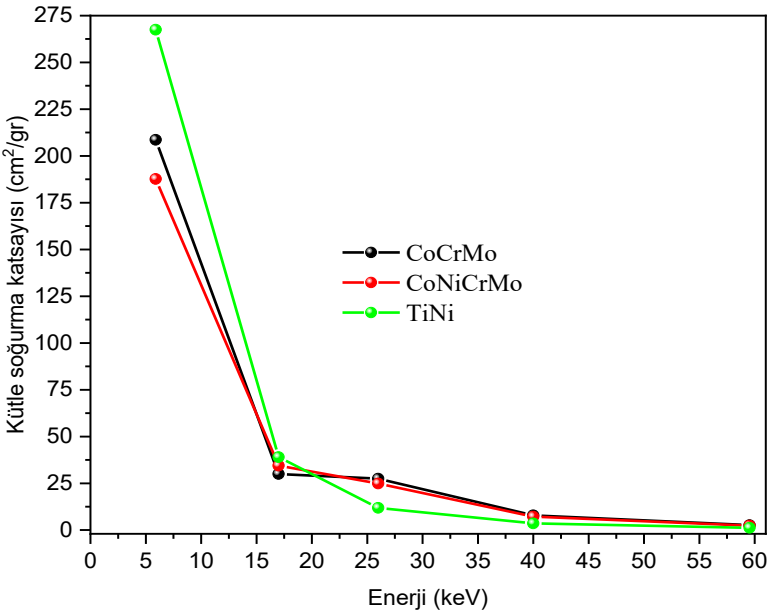

Şekil 2. 5,9 keV,*17 keV, 26 keV,40 keV ve 59,543 keV'de kütle soğurma katsayıları*

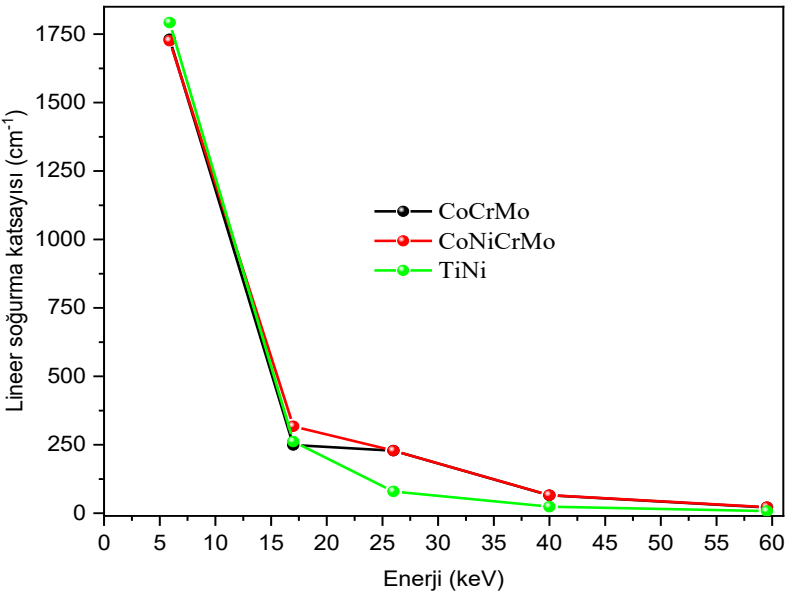

Şekil 3. 5,9 keV,*17 keV, 26 keV,40 keV ve 59,543 keV'de lineer soğurma katsayıları*

Elde edilen veriler, yüksek yoğunluklu ve çok bileşenli alaşımların elektromanyetik radyasyonu daha etkili bir şekilde soğurduğunu göstermektedir. Özellikle CoNiCrMo alaşımı, içerdiği nikel ve molibden nedeniyle yüksek μ/ρ değerlerine sahiptir ve yoğunluğunun da yüksek olması nedeniyle, lineer soğurma katsayısı en yüksek olan materyal olarak öne çıkmaktadır. Bu durum, radyasyonun etkili şekilde sönümlenmesini sağlar ve biyomedikal uygulamalarda koruyucu bir yapı görevi görebileceğini gösterir.

TiNi alaşımı ise daha düşük yoğunluğu ve buna bağlı olarak daha düşük lineer soğurma katsayısı ile hafiflik ve esneklik gibi avantajlar sunarken, elektromanyetik geçirgenliği daha yüksektir.

Bu da onu düşük radyasyon gereksinimi olan uygulamalarda avantajlı kılabilir.

Bu veriler ışığında, yüksek atom numarasına ve yoğunluğa sahip alaşımların, özellikle düşük enerjili fotonlarla çalışılan durumlarda daha fazla radyasyon soğurduğu görülmektedir. Bu durumun, tanı ve tedavi amaçlı kullanılan radyasyon kaynakları ile etkileşime giren biyomalzemelerde dikkate alınması, hem hastanın hem de görüntüleme kalitesinin korunması açısından kritik öneme sahiptir.

5. Sonuç

CoCrMo, CoNiCrMo ve TiNi alaşımlarının elektromanyetik radyasyonla etkileşimleri, yoğunluklarına ve içeriklerine bağlı olarak farklılık göstermektedir. CoNiCrMo, yüksek lineer soğurma katsayısı ile elektromanyetik ekranlama açısından en etkili malzeme olarak öne çıkarken, TiNi, daha hafif ve geçirgen bir yapıya sahiptir. Bu sonuçlar, işitme cihazları gibi biyomedikal uygulamalarda malzeme seçiminde yalnızca mekanik ve biyouyumluluk değil, aynı zamanda elektromanyetik soğurma özelliklerinin de dikkate alınması gerektiğini ortaya koymaktadır.

İşitme sistemine entegre edilen biyomalzemelerin radyasyonla olan etkileşimleri, odyolojik performans, güvenlik ve cihaz ömrü açısından stratejik önemdedir. Özellikle radyasyon tedavisi gören veya nükleer görüntülemeye maruz kalan hastalarda, bu biyomalzemelerin radyasyon soğurma katsayıları dikkate alınmalıdır. Gelecekte nanokompozit malzemeler, akustik-mekanik adaptasyonu optimize ederken aynı zamanda elektromanyetik ve radyasyon koruması sağlayabilir. Bu da kişiye özel, daha hassas ve uzun ömürlü işitme cihazlarının geliştirilmesine olanak tanıyacaktır.

KAYNAKLAR

Agar, O., Sayyed, M. I., Akman, F., Tekin, H. O., & Kaçal, M. R. (2019). An extensive investigation on gamma ray shielding features of Pd/Ag-based alloys. Nuclear Engineering and Technology, 51(3), 853–859. https://doi.org/10.1016/j.net.2018.12.014

Bertin, E.P. (1975). Principles and Practice of X-Ray Spectrometric Analysis. 2nd Edition, Plenum Pres, New York, 1079s.

Demir, M. (2024) Nükleer Tıp Fiziği ve Klinik Uygulamaları E-İstanbul Üniversitesi–Cerrahpaşa Üniversite Yayınevi Seri No: 80 ISBN: 978-605-7880-99-4

Gümüşderelioğlu, M., (2002). Biyomalzemeler. *Bilim ve Teknik Dergisi*, TÜBİTAK, Temmuz özel sayısı, 2002.

Hubbell, J. H. (1999). Review of photon interaction cross section data in the medical and biological context. Physics in Medicine and Biology, 44(1). https://doi.org/10.1088/0031-9155/44/1/001

İçelli, O. (2002). "Bazı Bileşik ve Kristallerde Lineer Diferansiyel Saçılma Katsayılarının Açısal dağılımının Ölçülmesi ve Etkin Atom numarasına Göre Değişiminin İncelenmesi", Yüksek Lisans Tezi, Fen Bilimleri Enstitüsü, Atatürk Üniversitesi, Erzurum, Türkiye.

Park, J.B., Kim, Y.K., (2000). *Metallic Biomaterials*. The Biomedical Engineering Handbook:Second Edition. CRC Press LLC, 2000.

Pasinli, A. (2004). Biyomedikal Uygulamalarda Kullanılan Biyomalzemeler Makine Teknolojileri *Elektronik Dergisi,* (4) 25-34.

Sayyed, M. I., Lakshminarayana, G., Dong, M. G., Ersundu, M. Ç., Ersundu, A. E., & Kityk, I. V. (2018). Investigation on gamma and neutron radiation shielding parameters for BaO/SrO–Bi2O3–B2O3 glasses. Radiation Physics and Chemistry, 145, 26–33. https://doi.org/10.1016/j.radphyschem.2017.12.010

CHAPTER 5

CHEMICAL BONDING AND MOLECULAR INTERACTIONS

FATMAGÜL TUNÇ[1]

Introduction

Chemical bonds and molecular interactions are fundamental forces that determine the relationships between atoms and molecules that constitute matter. These forces shape the physical and chemical properties of molecules—everything from a substance's hardness and boiling point to its reactivity and biological functions depends on them. In this section, chemical bonds are categories as ionic, coordiate covalent, and metallic, while molecular interactions are examined in terms of Van der Waals forces, hydrogen bonds, and ion-dipole interactions.

Chemical Bonding

A chemical bond refers to the interaction that binds atoms together within a molecule (IUPAC, 1997). Chemical bonds form to achieve the most stable electron arrangement, which corresponds to a filled outermost electron shell.

[1] Assist. Prof. Dr., Artvin Coruh University, Vocational High School of Health Services, Artvin/TURKIYE, Orcid: 0000-0003-3700-450X

There are two main mechanisms through which atoms achieve a stable electronic configuration, by the transfer or the sharing of electrons. Ionic bonds result from the transfer of one or more electrons from one atom to another. As a result, charged ions are formed and subsequently stabilized through electrostatic interactions. Conversely, covalent bonds arise when atoms share one or more pairs of electrons. It is important to note that these bonding types represent idealized extremes. In practice, many chemical bonds exhibit a combination of characteristics, displaying a partial ionic or covalent nature. For most elements, atoms in a bonded state attain a more stable, lower-energy configuration compared to their unbonded counterparts in the ground state. This implies that bond formation leads to a lower energy state and the release of energy. Therefore, creation of chemical bonds is an exothermic reaction. On the other hand, breaking chemical bonds requires an input of energy, thereby making processes such as pyrolysis endothermic in nature.

Atoms are composed of a central nucleus—containing positively charged protons and electrically neutral neutrons—surrounded by electrons in continuous motion (IUPAC, 1997). These electrons occupy distinct energy levels, commonly identified as electron shells or orbitals. Each shell corresponds to a specific energy level and can accommodate a fixed number of electrons. Table 1 illustrates the principal electron shells and their maximum electron capacities.

Table 1. Electron shells and their associated properties

Shell number	Type of orbital	Orbital electron capacity	Shell electron capacity	Total electron capacity
1	s	2	2	2
2	s	2	8	10
	p	6		
3	s	2	18	28
	p	6		
	d	10		
4	s	2	32	60
	p	6		
	d	10		
	f	14		
5	s	2	32	92
	p	6		
	d	10		
	f	14		
6	s	2	18	110
	p	6		
	d	10		
7	s	2	8	118
	p	6		

Each ground-state atom possesses a unique electronic configuration. This configuration can be determined from the periodic table of elements (Figure 1). The number of electron shells in an atom corresponds to its row in the periodic table. For example, hydrogen (H) and helium (He) have one shell, carbon (C) has two shells, and sodium (Na) has three shells. The outermost shell of an atom is referred to as the valence shell, and it determines the atom's bonding characteristics. The column number indicates the number of electrons in the outermost orbital of the valence shell. The electronic configurations of some ground-state atoms are as follows (Figure 2 provides the relevant diagrammatic representations):

Figure 1. *Periodic table of elements*

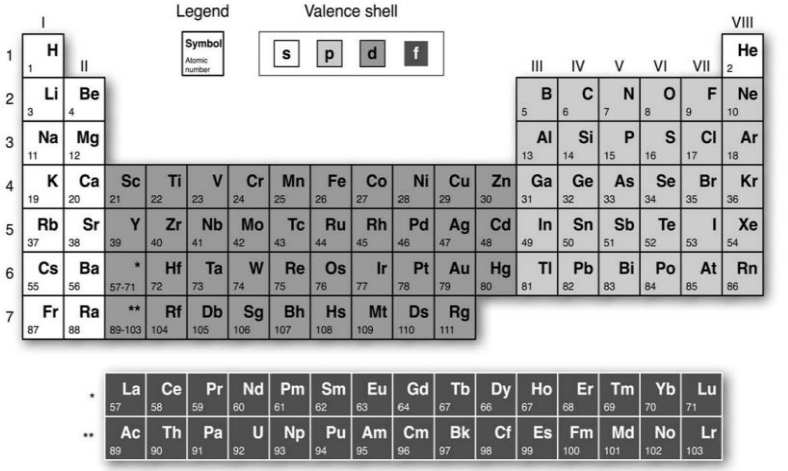

Hydrogen: $1s^1$

Carbon: $1s^2\ 2s^2\ 2p^2$

Neon: $1s^2\ 2s^2\ 2p^6$

Oxygen: $1s^2\ 2s^2\ 2p^4$

Chlorine: $1s^2\ 2s^2\ 2p^6\ 3s^2\ 3p^5$

Note: For transition metals and inner transition metals, the relationship between group number and valence electron count is more complex due to the involvement of d- and f-orbitals.

Figure 2. *A schematic representation of the ground-state electronic configurations of selected elements*

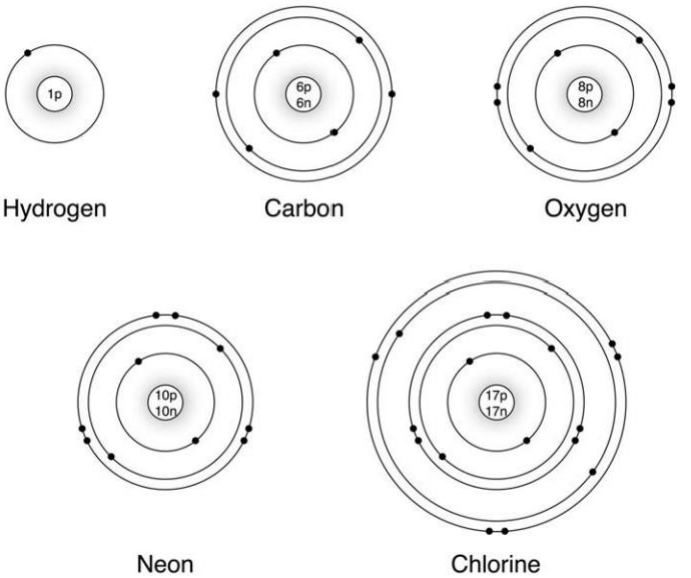

(IUPAC, 1997)

A stable electronic configuration in a molecule is attained when the valence shells of its constituent atoms contain the maximum number of electrons. Noble gases, which are located in the last column of the periodic table, are uniquely stable in their ground states. This stability results from the presence of a complete outer electron shell and is exemplified by neon, a noble gas with a fully occupied valence shell (Figure 2). In most stable molecules, atoms conform to the octet rule, typically forming chemical bonds that lead to eight electrons in their valence shell—except for the first shell, which can accommodate only two electrons. The valence electrons of an atom can interact with those of other atoms to form chemical bonds. The number of valence electrons an element has is determined by its position in the periodic table, specifically its group

number. Excluding transition metals, the group number usually corresponds to the number of valence electrons in an atom. For example, beryllium (Be) has two valence electrons, aluminum (Al) has three, and carbon (C) has four. Noble gases, found in Group 18, have eight valence electrons, indicating that their outer electron shells are complete. The periodic table also provides essential information about the total number of electrons in an atom. The atomic number (Z), which indicates the number of protons in the nucleus, is equal to the number of electrons in a neutral atom, since atoms are electrically neutral in their ground state.

- **Ionic Bond**

An ionic bond occurs when electrons are fully transferred between atoms, resulting in the formation of positive and negative ions. A positively charged ion (cation) forms when an atom loses one or more electrons, while a negatively charged ion (anion) forms when an atom gains electrons. This electron transfer creates an electrostatic attraction between the oppositely charged ions, leading to the formation of the ionic bond. Sodium chloride (NaCl) is a common example of an ionic compound, and Figure 3 demonstrates this type of bonding.

The atomic number of sodium (Na) is 11, meaning that a sodium atom contains 11 protons and 11 electrons. The electron configuration of sodium is written as $1s^2\ 2s^2\ 2p^6\ 3s^1$, which reflects the distribution of electrons across the respective energy levels. In this configuration, there is only one electron in the valence shell. Sodium tends to lose this electron to achieve a more stable electronic configuration, in which the second energy level becomes fully occupied. By losing one electron, sodium becomes ionized and forms a positively charged Na^+ ion.

Figure 3. Schematic illustration of NaCl

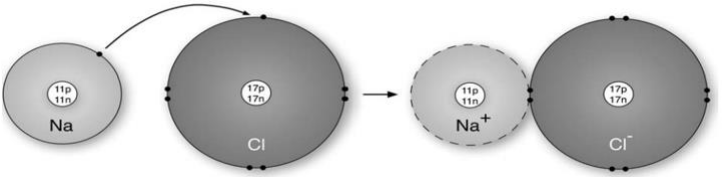

(IUPAC, 1997)

Another atom involved in the formation of salt is chlorine (Cl). Chlorine has an atomic number of 17, and its electron configuration is $1s^2\ 2s^2\ 2p^6\ 3s^2\ 3p^5$. This configuration shows that chlorine has seven electrons in its outermost shell. When chlorine gains an electron, it completes its third electron shell, resulting in a more stable configuration. Consequently, chlorine forms a chloride ion (Cl^-). Since sodium tends to lose an electron and chlorine has a strong tendency to gain one, the two elements readily form an ionic bond. The electron transfer between sodium and chlorine leads to the formation of Na^+ and Cl^- ions, which are held together by electrostatic forces.

Ionic bonds are prevalent in inorganic chemistry, whereas their occurrence is relatively rare in organic chemistry.

- **Coordinate Covalent Bond**

A covalent bond forms when atoms share one or more electrons. This type of bond results from the overlap of atomic orbitals (McMurry, 1988). Figures 4–6 illustrate this process. In covalent bonding, each shared electron contributes to the valence shell of both atoms, in accordance with the octet rule. In a *single bond*, one pair of electrons is shared, with one electron contributed by each atom. *Double bonds* involve the sharing of two pairs of electrons, while *triple bonds* involve three pairs. Bonds in which

more than one pair of electrons is shared are referred to as *multiple covalent bonds*.

Figure 4. Formation of a σ bond through the overlap of two s orbitals

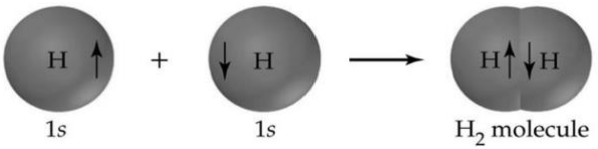

Figure 5. Formation of a σ bond through the overlap of an s orbital and a p orbital

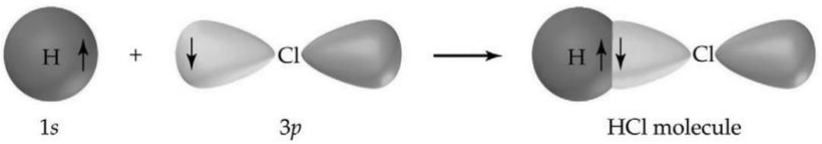

Figure 6. Formation of a σ bond through the overlap of two p orbitals aligned parallel to the nuclear axis

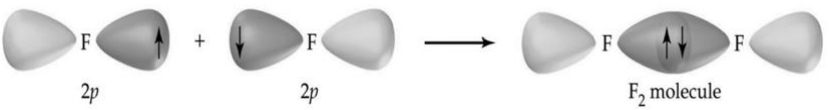

(McMurry & Fay, 2003)

A sigma bond (σ) occurs when electrons are shared between two s orbitals in a single covalent bond (Figures 4–6). Sigma bonds are the strongest type of covalent bonds. A sigma bond may also arise when an s orbital overlaps with a p orbital, or when two p orbitals overlap head-on along the axis between the nuclei.

A pi (π) bond forms from the lateral overlap of two p orbitals oriented perpendicular to the internuclear axis. In the context of multiple bonds, the initial bond formed is always a sigma (σ) bond, while the subsequent bonds are π bonds. In a double bond, one σ

bond and one π bond are present, whereas a triple bond comprises one σ bond and two π bonds. Despite π bonds being relatively weaker than σ bonds, the combined strength of these bonds results in the overall stability of the multiple bond structure.

For instance, water (H_2O) contains two sigma bonds, each linking a hydrogen atom to the oxygen atom, whereas in carbon dioxide (CO_2), each oxygen atom is bonded to the carbon atom through a double bond. The double bond in CO_2 consists of one σ bond and one π bond, contributing to its greater bond strength and shorter bond length relative to a single bond.

- **Metallic Bond**

Metal atoms, having relatively few valence electrons, are efficient electron donors. These electrons can be easily transferred into a freely moving "electron cloud." In metallic elements, atoms are closely packed in an orderly arrangement. The metallic core contains positively charged ions surrounded by a "sea of free electrons" (Figure 7). This configuration allows the electron cloud to move freely throughout the material, forming the basis for many of its properties.

Unlike covalent bonds, metallic bonds are non-directional, meaning the bonding between atoms is not confined to specific orientations. This contributes to the flexibility and malleability of metallic materials. The strength of metallic bonds can be quantified using measures such as sublimation enthalpy (the heat required to turn a substance from solid to gas without melting). For instance, the standard enthalpy of sublimation of aluminum is about 325 kJ/mol, whereas that of titanium is higher, approximately 475 kJ/mol, suggesting stronger metallic bonding in titanium.

The presence of the free electron cloud also enables metals to exhibit high electrical and thermal conductivity. The mobility of these electrons facilitates efficient charge transport and heat

distribution. The key attributes of metals—such as high conductivity, malleability, and bond strength—are a direct result of the structure composed of positive ions and the presence of freely moving electrons (Tanzi, Faré & Candiani, 2019).

Figure 7. Metallic bonds

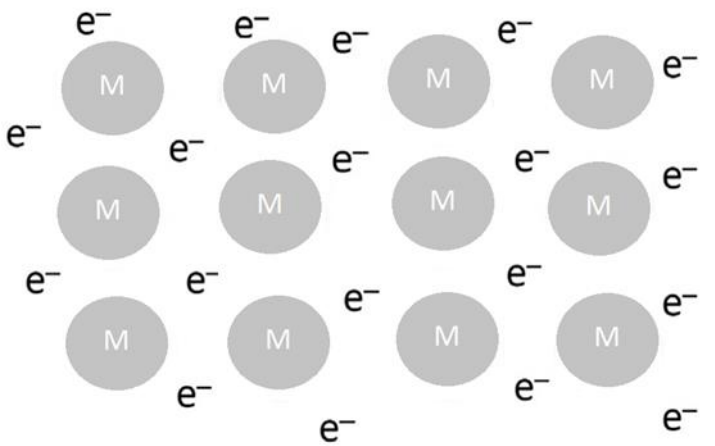

(Tanzi, Farè & Candiani, 2019)

Molecular Interactions

Strong bonds in a substance's chemical structure may be accompanied by weaker ones. These weaker bonds can be either intermolecular (between molecules) or intramolecular (within a molecule) and generally have lower energy. The energy associated with non-covalent bonds usually ranges from about 4 to 40 kJ/mol, which is significantly lower than the bond dissociation energy of covalent bonds. Given that the average kinetic energy of molecules at 25 °C is approximately 2.5 kJ/mol, a number of molecules are capable of breaking these bonds due to having enough energy. Non-covalent bonds are less directional because they do not involve electron transfer or sharing, and their bond strength is generally less than 10% of that of a covalent bond. However, these bonds play a

crucial role, particularly they significantly affect the characteristics of substances like polymers. Weak interactions include types such as Van der Waals interactions, hydrogen bonds, and ion-dipole interactions.

Molecular interactions examine the fundamental concepts and mechanisms of intermolecular forces. When molecules approach each other, the balance between the attractive and repulsive forces between them becomes important. At long distances, attractive forces dominate, while at very close distances, when the electron clouds overlap, repulsive effects come into play. The attractive interactions between molecules are generally grouped under Van der Waals forces. These forces govern the attraction between molecules at long distances and the emergence of repulsive forces at short distances (March & Mucci, 1993).

- **Van der Waals Forces**

Intermolecular interactions, which account for the attraction or repulsion between atoms and molecules, can be categorized into three primary types: electrostatic, polarization, and electrodynamic forces. The term Van der Waals forces encompasses all of these low-energy interactions, which are typically weaker than bonding energies. These forces have a significant impact on the behavior of atoms and molecules, influencing various physical properties. Van der Waals forces include both attractive and repulsive components and operate across all molecules and atoms, regardless of their specific chemical nature (Parsegian, 2005). The total van der Waals force, expressed as a function of separation distance (r), can be written as:

$$V_{VdW}(r) = V_e(r) + V_p(r) + V_{ed}(r) \quad (1)$$

Here, $V_e(r)$, $V_p(r)$ and $V_{ed}(r)$ represent the electrostatic, polarization, and electrodynamic components, respectively. As outlined below and presented in Figure 8, each term has its own

physical origin. However, all of them exhibit the same functional dependence on r, b/r^6, where b is a constant (Israelachvili, 2011).

1. Keesom Forces (Dipole-Dipole Interactions)

Keesom forces arise from interactions between molecules that possess permanent dipoles. A permanent dipole occurs due to the asymmetric distribution of electrical charges within a molecule, resulting a positive and a negative charged pole. Keesom forces are a result of the electrostatic attraction and repulsion between these poles.

Since this interaction is purely electrostatic, it is only effective between permanent dipoles. The strength of the force depends on the relative orientation of the dipoles: the way in which the poles are aligned with respect to each other determines the magnitude of the interaction.

The binding strength also varies based on the magnitude of the dipole moments and the distance between the molecules. This interaction is sometimes referred to as the orientation force because of its sensitivity to dipole alignment.

2. Debye Forces (Dipole-Induced Dipole Interactions)

Debye forces arise from interactions in which a permanent dipole disturbs the electron distribution of a neighboring molecule, thereby inducing a dipole (polarization) within it. In this case, a permanent dipole creates a temporary dipole in another molecule.

This force is associated with the interaction between a permanent dipole and an induced dipole. The permanent dipole causes the electrons in a neighboring neutral molecule to shift, leading to polarization. This polarization results in the formation of an induced dipole, and the electrostatic attraction between the permanent and the induced dipoles gives rise to the Debye force.

Debye forces depend on the magnitude of the permanent dipole moment of the molecule and the polarizability (induction capacity) of the neighboring molecule. This force is generally weaker, as the induced dipole moment is always limited by the strength of the permanent dipole's effect.

3. London Forces (Dispersion Forces)

London forces arise from interactions between temporary dipoles. Since all atoms and molecules possess electrons, at any given moment, the distribution of these electrons may be asymmetric, leading to the formation of a temporary dipole. These temporary dipoles can induce similar dipoles in neighboring molecules, leading to mutual attraction.

This force is based on the polarizability of atoms or molecules. As electrons move and redistribute, temporary dipoles are formed within atoms or molecules, leading to temporary dipole-dipole interactions. London forces are among the most prevalent intermolecular interactions and are effective in all types of molecules, because temporary dipoles can form in any atom or molecule.

The strength of London forces depends on the distance between molecules and their molecular size. Typically, as molecular size increases (i.e., the number of electrons increases), the strength of the London forces also increases.

Figure 8. Schematic representations of the various Van der Waals forces: Keesom forces arise from interactions between permanent dipoles, London forces result from interactions between induced dipoles, and Debye forces involve interactions between a permanent dipole and an induced dipole (the elliptical charge distributions (permanent dipoles) and circular charge distributions (induced dipoles))

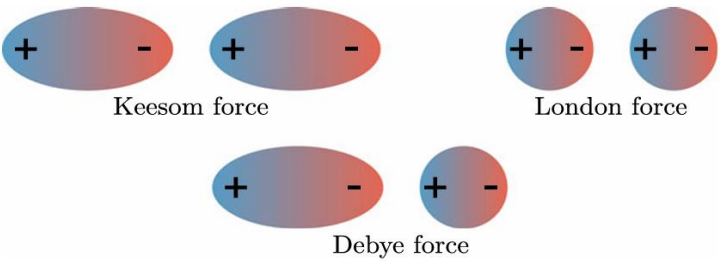

(Israelachvili, 2011)

- **Hydrogen Bonds**

Hydrogen bonds are a specific type of dipole-dipole interaction. Typically, a hydrogen atom (H) bonds to another atom via a single covalent bond. However, when hydrogen is covalently bonded to an electronegative donor atom (D), it can also interact weakly—but significantly—with an electronegative acceptor atom (A). This interaction is known as a hydrogen bond (see Figure 9).

For a hydrogen bond to form, the donor atom must be sufficiently electronegative to polarize the D–H bond, creating a partial positive charge (δ^+) on the hydrogen atom. The acceptor atom must also be electronegative and possess at least one lone pair of electrons, allowing for electrostatic attraction with the hydrogen.

Figure 9. Hydrogen Bond (indicated in blue)

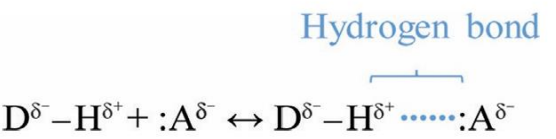

A classic example of hydrogen bonding occurs between water (H_2O) molecules. In this case, a hydrogen atom from one water molecule interacts with the oxygen atom of another. This interaction arises from the partial positive charge (δ^+) on the hydrogen being attracted to the partial negative caherge (δ^-) on the oxygen. Oxygen, being highly electronegative, pulls electron density toward itself, inducing partial charges that facilitate the formation of hydrogen bonds. These interactions can occur both within the same molecule (intramolecular) and between neighboring molecules (intermolecular) (Figure 10).

The strength of a typical hydrogen bond—such as the one formed between O–H ⋯ O groups—is around 20 kJ/mol, which, while significantly weaker than covalent bonds, is strong enough to influence molecular structure, boiling points, and many biological processes.

Figure 10. Hydrogen bonds between two water molecules.

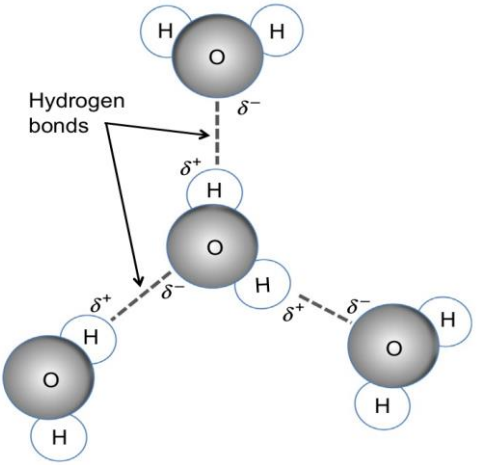

(Tanzi, Farè & Candiani, 2019)

- **Ion-Dipole Interactions**

Ion-dipole interaction is the attractive force between an ion (a charged atom or molecule) and a dipole. The ion influences the polarity of surrounding molecules by interacting with their oppositely charged regions. For example, a positive ion (Na^+) creates an attraction by approaching the negative pole (oxygen atom) of water molecules. This causes the dipoles of the molecules to orient in a specific direction during the interaction with the ion. For instance, when a water molecule interacts with a Na^+ ion, the oxygen part of the water molecule is attracted to the Na^+ ion, while the hydrogen atoms are oriented towards the negatively charged ions (Figure 11).

Figure 11. Ion-dipole interaction between a Na^+ ion and water molecules. Oxygen atoms face the ion, while hydrogen atoms point outward.

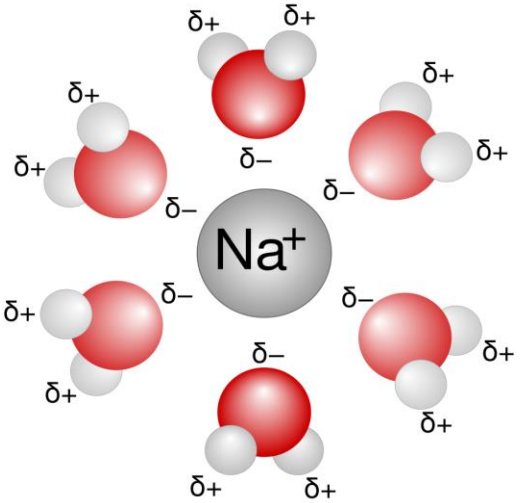

(Calmes & O'Brien)

The strength of ion-dipole interactions relies on factors such as the ion's charge, the magnitude of the dipole moment, and the distance between the interacting particles. The greater the ion's charge, the stronger the interaction. For example, the interaction between a Na^+ ion and H_2O is weaker than that between H_2O and a divalent ion, such as Ca^{2+}, which carries twice the charge. The strength of the dipole also affects the interaction strength; strong dipoles, such as water, exhibit stronger interactions. As the distance between the ion and dipole increases, the interaction strength decreases. According to Coulomb's law (the law of electrostatic forces), the attractive force weakens as the distance between charges increases. Ion-dipole interactions play a significant role in many areas, including chemical reactions, solubility, and the physical properties of solutions (McMurry & Fay, 2017).

REFERENCES

International Union of Pure and Applied Chemistry. (1997). Bond. In IUPAC Compendium of Chemical Terminology. Research Triangle Park, NC.

International Union of Pure and Applied Chemistry. (1997). Atom. In IUPAC Compendium of Chemical Terminology. Research Triangle Park, NC.

McMurry, J. (1988). Organic chemistry (2nd ed.). Brooks/Cole Publishing Company.

McMurry, J., & Fay, R. C. (2003). Chemistry (4th ed.). Prentice Hall.

Tanzi, M. C., Farè, S., & Candiani, G. (2019). Chapter 1 - Organization, structure, and properties of materials. In Foundations of Biomaterials Engineering (pp. 3-103).

March, N. H., & Mucci, J. F. (1993). Molecular interactions. In Chemical Physics of Free Molecules, Springer.

Parsegian, V. A. (2005). Van der Waals forces: A handbook for biologists, chemists, engineers, and physicists. Cambridge University Press.

Israelachvili, J. (2011). Intermolecular and surface forces (3rd ed.). Academic Press.

McMurry, J., & Fay, R. C. (2017). Chemistry: The central science (13th ed.). Pearson Education.

Calmes, J., & O'Brien, T. (n.d.). Ion-dipole interactions. Brilliant. https://brilliant.org/wiki/ion-dipole-interactions/

CHAPTER 6

THIN FILM PRODUCTION TECHNIQUES

1. Handan AYDIN[1]
2. Mehmet ODAK[2]
3. Cihat AYDIN[3]

INTRODUCTION

Since the 1940s, interest in thin film technology has grown, and it has continued to this day, thanks to the centuries-old usage of noble metal thin films as ornamentation on glass and ceramics. One of the most researched subjects at the moment is thin films, which serve as the foundation for the micro- and nano-structured materials sector and play a significant role in scientific and technological research. Thin films, which are typically less than 1 μm thick, are materials that are created as a thin layer by arranging the atoms or molecules of the substance to be coated using various production procedures on a base that aids in the development of the film by supporting the film (Bilgin V., 2003). Thin film materials

[1] Assoc. Prof. Dr. Munzur University, Department of Medical Services and Techniques Optician Program. ORCID: 0000-0002-0141-9773.
[2] Master, Munzur University, Department of Computational Sciences and Engineering.
[3] Prof.Dr. Firat University, Department of Airframe and Powerplant Maintenance, School of Civil Aviation. ORCID:0000-0001-9997-6326.

have undergone tremendous transformation and change in this century, which has created new processes and opportunities for material and technology development. As a result, numerous experiments have been carried out to advance this field and enhance the previously understood fundamental physical and chemical characteristics linked to thin film performance and structure in diverse applications. These experiments have also produced numerous new systems (Horzum Ş. 2005).

Thin films, which have gained great importance in today's scientific studies, are the basis of electronic technology. The performance and usefulness obtained from thin films, which have a wide range of uses, is a very important content. This is because the performance shown at the end of the work is related to the production techniques. Changes in production techniques and production conditions reveal many features that are not found in thin films. These properties in thin films give thin film materials more properties than bulky materials and pave the way for new scientific studies. Other production technologies have evolved in the production of thin films as a result of technological advancements. Thin films in three distinct phases—solid, liquid, and gas—were investigated in this work, and their benefits and drawbacks were thoroughly discussed along with their subtypes (Sonmezoglu et al. 2012).

THIN FILM PRODUCTION TECHNIQUES

Unlike the properties of tools and materials, the bulk coating or layer formed near the surface is called a film. In order for a film to be qualified as a thin film, its thickness must be 1 μm or less than 1 μm. Thin films, which have an important place in scientific and industrial fields, were first used for decoration purposes on ceramic and glass surfaces. In the following periods, silver salts were used to produce silver films on glass surfaces. The

first thin film was obtained by the “electrolysis” method in 1838. This production was followed by Bunsen “chemical reaction” in 1852, Faraday “evaporation in inert gas”, Nahrwold and Kundt “Joule heating” methods (Zor. M. 1982).

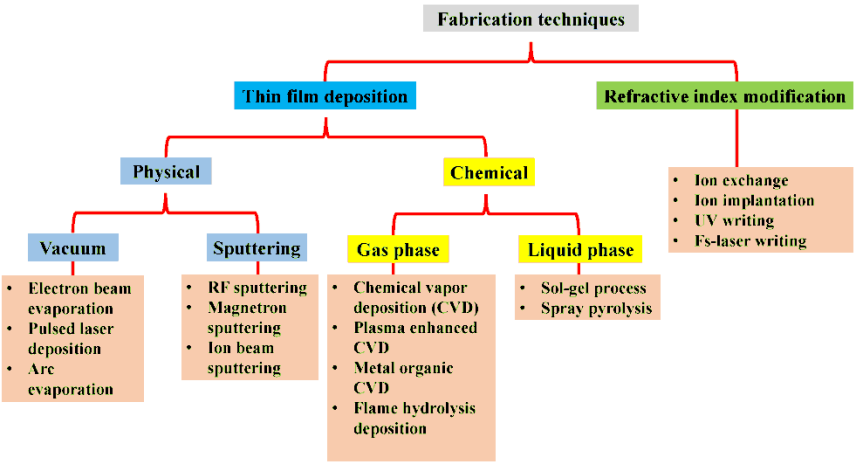

Figure 1. Thin Film production techniques (Butt M. *et.al*, 2022)

Vapor Phase Growth Technique

Chemical vapor deposition and physical vapor deposition are the two types of vapor phase coating processes that enable the production of high-quality coatings.

Physical Vapor Deposition

Physical characteristics like melting, oiling, and evaporation temperatures are unique to each substance. This method involves first heating the substance we wish to apply as a thin layer to the temperature needed for evaporation. The process of condensation, also known as evaporation, then occurs when the heated and evaporated material is transferred to the base in the colder temperature zone. The substance is heated in different ways to

create a vapor phase in accordance with the evaporation process. The generated vapor is transported to the area of low temperature, where it condenses on the carriers. Either an inert gas environment or a high vacuum environment can be used for this process. Resistance, induction, arc, and electron are the categories of physical vapor coatings produced by the evaporation process.

Physical vapor coatings obtained using the evaporation process are grouped as resistance, induction, arc, electron bombardment and laser evaporation.

Vaporization

Every substance has unique physical characteristics, including temperatures at which it melts, boils, and evaporates. The temperature necessary for evaporation is first raised for the item we wish to cover in a thin layer. Evaporation occurs when the heated and evaporated substance is transferred to substrates in the colder temperature range and condensed. The substance is heated in different ways to create a vapor phase in accordance with the evaporation process. The generated vapor is transported to the area of low temperature, where it condenses on the carriers. Either an inert gas environment or a high vacuum environment can be used for this process. Resistance, induction, arc, electron bombardment, and laser evaporation are the categories for FBB coatings produced by the evaporation method. (Gerhard W., 2009).

Vaporization with Residence

In the resistance evaporation method, the coating material to be evaporated is placed in a refractory crucible with high resistance to oxidation and temperature, and the heating process is carried out with the help of resistance wires wrapped around the crucible. This method, in which ceramic composite of refractory metals such as tungsten, tantalum, molybdenum is generally used as crucible material, is used for evaporation of materials with low melting

temperature such as aluminum, magnesium, silver, copper and lead (Türküz C. 1997, Özgüzar, 2017).

Inductive Vaporization

In the inductive technique, the heat source is the induction current applied to the copper wires wrapped around the crucible. In the system that provides melting temperature up to 2100 degrees Celsius, high cost is the most important disadvantage (Türküz C. 1997,Özgüzar, 2017).

Vaporization by Arc

In the arc method, the target material is ionized or vaporized by the use of arc. In the vacuum, the material to be vaporized is positioned as the cathode and the sub-stone as the anode. The applied high current (30-300 A) and low voltage (10-40 V) ensures the formation of an "arc". This method stands out due to its ability to coat with the desired composition, high ionization amount, successful coating even at low temperatures, and high coating speed. One of the main disadvantages of the system is the deposition procedure that causes droplet formation (Smallman and Ngan, 2007,Özgüzar, 2017).

Electron Beam Vaporization Method

The electron beam evaporation method is based on the principle that high-energy electrons (~15 keV) provided by an electron source are directed at the target material and the energy released as a result of directing the electrons at the target material vaporizes the material. In this method, which allows materials with high melting temperatures (up to 4000 °C) to be vaporized, there is a bombardment that can create regular vaporization with the advantage of directing electrons (Rointan F. 2001).

Laser Vaporization Method

The target material to be coated is vaporized in a vacuum chamber using a laser source in the laser vaporization method. This technique allows for the vaporization of metals that can absorb the laser beam and have a high melting temperature.

Application -Optimization

The vacuum's quality and the material's purity determine how pure the film is. The evaporation chamber's geometry has an impact on the film's thickness. The consistency of the thickness is disrupted by collisions with leftover gasses. Thick films cannot be coated by wire filaments. This is due to the fact that the amount of material to be coated is influenced by the filament's size. Thick coatings are made possible by crucibles and evaporation vats. Compared to the sputter method, thermal evaporation offers a faster rate of evaporation. Thicker film coatings are possible with crucible-based techniques like flash evaporation. The electron beam technique allows tight control of the evaporation rate. Therefore, it is possible to coat chemical compounds or composite materials with multiple beams and multiple material sources in the electron beam system.

Benchmarking with Similar Methods

It provides better step-by-step coating than sputtering and chemical evaporation methods. This can be an advantage or disadvantage depending on the desired result. With the sputter technique, materials are coated more slowly. In the sputter technique, plasma is used and high-speed atoms can damage the base. In the PVD technique, the vaporized atoms show a Maxwelian energy distribution, which reduces the high speed and depends on the temperature of the material. However, the electron beams generate X-rays and free electrons. These can also damage the substrate.

Advantages

- PVD coatings provide a harder and more corrosion resistant coating than electroplating.
- Most coatings have high temperature and impact resistance.
- Very abrasion resistant materials are obtained.
- Allows almost all types of inorganic and some organic coatings.
- Provides a high film coverage rate.
- Atomic collisions with less damage to the substrate.
- Excellent purity due to high vacuum conditions.

Disadvantages

- Complete coverage of bases with complex geometry cannot be achieved.
- Requires a vacuum environment and high temperatures
- Requires cooling systems
- Hot objects such as flames create vapors that adversely affect vacuum quality.
- Uneven coatings occur if the base has a rough surface.
- The material to be coated must be able to be vaporized by the system. This makes it difficult to coat heat resistant materials such as tungsten without using the electron beam evaporation method
- More difficult to control the film components compared to the sputter method

- It does not allow in-situ base cleaning, which is possible in the sputter system.
- Step-by-step coating is more difficult than with sputtering.
- When the electron beam is used for evaporation, the X-ray can damage the base.

Applications

- Space studies
- Automotive
- Medical materials
- Cutting tools
- Firearms
- Optical instruments
- Watches
- Glass films, thin films such as food packages
- Astronomical telescope mirrors
- Aluminum PET films
- Micro fabrication

Splashing Technique

This technique uses a plasma or ion gun to accelerate high-energy gas ions of atomic size, which are then blasted onto the surface to be coated. By bouncing the atoms off the substrate, coating is achieved. The atoms that are separated from the target material's surface then enter the vapor phase. Today, this technique is used in thin film coatings, surface analysis, surface cleaning and etching processes (Oktay G. 2005,Özgüzar, 2017). FBB coatings

obtained using the sputtering process are grouped as diode, triode, magnetic field sputtering and ion beam sputtering.

Diode Splashing Method

An anode and a cathode are two planar electrodes positioned opposite one another that make up the diode sputtering system. A water-cooled chamber is located beneath the cathode, and a coating material is present on the top surface of the cathode that is in contact with the plasma. An inert gas, such as argon gas, is supplied into the splash chamber at a pressure of 13.3 Pa after the chamber has been brought under vacuum. A flash discharge is produced when a voltage of several kV and a resistance of 1–10 kΩ is applied between the electrodes. A thin layer is created on the surface to be coated when the positive ions in the flash discharge strike the cathode surface and splatter the coating material from there (George, 1992).

The lack of secondary electrons, low deposition rate, warming of the substrate from high-energy particle bombardment, and extremely small deposition surface area are just a few of the drawbacks of the diode sputtering technique, despite its widespread use due to its simplicity (Özgüzar, 2017).

Triode Sputtering System

To increase ionization at low pressures and to maintain the flash discharge, the diode system is supplemented by a heater and a positive potential electrode. The heater and electrode increase the sputtering efficiency by increasing the degree of gas ionization. The primary anode, placed opposite the cathode, has a potential close to the potential of gas ionization, which allows the plasma to form. Under these conditions, it offers the opportunity to obtain a homogeneous plasma even at low pressure values (Cansever, 2001).

Magnetic Field Splashing Method

The target material is positioned on a holder made of electromagnets or water-cooled magnets in the magnetic field sputtering technique. The magnet's first pole is positioned on the coating material's center axis, and its second pole is positioned on its edges. The electric and magnetic fields on the cladding material are guaranteed to be perpendicular to one another thanks to this magnet arrangement. The plasma's electrons go in the direction of ExB. Stated differently, electron motion is perpendicular to the magnetic field (B) and the electric field (E). The electrons' channel of movement in the ExB direction forms a closed ring and runs parallel to the coating material's surface (Cansever, 2001).

Advantages

- Ambient conditions facilitate the maintenance of the plasma state.
- The process can be carried out at lower pressures.
- More uniform coating due to fewer gas collisions.
- It is possible to successfully deposit alloys with varying evaporation rates at varying vapor pressures without altering their composition.
- Extremely little chance of macroparticles getting into the film structure.
- Excellent coating adherence to the substrate. Splash washing the substrate might enhance it even further.
  The film's structure and quality are superb.

Disadvantages

- Limited coating thickness.
- High cost.
- Dielectric materials have low heat conductivity and high coefficient of thermal expansion, resulting in larger thermal gradients during ion bombardment. This can cause patterning on the target.
- It has a lower coating speed compared to arc technology.
- Lower plasma density (~5%) compared to arc technology reduces the adhesion rate of the coating and the density of the scattered layers may be lower.

Applications

- Bioactive ceramic coatings
- Ceramic coatings on implant materials
- Dynamic ram (random access memory) applications
- Surface acoustic wave applications
- Electrical insulation applications
- Obtaining nanocrystalline powders
- Dielectric thin films
- Electronic and optoelectronic applications

Chemical Vapor Deposition

In a confined space, the chemical compound that passes from the solid phase to the gaseous phase is carried by the carrier gas and deposited on the base material by diffusion, this is known as chemical vapor deposition method. The coating thickness is thinner

than 10 micrometers. Depending on the type of material, the temperature is usually up to 1100°C. The process time depends on the thickness of the material to be produced. The stoichiometry, morphology and crystal structure of the material can be controlled by changing the coating parameters (Coşğun et al., 2021).

Liquid Phase Magnification

Liquid phase growth techniques are divided into 3 groups: sol-gel, chemical bath and electrochemical methods. These techniques are discussed in detail below.

Sol-Gel Method

A very practical technique for creating thin films is the sol-gel process. Generally speaking, the system moves from the liquid phase (sol) to the solid phase (gel) during the sol-gel process. This process can be used to create a variety of glass and ceramic materials. Microporous inorganic membranes, ceramic fibers, thin film coatings, and extremely pure and spherical powders are among them. The components that comprise the sol do not sink to the bottom due to their greater strength than monolithic materials. This material is referred to be a gel if the molecule grows significantly in size while in solution. The gel's elastic quality comes from the solid structure's continuity. There are numerous benefits to the solgel technique. The tools and materials used in this method are very simple (Hasançebi, 2006).

A pure coating is produced, and the films made using this technique have the same thickness across the surface. Energy is saved, no interaction with the prepared medium occurs, and materials of any geometric shape can be covered with pure, homogenous films made at low temperatures. The primary benefit is the easy controllability of the coated film's microstructure. This technique can be used to create films with a low refractive index because it yields a porous structure. Furthermore, the technique is

not constrained by the object's geometry and multi-layer coating is feasible. But in addition to these benefits, there are also drawbacks. Some of them have high material costs and significant material loss during coating. Furthermore, there is a significant chance that the carbon solution will remain in the films, and the chemicals utilized may be hazardous to health (Sönmezoğlu et al., 2017).

In the sol-gel process, the fluid sol or solution prior to gelation can be coated onto any surface by commonly used dipping, spraying and spinning techniques.

Coating Method with Rotation

It is a process used to produce thin films on a rigid sheet or slightly curved substrates. The substrates used for this process are reduced to a smaller size. Film coating by the spinning process can be divided into 4 phases. These phases are: coating, spinning, end spinning and evaporation. In the coating phase, some liquid is poured onto the surface. In the second stage, rotation, the liquid flows radially out of the carrier surface due to centripetal force. At the end of the rotation, the excess liquid overflows from the carrier surface and leaves the surface. As the film thickness decreases, the amount of liquid overflowing from the surface decreases. The reason for this phenomenon can be explained as the increase in the resistance to fluidity with the thinning of the film. At the same time, the increase in the concentration of non-volatile substances leads to an increase in the resistance to viscosity. The evaporation phase is the last and most important phase in the thinning of films. An advantage of spin coating is the uniform distribution of the film that begins to form on the surface as the film is forming. As a result, the film thickness is homogeneous across the surface. As long as the viscosity of the sol does not change, the film thickness remains the same. Two main forces are effective in the uniformity of the film thickness. These are the centripetal force that causes the

liquid dripped on the carrier to flow radially outward and the friction force in the opposite direction. The centripetal force in the rotation phase causes the gravitational force to be neglected. Thus, there is only centripetal force in the thinning stage of the film (Alan P.C., 1998).

Advantages

- The film thickness can be easily changed by changing the rotation speed.
- The film thickness can be easily changed by using a solution of different viscosity.
- It is easy to change the coating thickness control parameters.
- It is low cost.
- The process does not take too long.
- It is a well-known process because it is widely used.

Disadvantages

- Large bases cannot be rotated at sufficient speed and therefore a film of sufficient thinness cannot be prepared.
- Material yield is not sufficient. (Approximately 5% of the material used is coated. The rest is wasted.

Applications

- In integrated circuits
- In optical mirrors
- For data storage on magnetic disks
- In solar cells
- In detectors

- In sensors
- In very large-scale integration
- In nano-sized devices
- In DVD and CD Rom production
- In silicon circuit plate coating with photo resistance in microcircuit production.
- In insulating layer coating such as polymers in microcircuits
- In plane screen coatings
- In antireflection coatings
- In gas sensors
- In LED manufacturing
- In high mobility ultra-thin semiconductor films
- In semi-metal dielectric applications
- In organic LED diodes

Immersion Coating Method

This method is generally used to produce transparent layers. The dip coating method is based on the principle of immersing the substrate material into the prepared solution at a certain speed and withdrawing it at the same speed. The dip coating method takes place in five stages. These stages are: dipping, pulling up, coating, filtration and evaporation. As a result of this process, a film is formed. In the immersion stage, the base is immersed into the sol at a constant speed, while in the pull-up stage, it is pulled up without waiting at the same speed as it was immersed. In the third stage, coating, the parts of the carrier that come into contact with the sol are coated. At this stage, the force of gravity, the carrier force

between the left and the base and the surface tension forces are effective. At the end of the immersion, the excess sol droplets leave the surface by draining from the edges of the base, while the sol droplets that cannot leave the surface with the filtration process evaporate and fly away. After all these stages, the sol remaining on the base turns into a film as a result of the annealing process. At the end of the immersion, the excess sol droplets leave the surface by filtering through the edges of the base, while the sol droplets that cannot leave the surface with the filtration process evaporate and fly away. After all these steps, the sol remaining on the base turns into a film as a result of the annealing process. One advantage of dip coating is that it is possible to coat bases of all shapes and sizes. With this process, a uniform and controllable thickness can be achieved. As a result, the film thickness is homogeneous across the surface (Jeffrey and George, 1990).

Advantages

- Allows simultaneous coating of the front and back side.
- Allows almost any type of material to be coated.
- No material is wasted.

Disadvantages

- All parts must be submersible. Otherwise masking may be required.

Spray Coating Method

The sputtering method involves combining aqueous solutions that have been prepared for the production of films, then atomizing them with the use of nitrogen gas or air to spray them onto the heated base. The simplest and least expensive technique for creating thin films is sputtering. Because it has a very straightforward structure, requires less expensive equipment,

allows for easy production process intervention, doesn't require a vacuum environment for thin film production, and allows for step-by-step production, the sputtering method is far more advantageous than other approaches. Both n-type and p-type doping are also possible with this technique. Experimental parameters including substrate temperature, sputtering rate, and film thickness affect the film's quality. A high-quality film can also be obtained by controlling experimental parameters including the spray nozzle's diameter, distance from the substrate, pure water ratio, and the amount of hydrochloric acid in solution. The quality of the film is significantly impacted by the size of the sprayed solution's droplets (Özkan, 2006).

Advantages

- The spraying method being quite simple in structure
- Being more economical in terms of the necessary equipment
- Being suitable for intervention during the production process
- Not requiring a vacuum environment for thin film production
- The ability to monitor the production process step by step
- Allowing n-type and p-type doping.
- Substrates with complex geometries can be coated.
- Relatively smooth and high-quality films can be obtained.
- Does not require very high temperatures during the process.

- It is suitable for automation. This also enables mass production.

Disadvantages

- The formation of non-homogeneous films with large particle sizes due to uncontrollable droplet size
- Wastage of the solution. For example, the low rate of effective coating of atoms on the substrate.
- Low coating rate.
- The coating on the substrate does not occur simultaneously.

Applications

The biggest feature of this method is its low cost. Therefore, it is increasingly being used in commercial transactions.

- For coating a transparent layer on glass
- To coat the layer in gas sensor applications
- In solar cell applications for layer coating
- To create anode in lithium-ion batteries
- It is used in the production of optoelectronic devices.
- In the synthesis of ceramic powders
- In high-capacity anode applications
- In nanowire synthesis

Chemical Bath Technique

This system mainly consists of a magnetic stirrer with heating capability, a reaction bath, a water bath, and a base arrangement. This technique is based on reducing the reaction rate of the ions

that will form a film within the solution. The advantages of the chemical bath technique over other methods include its applicability at low temperatures and atmospheric pressure, low cost, rapid and safe application, and suitability for thin film coating on large surfaces (Canci, 2009).

Electrochemical Method

The electrochemical (electrolysis) deposition technique involves coating thin films from solutions, with the material being deposited on either metallic or non-metallic substrates. Especially in the formation of desired shapes and the coating of large areas, this method provides a significant advantage. This method, depending on whether the controlled variable is potential or current, is divided into potential-controlled and current-controlled electrolysis methods. In current-controlled electrolysis, maintaining a constant current despite the decreasing concentration of the substance during the electrolysis process is achieved by increasing the applied potential. n order to eliminate the disadvantages that this increase in potential will cause, the usually consumed substance is constantly added and the concentration is kept constant (Kaya, 2005). The potential-controlled electrolysis collection technique excels in situations requiring successive electron exchange. Dec. It is also used to prepare a sufficient amount of reaction product to be determined in the application of traditional analytical techniques. If there is a possibility of different reactions occurring at different potentials in the electrolysis environment, the desired product can be achieved by a potential-controlled electrolysis. There are some parameters that affect the quality of the thin film formed in the electrochemical deposition technique. By changing these parameters, it is possible to produce thin film according to the desired properties.

These parameters are;

- Deposit potential,
- The type and amount of substances participating in the electrolyte,
- Solution pH,
- Current density,
- Electrolyte temperature,

It can be sorted in the form of chemical additives added to the solution (Özdemir, 2010).

Magnification in the Solid Phase

In the solid phase, which is less preferred than the vapor and liquid phase, the enlargement process is mainly divided into two, mechanical etching and devitrification.

Mechanical Etching

Mechanical etching is used to produce nanostructured materials by structural decomposition of coarse grains as a result of many plastic deformations. Mechanical etching covers the repeated joining, breaking and re-joining processes of powder particles in high-energy mills. With these processes, nanocrystalline thin film structures are obtained in pure metals, intermetallic components and immiscible alloy systems. It has been observed that after sufficient grinding time, nanometer-sized grains are obtained in any material. It has been observed that the grain sizes decrease towards a minimum value (inversely proportional to the melting temperature) with the grinding time. In recent years, it has been observed that ultrafine granular structures have been obtained as a result of processes in which mass solids undergo a large number of plastic deformations. Although the grain sizes are not exactly nano-sized (usually 3-5 μm), there are many research studies on products

made with this method. However, scientifically, there are concerns that this mechanical grinding process will cause the formation of impurities, that the size distribution and surface properties cannot be controlled. What is usually expected here is to increase the possibilities of producing volumetric high-purity materials by working in sub-micron grain sizes (Schweitzer, 1988).

Devitrification

Devitrification is also known as the rapid solidification method. The controlled crystallization of these amorphous alloys (by increasing the nucleation rate and decreasing the growth rate) is used in the synthesis of nanostructured materials. This simple method is a common method in studies of the magnetic properties of nanocrystalline materials. it is to crystallize the glassy phase at lower temperatures. Because porous samples can be produced, different grain-sized samples can be produced by controlling the crystallization parameters, and large quantities of materials can be produced. Furthermore, if it does not contain any artificial synthesis process, the interfaces are clean and the product is dense (Suryanarayana and Koch, 1999 Dec).

RESULT

The indispensable first step for new developments in the field of nanotechnology, which covers the design, production and functional use of nanostructured materials and devices, is the production of thin films. Intensive studies are being carried out in both academic and industrial fields in order to increase the performance and reduce the costs of thin films, which are frequently used in device technology applications. The increasing number of scientific studies conducted in this field all over the world every day and the large investments made by technology companies in this field are an indicator of how important thin films are as a field of study. In thin film production techniques, it is

observed that parameters such as the pH value, temperature and reaction time of the solution, solvent concentration, structure and concentration of the catalysts used, annealing temperature and duration, drying and drying atmosphere, substrate used have effects on the quality, thickness and production cost of the film. In addition, it is clearly seen that each technique has advantages and weaknesses compared to the other technique. While high temperature and vacuum are not required in liquid phase magnification techniques, vacuum and high temperatures are required in vapor phase magnification techniques. However, in vapor phase magnification techniques, higher quality and nano-sized thin films are obtained compared to liquid phase magnification techniques. Solid phase magnification techniques are the techniques commonly used in the production of superconducting films. For example, in the widely used sol-gel method, it is an advantage that the coating can be made without the need for very high temperatures, while the need for a large amount of chemical materials and carbon deposits formed in thin films are a significant disadvantage. Likewise, MOCVD, the most important technique of chemical vapor deposition method, is an important epitaxial enlargement technique that has proven itself in terms of its advantages in producing high-quality epitaxial layers, sharp interfaces and multilayer structures with a thickness of several atoms, but it provides a serious disadvantage due to its high cost. For this reason, it would not be the right approach to say that it is more advantageous for any technique than others. The technique to be used is determined only according to the type and size of the substrate to be coated with thin film, the temperature to be coated, the coating material, the available budget and, most importantly, the intended use of thin film.

REFERENCES

Alan P.C., 1998. Introduction to Sol--Gel Processing: The International Series in Sol-Gel Processing: Technology & Applications, s. 408, Kluwer Academic Publisher.

Bilgin, V., 2003. The Effect of Tin Doping on the Electrical, Optical, Structural and Superficial Properties of ZnO Films, PhD Thesis, Osmangazi University, Eskisehir.

Butt, M. A. *et. al.*, 2022. Optical Thin Films Fabrication Techniques—Towards a Low-Cost Solution for the Integrated Photonic Platform: A Review of the Current Status. *Materials*,*15*(13), 4591.

Canci, U., 2009. Determination of Electrical and Optical Properties of Doped and Undoped CdS Thin Films Prepared by CBD Method, Master's Thesis, Gebze Institute of Advanced Technology, Institute of Engineering and Science, Gebze.

Cansever, N., 2001. Recent Developments in Particle Splashing Method in Magnetic Field, Engineer and Machinery, 496.

Coşğun ve ark. 20210., Chemical Vapor Deposition Method and Types in Thin Film Production. Mehmet Akif Ersoy University Journal of Institute of Science and Technology 12(2): 351-363.Burdur.

George, J., 1992, Preparation of Thin Films, Marcel Dekker, Inc., New York.

Gerhard, W., 2009. Nanostructured Materials, s. 384, Elsevier Science.

Hasançebi, Ö., 2006. Electrical, Structural and Optical Properties of Copper Oxide Thin Films Prepared by Sol-Gel Method, Yüksek Lisans Tezi, Ankara University, Ankara.

Horzum, Ş., 2005. Investigation of Structural, Electrical and Optical Properties of Chemically Coated CuO2 Thin Films, Master's Thesis, Ankara University Institute of Science and Technology, Ankara.

Jeffrey B.C., George, W., 1990. Scherer Sol-gel Science: The Physics and Chemistry of Sol-gel Processing, s. 908, Gulf Professional Publishing.

Kaya, H., 2005. Electrochemical Eldition of CoNiFe Thin Film Alloys and Investigation of Their Properties, Master's Thesis, İnönü University Institute of Science and Technology, Malatya.

Oktay, G., 2005. Physical Vapor Deposition (PVD) Method, Galvanoteknik, 2006. Ürgen, M., Modern Surface Modif. Tech. Lecture Notes, I.T.Ü., Istanbul.

Özdemir, R., 2010. Investigation of Electrical Resistivity Properties of ZnFe Thin Films Obtained by Electrodepolama Method with the Help of Intuitive Methods, Master's Thesis, Kilis 7 Aralık University, Institute of Science and Technology, Kilis.

Özgüzar H.,2017. Improving the stability of thin films rich in amine groups for biomedical applications: n-hexane substrate film application with plasma polymerization method.Master's thesis,Ankara.

Özkan, İ., 2006. Improvement of Surface Properties of Materials with Nanotechnological Methods, Master's Thesis, Dokuz Eylül University Institute of Science and Technology, İzmir.

Rointan, F., 2001. Handbook of Hard Coatings, Deposition Technologies, Properties and Applications, Noyes Publications /William Andrew Publishing, LLC., U.S.A.

Schweitzer, P., 1988.Corrosion and Corrosion Protection Handbook, s. 682, CRC Press.

Smallman, R.E. Ngan., 2007. A.H.W., Physical Metallurgy and Advanced Materials, Seventh Edition, s. 672, Butterworth, Heinemann.

Sönmezoğlu ve Ark., 2012. Thin film production techniques. Erciyes University Journal of Institute of Science and Technology, 28(5):389-401.

Suryanarayana, C., Koch C.C., 1999. Non-Equilibrium Processing of Materials; Nanostructed Materials, Pergamer Materials Series, New York, USA, 313-344.

Türküz, C., 1997. Characterization and Performance Investigation of TiN Coated Cutting Tools with Arc PVD Method, Master's Thesis, ITU Institute of Science and Technology, Istanbul.

URL-1,2023.https://yusufbilgen.wordpress.com/2015/01/16/ince-film-teknikleri/ Erişim Tarihi:18.05.2023

Zor, M., 1982. Some Physical Properties of AgInS2 Compound Obtained by Spray-Pyrolysis, Associate Professorship Thesis, Ankara.

CHAPTER 7

EXAMPLES OF KONYA'S HISTORICAL CARPET MOTIFS IN THE LIGHT OF CRYSTALLOGRAPHY AND SYMMETRY

BÜŞRA SAYIN[1]
CEM CÜNEYT ERSANLI[2]

Introduction

Carpets, as valuable artifacts of cultural heritage, have played an extraordinary role throughout history as a decorative and functional component. The art of carpets, more specifically in the Turkish world, has developed as a method of expression that carries aesthetic and cultural importance and conveying social order and values. It is emphasized in the majority of the studies that carpets, beyond being practical objects used on a daily basis, carry deep symbolism and beautiful mathematical patterns. Konya carpets are one of the most unique examples of Turkish handicrafts from both the aesthetic and cultural sides. Especially with their rich history

[1] Sinop University, Institute of Graduate Studies, Department of Physics, Sinop/Turkey, Orcid: 0009-0007-7100-4913, busrakaratay@gmail.com
[2] Prof. Dr., Sinop University, Faculty of Arts and Science, Department of Physics, Sinop/Turkey, Orcid: 0000-0002-8113-5091, ccersanli@sinop.edu.tr, ccersanli@gmail.com
This study was produced under the supervision of the second author from the first author's master seminar.

dating back to the Anatolian Seljuk period, these carpets are not just a handicraft commodity; they are also multi-layered cultural texts that have strong symbolical expression (Erdoğan, 2015; Öztürk, 2019). The organization of the geometrical motifs is not just an articulation of traditional notions of aesthetic knowledge, but also of universal principles of symmetry. Here, research into Konya carpets offers a topic deserving of examination not just in the eyes of art history and ethnography, but also by natural sciences such as crystallography and symmetry theory (Critchlow, 1976; Grünbaum & Shephard, 1987). Symmetry is where science and art converge. The translation symmetries, rotation, reflection, and sliding symmetries one finds in carpet patterns demonstrate that handicrafts are not just for adorning but also have a mathematical order (Weyl, 1952).

By putting symmetry on a scientific basis, crystallography provides an important framework for explaining repetition patterns on two-dimensional surfaces. Just as crystal structures are formed by the arrangement of atoms according to certain symmetry rules, carpet patterns are similarly formed by the symmetrical repetition of motifs (Giacovazzo, 2002; Hahn, 2002). This parallelism makes it possible to match the carpet patterns to crystallographic plane symmetry groups (*e.g.*, P2 and P4m) (Schattschneider, 1978). Octagonal and star motifs frequent in Konya carpets can be considered as visual projections of the crystal structures in nature. Symmetry of the patterns also supports Islamic arts strive to represent the cosmic order and infinity (Denny, 2002a; Broug, 2008). In addition, such symmetrical compositions make Konya carpets not only an art product but also an interdisciplinary science that can be the subject of scientific study (Kaya, 2016). The present study emphasizes how the geometric symmetry in traditional patterns meets the symmetry policies often seen in science and thus introduces an interdisciplinary approach that brings together art and

science. The examination of the patterns of Konya carpets enables us to evaluate cultural life from a broader base and is important in that these patterns can be advertised with the help of modern science. The correspondence of carpet motifs with the rules of symmetry is concurrent with the characteristics of crystallographic structures. Revealing this connection not only makes the examination of cultural values possible in another aspect but also provides a new perspective to art products. With this study, readers will better recognize carpet aesthetic values reflecting the Konya cultural heritage and will be able to learn how scientific concepts such as symmetry, crystallography and geometry are realized in traditional designs. Thus, a holistic approach in art and science will be developed by linking different disciplines.

The Relationship of Carpet Design, Motif, Symmetry and Crystallography

Carpet art is one of the greatest examples of ancient Turkish handicrafts that developed during history and reached the present time. Carpets are not only functional objects but are also precious cultural ones expressing the aesthetic knowledge and symbolic universe of a culture in the shape of color, pattern, and symbol. Archaeological findings suggest that carpet weaving originated in the 4th-5th centuries BC and this art began in Central Asia. In Anatolia, especially in the period of the Seljuks in the 13th century, great progress was experienced and the craft of carpet has lived on to the present without a break. Carpet is one of the only weaving materials to have retained its importance without changing its very nature in the last 3000 years (Öztürk, 1992; Yılmaz, 2017). The history of the word carpet is also noteworthy with cultural transformation. In the Ural Altaic language family, the word “thick” conveys the meaning of dowry or dowry. This term has, throughout history, taken many different forms in various Turkic dialects and languages: “kalın” in Chagatai, ‘kilem’ in Crimean

Turkish, ‘kalı’ in Anatolian Turkish, ‘haliya’ in Bulgarian, ‘kalın’ and ‘halım’ in Yakut, and ‘kalice’ in Persian. This term has, throughout history, evolved into the modern form “carpet” by being taken from the Turkish verb “kal” (Yılmaz, 2017). Carpet art has gained a central position in every society as an expression of the socio-cultural and economic standing of people. Turkish carpet art, which has been successful globally in terms of quality and quantity, has a special value in terms of art history. Even though initial carpets were woven for utilitarian use, they later evolved to have a rich visual vocabulary by taking on aesthetic, symbolic and cultural roles. Here, carpets have been a part of the homes of different societies from nomads to empires. The motifs within carpet weaving are one of the basic elements of cultural expression. Motifs in different activities such as literature, music, visual arts and architecture are structures that emphasize a specific theme or message by utilizing their repetitive structure. Motifs, which multiply the levels of meaning of a work through repetition, have the function of directing attention on the part of the viewer. As an example, in a work that has light vs. darkness as its theme; repeated recurrence of symbols of darkness is considered a motif. To this extent, the motif facilitates the theme to be concretized. Symmetry is another important element of art works. Symmetry is where an object overlaps with itself through operations such as rotation, reflection or traveling around a specific axis, plane or point. The aesthetic appeal of perception of symmetrical forms by the human eye has seen symmetrical forms used on a large scale in works of art (Weyl, 1952). The patterns in carpet weaving are generated within the constraints of certain symmetrical structures and this regularity produces visual harmony (Grünbaum and Shephard, 1987). Geometric designs, especially common in Islamic art, are considered to be representative of universal and cosmic order. This consideration is also found in carpet designs; the repeating character of the patterns is welcomed as a depiction of the concept

of infinity (Critchlow, 1976). The place of symmetry in art takes on even larger importance in the scientific discipline of crystallography. Crystallography is a scientific discipline that investigates the atomic and molecular structure of solid materials. Based on the concept of symmetry, the discipline investigates the effects of the order in the internal structure of crystals on physical properties.

Crystallography has widespread application in physics, chemistry, biology, pharmacy, and material engineering in the determination of the structure of a vast array of materials ranging from minerals to proteins (Bragg and Bragg, 1915; Giacovazzo, 2002). Crystallography utilizes techniques such as X-ray diffraction in the investigation of crystal structures. Max von Laue's discovery of the diffraction of X-rays in crystals in 1912 laid the foundations of crystallography on the modern scale. Crystal structures are a result of the arrangement of atoms following certain rules of symmetry. Symmetric structures are described by crystallographic symmetry groups (space groups) (Hahn, 2002). As it happens, there is a corresponding symmetrical order in carpet patterns. Carpet designs are periodic, repeating and symmetrical patterns such as the atomic structure of crystals. Konya carpets, in particular, attract attention with geometrical designs and unique motifs; it is noted that the majority of the designs in the carpets match one of the 17 plane symmetry groups (Schattschneider, 1978). This suggests that carpet art has, besides a cultural, also a mathematical and scientific dimension. The aesthetic balance of Konya carpets both attract the attention of art lovers and offer researchers a rich field of study on the congruence of motif symmetry (Denny, 2002a).

Historical and Cultural Background of Konya Carpet Art

Konya, as one of the provinces with the longest-established carpet weaving tradition in Anatolia, has a central position in

Turkish carpet art in historical and cultural terms. Konya carpets have been identified with the Anatolian Seljuk Empire, especially since the 13th century, and continued to develop both in terms of production and aesthetics during the Ottoman Empire. With their weaving techniques, motifs and symmetrical patterns, these carpets are important cultural heritages that reflect the visual and symbolic codes of not only Anatolian culture but also Islamic art (Yetkin, 1981). Konya carpet weaving was carried to the region as the cultural heritage of the Turkish communities migrating from Central Asia to Anatolia and gained a unique identity here. Carpet weaving showed a great development during the Seljuk period; especially the carpets used in public buildings such as mosques, madrasas and palaces reflected the aesthetic understanding of this period and the motif world based on geometric symmetry (Denny, 2002b). Octagonal forms, stars and other geometric patterns are predominant in these carpets (Critchlow, 1976). During the Ottoman period, both pattern and color diversity increased in Konya carpets. Floral forms, medallion-type central motifs and stylized figurative elements began to be widely used. The carpets produced during this period were in high demand not only in the local market but also in Europe and spread over a wide geography through trade routes (King and Sylvester, 1983a). Indeed, the frequent inclusion of Konya carpets in the works of European painters in the 16th and 17th centuries increased the international recognition of these carpets (Mackie, 1989). In technical terms, Konya carpets are traditionally woven with the Turkish knot (Gördes knot). This knotting technique increases both the durability of the carpet and the clarity of the motifs (Erdmann, 1960). The yarns used in the carpets are usually obtained from local sheep wool, while the colors are created with natural vegetable dyes. Traditional herbal sources such as root dye, walnut and pomegranate shells create the rich and long-lasting color palettes of the carpets (Böhmer, 2002). Konya carpets are not only aesthetic

and functional objects; they are also carriers of social identity, cultural values and individual narratives. The motifs on the carpet are often reflections of the weaver's personal feelings, beliefs and environmental observations. For example, the "ram's horn" motif symbolizes power and fertility, while the "tree of life" motif symbolizes immortality and paradise (Ögel, 1987a). However, Konya carpet weaving also functioned as an element that increased the economic contribution of women in social life. Carpets woven in the home environment allowed women to contribute to the family budget and this tradition was passed down from generation to generation (Atasoy, 1988). In this respect, carpet weaving is not only a cultural but also a socio-economic practice. The aesthetic value of Konya carpets becomes evident with their symmetry, color harmony and pattern diversity. Symmetry and geometric order are the basic elements representing cosmic order and infinity in Islamic art and this understanding is clearly seen in Konya carpets (Grünbaum and Shephard, 1987). With these characteristics, Konya carpet art preserves its importance both as an example of traditional Turkish handicrafts and as an area of intercultural interaction.

Cultural and Scientific Value of Konya Carpets: The Contribution of Carpet Patterns to Cultural Heritage and Global Change

Konya carpets, as one of the finest works of Turkish carpet art, both play a great role in passing on local cultural heritage and participating in cultural exchange at an international level. The carpets, by carrying the aesthetic as well as technical imprints of ancient Turkish art and craftsmanship from Central Asia, have become a tangible symbol of cultural identity. While the motifs of the weft of carpets reflect strong symbols of the believing systems, lifestyle and historic memory of the locals, they are also among the most precious cultural items with great artwork and economic value in the world. Especially Konya carpets, preserved from

Seljuk ages to the present time, are typical examples showing the continuation of traditional weaving traditions. These carpets are charged with geometric ornamentation, floral motifs and embellishments, animal depictions and symbolic themes, and embody multiple layers of meaning reflective of Turkish Islamic art's aesthetic sense and metaphysical imagination (Erdoğan, 2015). The mentioned motifs were not only thought to be merely decorative in character, but also symbolic elements that indicated the harmony of the universe, man's existence in relation to God and cyclical character of life (Çolak, 2017). The symbolic themes that emerged in the carpets designed specifically for religious buildings during the Seljuk era were based on the aesthetic principles of Islamic art and carried a religious meaning appropriate for the purpose for which the carpet was created (Öztürk, 2019). The processes of modernization and globalization have directly influenced Konya carpets as well as traditional handicrafts. Most importantly, the widespread application of industrial manufacturing techniques has led to the replacement of hand-made carpet production techniques with mass production. However, the artistic sophistication and historical integrity of Konya carpets still make them valuable in the global market. Konya carpets are among the cultural goods that museums, art galleries and collectors wish to obtain; they generate international interest in both their aesthetic values and the meanings they carry in a cultural context (Altınsoy, 2018). In this context, Konya carpets are not only an art piece, but also a communication tool that ensures intercultural communication and a symbolic element of Turkish culture. Increased worldwide interest has also encouraged the preservation of ancient patterns and the type of weaving, encouraging carpet producers to keep cultural authenticity (Güleç, 2020). Preserving and selling Konya carpets is therefore a vital cultural responsibility both on the local as well as global fronts. These rugs are worthwhile objects of study for disciplines such as ethnography,

cultural anthropology, art history and archaeology; they become a site for interdisciplinary study by being evaluated under many categories ranging from weaving method to the materials employed, from symbolic meaning of motifs to their socio-cultural explanations (Kaya, 2016). Furthermore, research into how Konya carpets were developed in the cultural field and how they diffused over the course of history verifies that Turkish carpet weaving is not only a regional artistic activity, but it also reveals its place and value in global art history. In this way, Konya carpets are both material cultural heritage objects that facilitate the passing on of existing systems of knowledge to the present and offer a rich and multi-faceted site of investigation for contemporary scholarship.

The Concept of Motifs in Crystals

The motif theme, a central one to understanding the inherent characteristics of crystal structures, is one of the most important supports of crystallography. The most basic repeating unit defining element in any crystal structure that forms a motif may be an atom, an ion or a cluster of molecules. This basic building block forms the entire crystal structure by repeating in certain symmetrical patterns in the crystal lattice (Cullity and Stock, 2001). Regularity found in crystal structures is really a result of repeating these motifs on a three-dimensional lattice structure under certain rules. This regular structure of motifs directly determines not only the geometric design of the crystal but also its physical and chemical properties. In crystals, motifs are repeatedly replicated in a three-dimensional lattice system by appearing at specific points. Such a three-dimensional lattice system is referred to as the crystal lattice, and the presence of a motif at each lattice point causes the structure to increase homogeneously and symmetrically (Kittel, 2004). In NaCl crystal, for example, the motif can be sodium (Na^+) and chlorine (Cl^-) ion. This ion pair is repeated in some order through the crystal and forms the cubic symmetry arrangement of the

crystal salt. This symmetry pattern is a determining factor for much of the crystal's properties, such as strength, solubility and optical properties. Motifs in crystals have purposes that are not structural order alone; they determine all of the substance's properties. The motif structure, place and number affect many parameters, from the crystal's hardness to its electrical conductivity, optical reflectance, and thermal characteristics. To this effect, differences between carbon-based crystals such as diamond and graphite arise from motif orientation. In diamond, each carbon atom is bonded to four neighbors in a three-dimensional arrangement with robust covalent bonds, while in graphite; each carbon atom is bonded to three and also held together in sheets by tenuous van der Waals forces (Ashcroft and Mermin, 1976). The differences in the physical properties exhibited by these two crystals of the same element most assuredly determine the determinism of motifs' arrangements in material behavior. The connection of motifs with crystal symmetry is likewise a major determiner in the classification of crystals. Crystal systems are investigated under seven distinct classes of symmetry where motifs appear in regular repetition: cubic, tetragonal, orthorhombic, hexagonal, trigonal, monoclinic and triclinic (Hammond, 2009). In each crystal system, motifs are fitted into the lattice structure in the realm of particular symmetry elements. These symmetry elements include geometric transformations such as axes of rotation, mirror planes and centers of inversion. The precise integration of motifs within such elements has immediate effects on the final arrangement as well as physical stability of the crystal. The symmetrical arrangement of motifs not only increases the crystal's resistance against external forces, but also promotes the thermodynamic stability of the internal structure. The motif part is in direct interaction with the crystal lattice structure. The arrangement of the lattice points where motifs are arranged forms the basis of the three-dimensional crystal structure. Here, 14 Bravais lattices describe the structure on which motifs

will be located (Cullity and Stock, 2001). Motifs in a cubic crystal shape are located within a cubic lattice structure where the structure can have highly symmetric and isotropic behavior. This interaction of the motifs with the lattice is crucial to describing the macroscopic properties of the crystal and the systematic cataloging of crystal structures. The spatial order of motifs in crystal structures also has important implications for materials science. Especially in semiconductor technologies, the spatial arrangement of motifs in certain patterns has a direct effect on the electrical conductivity and function of the material. For example, suitable motif alignment in silicon crystals optimizes semiconductor behavior by enabling free electrons to travel (Kittel, 2004). Similarly, photonic crystal motif arrangements used for opto-electronic applications are made such that transmission or reflection of light is possible at selected wavelengths. Arrangements are utilized in the majority of advanced technologies from laser technology to sensor systems. Lastly, in knowing and development of crystalline structure functions, the concept of motifs not only provides a theoretical foundation, but also is of strategic importance with respect to real application.

The Idea of Symmetry and Its Implication in Crystallography

Symmetry, as a fundamental property of nature and art, is not only an indicator of aesthetic order but also a decisive principle in the operation of nature (Weyl, 1952). Symmetry in crystallography is a fundamental property that governs the order of the internal arrangement of crystals and thus their physical and chemical properties (Kittel, 2004). Crystals are characterized by atomic structures repeating in three-dimensional space in a specific order, and this order is explained by the principles of symmetry. Symmetrical structures directly affect the refractive, conductivity and optical properties of crystals. Therefore, the principle of symmetry is a critically essential tool for explaining and classifying crystal structures.

Bravais Braids and Crystal Systems

In crystallography, the atomic structure of a crystal is described in terms of the smallest repeating unit called a “unit cell”. The three-dimensional stacking of these unit cells in a periodic fashion constitutes the entire crystal. The mathematical representation of this order is provided by Bravais lattices. Formulated by Auguste Bravais in the 19th century, this theory unveiled that crystals can be arranged in only 14 ways (Figure 1).

In three dimension space, these 14 Bravais lattices are grouped into 7 crystal systems: cubic, tetragonal, orthorhombic, monoclinic, triclinic, trigonal (rombohedral) and hexagonal (Hammond, 2009). Each crystal system is characterized by particular axis lengths and angles. For example, in the cubic system, all the axis lengths are identical and the angles between axes are 90°. In the hexagonal system, two of the axes have the same length and make an angle of 120° with one another, and the third axis is at right angles to this plane. All these geometric characteristics have a direct effect on the crystal’s symmetry elements and physical behavior. The following Table 1 gives the basic geometric properties and example structures of crystal systems:

Table 1. Properties of Bravais lattice and crystal systems.

Crystal System	Unit Cell Types	Number of Bravais Lattices	Features
Hexagonal	Simple Hexagonal (atoms arranged in a hexagonal structure. Example: graphite, zinc)	1	Two sides equal, angles 120° and 90°
Cubic	Simple Cubic (atoms are located only at the corners), Inner Centered Cubic (contains corners and an inner center atom. Example: iron), Surface Centered Cubic (contains atoms at the corners and in the middle of the surfaces. Example: copper)	3	All sides equal, all angles 90°
Tetragonal	Simple Tetragonal (atoms at the corners), Centered Tetragonal (atoms at the corners and one atom in the center)	2	Two sides equal, all angles 90°
Orthorhombic	Simple Orthorhombic (containing only corner atoms), Base-Centered Orthorhombic (center atoms at two bases), Inner-Centered Orthorhombic (containing inner center atoms), Surface-Centered Orthorhombic (containing surface center atoms)	4	All edges are different, all angles 90°
Trigonal (Rhombohedral)	Simple Trigonal (atoms at corners and in rhombohedral arrangement)	1	All sides equal, all angles equal but not 90°
Monoclinic	Simple Monoclinic (containing corner atoms), Base Centered Monoclinic (containing center atoms at the bases)	2	Two angles 90°, one angle different
Triclinic	Simple Triclinic (containing only corner atoms)	1	All edges and angles are different

Bravais lattices provide a crucial classification system in crystallography by demonstrating that the entire structure of a crystal can be constructed solely based on its fundamental symmetries.

Figure 1. Fourteen Bravais lattices grouped in seven crystal systems.

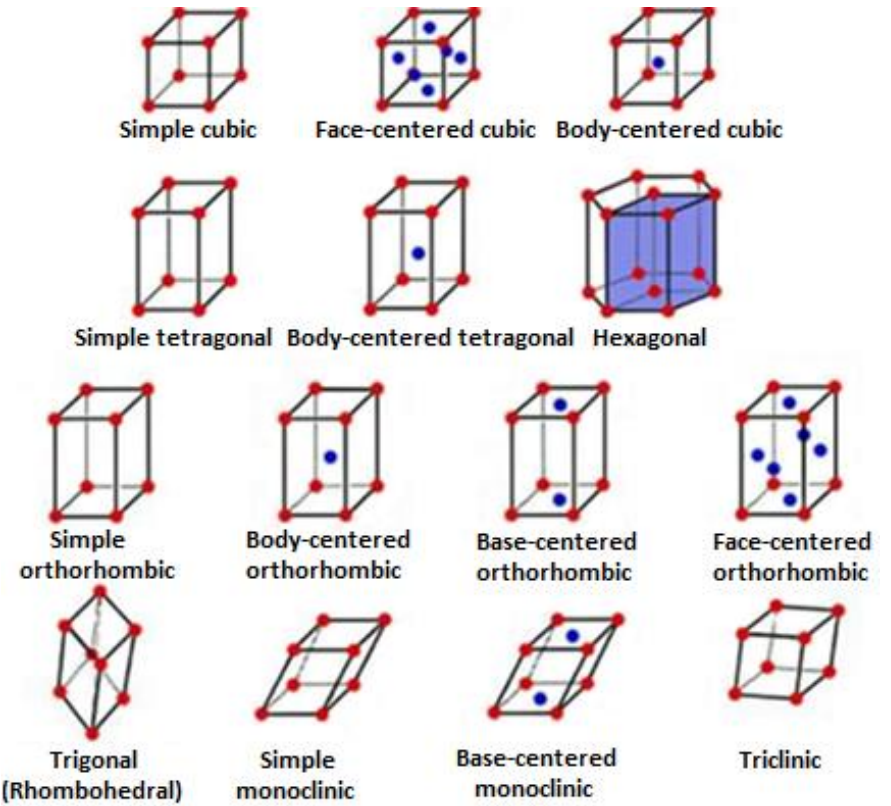

Space Groups and the Classification of Crystal Structures

The concept of symmetry in crystallography is not only applicable to the look of the crystals on the exterior, but also as a mathematical term for their internal structure. Crystals are distinguished by recurring symmetry elements in space three-dimensionally. These are operations such as rotation, reflection or

mirror planes, inversion, and roto-translation or screw axes and glide planes. When such operations of symmetry are applied to any point in the crystal, the resulting physical or geometric shape is not altered. By considering all the combinations of these symmetry elements, crystal structures are classified into a total of 230 distinct space groups (Table 2). All the symmetry elements that a particular crystal structure can be endowed with belong to each space group. These groups also represent individual crystal systems, and each crystal system contains a definite number of space groups. For example:

Table 2. Number of space groups for each crystal system.

Crystal System	**Space Group Number**
Cubic	36
Tetragonal	68
Orthorhombic	59
Hexagonal	27
Trigonal (Rhombohedral)	25
Monoclinic	13
Triclinic	2

Space groups are the standard of reference for crystal analysis through techniques such as X-ray diffraction. The space group a crystal belongs to is crucial in determining its symmetric properties and also its physical behavior (*e.g.* piezoelectricity, optical birefringence, *etc*.) (Kittel, 2004). As an example, crystals

that exhibit piezoelectric properties exist only in space groups that do not have central symmetry.

Interdisciplinary Relevance of Symmetry and Crystallography Applications

Crystal symmetry is not a mere concept, but has its relevance in many disciplines such as chemistry, physics, materials science and biochemistry. In material science, the electrical, magnetic and mechanical properties of crystals rely significantly upon symmetry. As an example, the semiconductors' band structure might be varied depending upon the symmetry properties of the crystal.

Symmetry and space groups play a vital role in the study of protein structures in bio crystallography. Proteins resolved through X-ray crystallography are simulated in specific space groups to gain information about their three-dimensional structure. This helps in understanding the structural properties of enzymes, drugs, and DNA-protein complexes. Crystallographic computer packages (*e.g.*, Vesta, Shelx, and Crystal) assist scientists in simulating crystal structures, symmetry analysis, and determining the space groups. These computer programs analyze symmetry for us, so increasingly and more complicated structures can be rapidly and precisely modeled. Symmetry is therefore no longer merely a way of describing structural order but central to explaining the physical properties of crystals. It combines scientific precision with aesthetic appeal, being one of the basic elements of crystallographic analysis.

The Connection between Motif, Symmetry, and Crystallography

The Relationship between Motif, Symmetry and Crystallography is presented in Table 3.

Table 3. The relationship between motif, symmetry, and crystallography.

Concept	Example and Definition	Connection
Motif	Groups of atoms or ions in a crystal. Geometric patterns in art.	Motifs create repeating patterns through elements of symmetry.
Symmetry	Organizations that do not change with symmetrical operations such as rotation, reflection or shifting.	Crystallography describes the formation of crystal structures through the symmetrical arrangement of motifs.
Crystallography	The branch of science that studies the arrangement of atoms and the repetition of motifs according to the rules of symmetry.	The combination of symmetry and motifs determines the internal structure of the crystal and affects its physical properties.

Types and Groups of Symmetry in Crystallography

Symmetry is a fundamental concept describing the geometric pattern and structure of crystal structures. Symmetry in crystallography is when a structure superimposes upon itself through one or more transformation operations. On this principle, four elementary types of symmetry are to be defined: rotational, reflection, translation, and composite symmetries. Rotational symmetry is a property of an object that looks the same when it is rotated by particular angles around a unique axis. A square looks

geometric in shape when rotated through 90°, 180°, 270°, and 360°. Reflection symmetry occurs if an object appears identical to its mirror image when reflected over a plane. Translational symmetry, on the other hand, refers to periodic structures created by the translation of a motif in a direction and at a constant interval. This type of symmetry is of great significance in crystals, where atom structures are translated at a constant distance. Crystallography entails plane (two-dimensional) and space (three-dimensional) group symmetries. These facilitate the characterization of the symmetric features of patterns and atomic structure both on a plane surface and in space (Hammond, 2009). Symmetry groups are used mathematically to classify such symmetry. Within the system, the most simple groups, called cyclic groups (C_n groups), include rotational symmetries. A model of an equilateral triangle, which can be rotated 120° and 240°, is the C_3 group. Dihedral groups (D_n groups), which include both rotational and reflectional symmetries, enable classification of more symmetrical complex shapes. For example, the group D_4 of a square possesses four rotational symmetries and two axes of reflection. The most extensive symmetry classification in crystallography exists in crystallographic space groups. There are several symmetry elements such as rotation, translation, reflection, glide planes, and screw axes present in these groups. Crystal structures are characterized through a set of 230 distinct space groups in three-dimensional space, which cover entirely all of the symmetrical features of a crystal (Glusker et al., 1994; Kittel, 2004). The systematicity of symmetry groups in this way is the foundation of a key tool in the study of crystal structures, the establishment of their physical and chemical properties, and the design of materials. Thus, in crystallography, symmetry is not just a geometric concept, but it is also a principle that directly influences structural properties.

Symmetry in Carpet Patterns: An Aesthetic, Cultural, and Practical Design Principle

Carpet patterns are not merely ornaments but also symbolic images charged with cultural heritage. Age-old Anatolian carpet production has produced significant motifs that give life to the lifestyle, ideologies, and cultural memory of a people. Symmetry in this case becomes a built-in design principle that governs both the aesthetic appeal and the multi-level meaning of carpet patterns. In woven carpets, symmetry not only contributes to visual harmony but also presents an impression of balance through regular repetition of motifs, which makes the viewer sense unity (Güzel & Aksu, 2013). Symmetry, similar to that in visual arts, is a fundamental aspect that heightens the aesthetic consciousness of the viewer in traditional textile arts. The human eye is naturally drawn towards symmetrical and organized composition; thus, the symmetrical compositions that are being used in carpets create a perception of balance, calmness, and visual ease. Symmetrical compositions in the categories of mirror symmetry (reflection), rotational symmetry, and translational symmetry can be seen to a great extent in Turkey's most important carpet-producing regions -*e.g.*, Konya, Uşak, Bergama, and Hereke-. Such symmetries enable both sides of the carpet to appear balanced, hence enhancing its beauty and achieving a harmonized composition (Kurt, 2018). Symmetry in the patterns of carpets is not just about beauty; it also has cultural and symbolic significance. Symmetry, for example, in Islamic art, is regarded as an aspect of perfection and universal order. Since figurative imagery is generally prohibited in Islamic society, vegetal and geometrical motifs have gained significance, highlighting the use of symmetrical patterns. The weavings of carpets also function as systems of symbols which illustrate the order of the cosmos, the harmony of creation, and one God. For instance, a medallion design in the center often symbolizes the

center of the cosmos, and the subsequent symmetrical patterns symbolize the orderly harmony of the universe (Çolak, 2015). These symmetrical compositions, which are a common selection among Konya carpets, turn the carpet into not only a floor covering but also into a means of narrating stories filled with symbolism. Symmetry also serves as a practical function in weaving procedures. Due to the requirement of consistency in the methods of knotting and pattern transfer operations, symmetrical motifs guide the weavers and reduce errors. In large-sized rugs, repetitive symmetrical motifs offer a more systematic and accurate production process. This efficiency minimizes production time and results in consistent quality throughout the entire rug surface (Öztürk, 2017). Symmetry thus not only simplifies pattern planning, but also production planning. Finally, symmetry improves the structural stability and longevity of rugs. Repeated use of motifs on a regular basis ensures even distribution across the surface, with immediate effects on the lifespan of the carpet. Symmetrical-surfaced motifs allow the carpet to appear even in all directions, hence providing a visually coherent look in the room. This creates spatial flexibility in placement and allows users to experience a uniform visual perception (Erdoğan, 2009). In short, symmetry in traditional carpet weaving is not a mere external appearance; it is a fundamental rule of design in carpet weaving with aesthetic, cultural, symbolic, and functional elements. Hence, it is one of the instrumental ingredients that boost the value of carpets in both artistic and crafts aspects.

Symmetries of Carpet Motifs and Their Relation to Chemical Structures

As part of classical art, carpet motifs have a specific order and symmetrical composition. Anatolian carpet motifs mostly consist of symmetrical compositions that not only ensure aesthetic equilibrium but also have cultural and symbolic significance. By

the change of types of symmetry, the motifs give a meaningful organization that is at the same time visual and symbolic. The symmetries that are employed on carpets are usually classified under reflection symmetry, translation symmetry, glide symmetry, and rotational symmetry (Grünbaum & Shephard, 1987). Reflection symmetry is where a motif is placed as the mirror image to a specified axis. Reflection symmetry is easily observed on geometric patterns that are commonly used in carpets. In particular, star and lozenge geometric shapes in Konya carpet designs are positioned in reflection symmetry, creating a balanced pattern of an equal nature around center motifs (Critchlow, 1976). Reflection symmetry introduces visual order and balance to the carpet and induces an impression of aesthetic harmony in perception. The creation of translation symmetry occurs with the repetition of a motif at regular intervals along a given length. This symmetry is most often utilized in carpet edges and is usually used in nature-based ornamentation such as floral and leaf patterns. These patterns are placed at a determined interval, providing eye continuity and some of the overall unity of carpet design. Translation symmetry helps in establishing a consistent order from all directions and therefore to the improved aesthetic perception of the carpet (Hahn, 2002). Glide symmetry is when a motif is translated over a certain distance and direction then reflected. This more complex type of symmetry is found mainly in geometric patterns. In Konya carpets, motif elements such as zigzag motifs and diagonal lines are described in terms of arrangements that include reflection as well as glide symmetry. Glide symmetry gives the carpet a dynamic texture and offers the viewer a visually interesting, rhythmic encounter (King & Sylvester, 1983b).

Turkish carpet designs typically have symmetrical arrangements that recall patterns of chemical structures. The symmetrical design of carpet compositions can sometimes be

identified with that of molecule structure, which offers a deeper conceptual correspondence. For instance, the geometric patterns that are found in carpets -particularly the ones in corner and center regions- usually have their configurations resembling crystalline arrays. Silica crystals (SiO_2) types of molecules form systematic, symmetrical patterns, and so do many carpet patterns, designed symmetrically around a point of axial symmetry (Grünbaum & Shephard, 1987). Moreover, the carbon skeletons of aromatic molecules exhibit an intriguing similarity with carpet motif configurations. Aromatic compounds like the benzene ring (C_6H_6) have a tendency to copy carpet pattern repetitive and border motifs. Such patterns are indicative of the symmetrical disposition of chemical structures and are meant to bring the visual continuity and coherence of the carpet. Similarly, more complex aromatic hydrocarbons like naphthalene ($C_{10}H_8$) and anthracene ($C_{14}H_{10}$) are found in accordance with intricate geometric motifs in carpet patterns. Naphthalene is of the two-ring type, whereas anthracene shows a more wider and complex symmetric shape (Grünbaum & Shephard, 1987). Symmetrical patterns are also found in metallic compounds as well as ionic compounds, which can be observed in the motifs of carpet patterns. Motifs in green, blue, and yellow color shades depicted in Turkish carpets can appear like cobalt(II) complexes with symmetrical patterns. Such metal-organic materials can duplicate the color transformation and geometric uniformity found in carpet designs. Cobalt(II) complexes, which are iconic in the field of metal-organic chemistry, could be depicted aesthetically in these designs (King & Sylvester, 1983b). Some motifs of carpets could even be inspired by the structural properties of organic compounds. Carbohydrates and polysaccharides, for instance, could be associated with vegetal motifs in most traditional designs. Cellulose ($C_6H_{10}O_5$), being a fundamental compound in nature, is symbolically utilized to represent organic shapes and nature designs in carpets. The same goes for natural acids such as ascorbic

acid ($C_6H_8O_6$), which can be equated with the minor lines and finer details of the texture in the carpet (Critchlow, 1976). Copper ions (Cu^{2+}) can be equated with some of the blue and green colors that are typical in Turkish carpets. These ionic forms are also in conjunction with the symmetrical polygonal patterns that are found in most designs. The crystalline form of copper salts is in line with the symmetrical shapes utilized in carpet motifs, hence increasing both the aesthetic and symbolic nature of the compositions (Hahn, 2002). Two-dimensional (2D) space groups, or wallpaper groups, dictate the periodic symmetry operations of a two-dimensional pattern. Mathematically, they classify the isometries of a plane - distance- preserving transformations, including translation, reflection, rotation, and glide reflection- into exactly 17 distinct symmetry groups. These 17 groups are classified in analogy with two-dimensional crystallography (Figure 2, Table 4).

Figure 2. Lattice units with symmetries of periodic plane patterns.

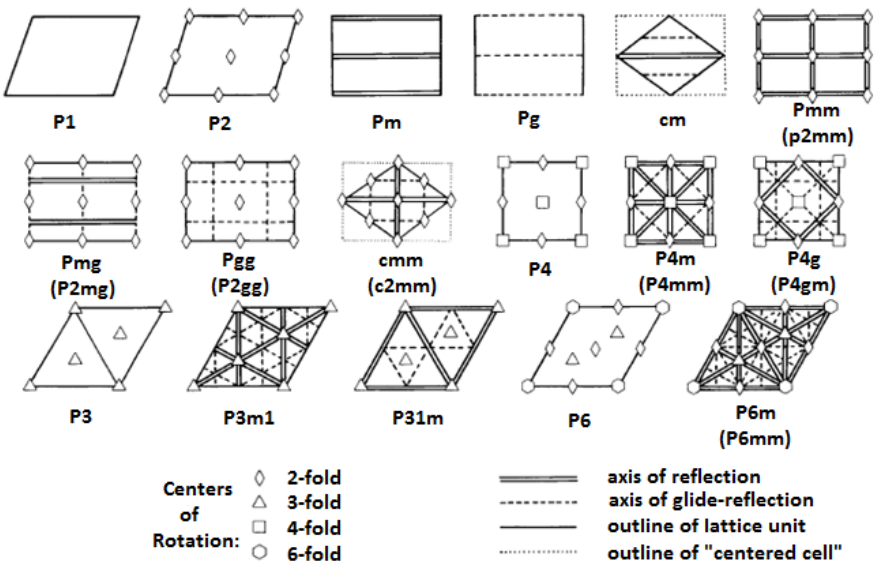

In this Figure 2: international notation identifies the seventeen two-dimensional crystallographic groups. The short form is given first,

with the full notation in parentheses (Schattschneider, 1978). Specifically, the entire group of 17 wallpaper groups has been found in Konya carpet patterns (Grünbaum & Shephard, 1987; Hahn, 2002).

Table 4. The 17 independent space groups resolved according to the rules of 2D crystallography.

No	International abbreviation	Notation (orbifold / Schoenflies *etc*. IUC)
1	P1	translation only
2	P2	2-fold rotation
3	Pm	reflection
4	Pg	shift reflection
5	cm	reflection + shift reflection
6	Pmm	double reflection + 2-fold rotation
7	Pmg	reflection + shift reflection + rotation
8	Pgg	double shift reflection + rotation
9	cmm	orthogonal reflection + center symmetry
10	P4	4-fold rotation
11	P4m	4-fold rotation + reflection
12	P4g	4-fold rotation + shift reflection
13	P3	3-fold rotation
14	P3m1	3-fold rotation + reflection (symmetric)
15	P31m	3-fold rotation + reflection (asymmetric)
16	P6	6-fold rotation
17	P6m	6-fold rotation + reflection

Explanations: Letters P and c indicate the type of lattice: P = primitive, c = centered. Letters such as m, g indicate that it contains mirror or glide reflection.

Geometric and Crystallographic Motifs

Motifs in the Konya carpets are not merely intended to be beautiful but are also of symbolic significance and of geometric patterns consonant with the principles of crystallography. Crystallographic analysis of motifs allows one to understand their symmetry properties as well as their spatial relation to group structures. The motifs employed in the Konya carpets are common and represent a cultural and artistic expression through geometric patterns and symmetry in composition. These motifs, while a symbolic language of Islamic art, also provide an aesthetic enriched by mathematical and crystallographic symmetries.

Hexagonal star motif, found frequently in Konya carpets, is one of the symbolic motifs of Islamic art. The motif is characterized through rotational symmetry of hexagons and, crystallographically, belongs to the P6m space group. Hexagonal compositions are repeated in the center and corner areas of Konya carpets in order to achieve aesthetic harmony. These symmetrical compositions with repeating elements represent the order and limitlessness of the universe. In Islamic art, repetitive symmetries are considered to be visual symbols of infinity (Ögel, 1987b). Hexagonal star symbol is widely used in the patterns of carpets, especially in middle fields and border decorations, to signify universal order (Critchlow, 1976).

Square symbols are forms generated through fourfold rotational symmetry and are part of the P4m symmetry group. These symbols are often used in borders and replicated at equal intervals in Konya carpets to create rhythm. Square motifs are utilized in the center as well as in the borders, producing visual balance. These symmetrical arrangements not only serve an aesthetic purpose but are symbolically employed as well. Fourfold rotational symmetry represents the four cardinal directions and cosmic balance (Ögel, 1987b). The repetitive recurrence of square

motifs represents balance and continuity in the overall structure of the carpet.

Zigzag designs, which are part of the Pg space group, contain glide reflection symmetry as well as translational symmetry. The designs tend to be aligned normally in border compositions in Konya carpets, repeated by translation to create a sensation of movement and continuity. The zigzag pattern offers visual movement without the representation of discontinuity. Glide symmetry adds dynamic structure to the carpet, creating a feeling of movement. In Islamic painting, these types of patterns symbolically represent the repetitive life process and cosmological change (King & Sylvester, 1983b).

The eight-pointed star design, with fourfold rotational symmetry and glide symmetry, belongs to the P4g symmetry group. The design occurs prominently on Seljuk-period carpets and adheres to a central arrangement. Octagram stars radiate from a central point, the intense visual focus, and are employed as symbols of cosmic order. The repeated and symmetrical pattern across the stars visually symbolizes the universe's order and has cosmological significance. This pattern has a symbolic articulation of the order of the universe and human being in Islamic cosmology (Broug, 2008; Critchlow, 1976).

Hexagonal and Polygonal Motifs: Symmetry and Transformations

The ubiquitous hexagonal and other polygonal patterns on carpet motifs are not only aesthetically pleasing but are directly associated with crystallography. These patterns, with their geometric arrangement and symmetry, reflect the regularities of the atomic structures of crystals. The hexagonal and polygonal motifs of the Konya carpets offer an interdisciplinary field of study by being both a work of art and an established sense of order. Apart

from their looks, the association of these motifs with crystallographic principles is intriguing.

Hexagonal motifs are among the most common motifs used in Konya carpets and play an important part in Islamic art. Hexagonal shapes, a standard finding in nature -like snowflakes and honeycombs, belong to the P6m crystallographic symmetry class. Such symmetrical shapes possess sixfold rotational symmetry and can offer perfect tessellation of surfaces. Hexagonal symmetry, through natural energy optimization, is the most effective form of spatial order (Grünbaum & Shephard, 1987; Broug, 2008). The prevalence of hexagonal motifs employed in Konya carpets is more than mere aesthetics and also follows the atomic structure of crystalline order and therefore adds profound mathematical and visual intensity to carpet design. Apart from that, the various forms of symmetry observed in polygon patterns constitute another significant feature commonly found in carpets.

Octagons, decagons, and n-gons of higher orders are duplicated by rotational and reflection symmetries. Octagons are often illustrated using the p8m symmetry group, and such symmetric designs give rise to visual harmony and aesthetic equilibration in carpets (Critchlow, 1976). Such designs in Islamic art are sacred symbols that represent motifs related to cosmic order and infinity. The rotation and reflection symmetries' pattern composition highlights a visual ordering of cosmic order (King & Sylvester, 1983b). Polygon motifs are usually adopted in Konya carpets, especially those that are dominated by geometry.

Such polygons as pentagons, hexagons, and octagons are used either along the edges or in the interior of the carpets, creating a sense of oneness. The connection between such polygons and crystallography may be based on their regular and repeating shapes. Likewise, crystal atoms are made up of regular, repeating arrangements (Hahn, 2002). Octagonal decorations, for instance,

are repeated exactly in square and control surfaces to create visual harmony. They adhere to the symmetrical pattern of crystal forms and indicate that carpet motifs depend on a deep sense of order. Hexagonal and polygonal patterns used in Konya carpets are not only symbolic of esthetic motifs but expressions of an artistic and mathematical understanding. Commonly employed in Islamic art, these motifs are where art and science cross paths. The connection of geometric patterns to crystallography enables a more sophisticated study of these motifs and enables an in-depth understanding from both an artistic and scientific perspective (Ögel, 1987).

Color and Pattern Harmony: A Crystallographic Perspective

Color and pattern harmony in carpet design is not simply a question of appearance; it's the successful articulation of natural order and symmetry standards. Such harmony meets halfway with the symmetrical shapes offered by crystallography, providing relevant guidance on carpet motif placement and color direction. Similar to the patterns of natural crystals, carpet motifs are repeated in specific symmetries. Symmetrical composition leads to a harmonious visual balance such that the motifs become components of a harmonious aesthetic whole. Contrast in colors of carpet patterns causes the symmetry to be more apparent. High-contrast colors allow for various arrangements of the patterns and highlight different motifs. This effect is equivalent to how atomic lattices are described in crystallography, whereby the symmetric lattice structures of atoms become revealed by X-ray diffraction. Particularly in geometric patterns, the congruence of colors with recurring motifs symbolizes the concept of universal order and infinity in Islamic art. This description in Islamic art prescribes the symmetrical arrangement of colors in carpets with added visual as well as metaphysical meanings.

From the crystallographic perspective, the harmony of color and pattern of carpets is not a composition visible to the naked eye but also an articulation of nature's inherent order of symmetry. The symmetrical arrangement of colors is viewed as a visual sign of the order that pervades the universe. Here, the carpet color schemes are on the periphery of art and science, striking a balance between the artist's creativeness and the mathematical harmonies of nature.

The Intersection of Art and Science: The Mathematical Aesthetics of Carpet Motifs

Konya carpets have a unique aesthetic that reconciles art as well as science. The designs in such rugs are not just a representation of art but also guided by patterns based on mathematical concepts. Mathematical beauty enhances not just the visual appeal of the designs but also makes them possess a regular, balanced, and symmetrical structure. In Konya carpets, the measurements and proportions of the patterns are calculated out, and the golden ratio -a very important mathematical key to achieving visual balance both in art and in nature- is frequently employed. The employment of the golden ratio in motif arrangement allows for the designs to be seen as visually balanced and pleasing to the eye. Besides this, the relative position of the central motifs and the border elements is also composed in relation to this principle.

Fractal geometry -a mathematical concept by which a pattern repeats at different scales, giving the impression of infinity- is extensively applied in Islamic art and, in particular, in Konya carpets. The patterns employed here symbolize infinity with repeated forms developing from small to larger. Patterns of "infinite knot" of carpets achieve a fractal shape with recurrence at a number of scales, both aesthetically and mathematically establishing continuity.

In the mathematical pattern of motifs in Konya carpets, plane symmetry groups theory of wallpaper is relevant. Similar to crystallography, designs of carpets may be classified by particular wallpaper groups. They specify the fundamental symmetrical patterns by which they repeat on two-dimensional planes. Conventional square and hexagonal designs of Konya carpets follow these symmetrical arrangements in relation to different wallpaper groups, creating an aesthetic as much as a mathematical equilibrium.

Crystallographic Transformations within Ancient Carpet Motifs

Motif development within the art of carpet weaving is the central factor culturally as well as aesthetically. Over time, social pattern changes, art preference changes, and mutual influences between different geographical areas have sparked the development of carpet motifs. But the development is not limited to visual and cultural developments-mathematical and crystallographic progress are also involved. Crystallographic developments of carpet motifs over time develop along with the progression of their symmetry properties. These variations enlighten us to the development of geometric shapes of motifs and how their symmetrical arrangement has become varied.

With the development of historical carpet motifs, the transformation in the geometric shapes used in design is a determining factor. For instance, as ancient carpets typically comprised less complex geometric shapes (squares, triangles, circles), more complex polygonal shapes (hexagons, octagons, stars) began to appear after some time. This growth influenced crystallographic symmetry of patterns, with some patterns growing into more complex structures made up of the superposition of multiple symmetrical arrangements. Crystallography is essential to

this growth, as crystallographic transformations provide a valuable tool for viewing changes in motifs' repeated symmetrical structures.

The geometrical shapes and symmetry changes of motifs share close resemblance to crystal structure changes. Therefore, motifs in carpets become more symmetrical and beautiful over the course of time as well. Crystallographic changes are the reason for the increasing complexity of carpet motifs both visually and mathematically. The symmetry patterns developed over time reflect a radical shift in art as well as science.

Examples of Historical Carpet Motifs in Konya

Examples of historical carpet motifs of Konya, employed in this research, are borrowed from Turkish Handwoven Carpets Volumes 2, 3, 4, and 5 published by the Republic of Turkey Ministry of Culture, Central Directorate of Revolving Funds (Republic of Turkey Ministry of Culture, Central Directorate of Revolving Funds, 1995, 1998a-c).

Figure 3. THC Pattern Code 0594.

Source: Republic of Turkey Ministry of Culture, Revolving Fund Enterprises Central Directorate, 1995.

First, the large motif in the middle of the carpet is divided into sub motifs in a symmetrical fashion in four directions; this division manifests the presence of a 90-degree (fourfold) rotational symmetry. Secondly, the overall pattern belongs to the P4g plane symmetry group. This group includes, besides the fourfold rotational symmetry, twofold (180°) rotation axes through the midpoints of these axes. This means the motifs are harmoniously repeated by 180-degree rotation at the corners and the edges. Thirdly, the P4g group does not have direct mirror symmetry, but there exist glide reflection axes in the diagonal directions. With these axes, the motifs are repeated in the diagonal directions by the combination of the reflection and translation operations. Finally, no mirror symmetry in the horizontal or vertical direction is found; there is only glide reflection symmetry in the diagonal directions. Taking all of these symmetric elements into account, it is clear that the carpet pattern falls into the **P4g** plane symmetry group. The P4g group, with fourfold rotations and diagonal glide reflections combined, has a more complex and richer symmetry structure than other plane groups.

Figure 4. THC Pattern Code 0547.

Source: Republic of Turkey Ministry of Culture, Revolving Fund Enterprises Central Directorate, 1995.

The carpet pattern belongs to the **P2** plane symmetry group and exhibits the following fundamental symmetric properties: Firstly, the pattern is translationally symmetric at periodic intervals in both the horizontal and vertical directions, which allows the motifs to form a 2D repeating pattern. Secondly, four 180-degree rotation centers that are located in the center of each cell indicate the pattern has twofold rotational symmetry. On the other hand, the pattern lacks any mirror reflection or glide reflection axes. This structure illustrates the presence of motifs placed symmetrically in square cells only through 180° rotations. The motif appears the same in visual shape under this transformation but lacks any symmetry of the reflection variety.

Figure 5. THC Pattern Code 0160.

Source: Republic of Turkey Ministry of Culture, Revolving Fund Enterprises Central Directorate, 1998a.

This woven carpet is of Pgg as its plane symmetry group and illustrates distinct symmetric properties. The patterns of birds repeat in the next row in a 180° upside rotation; this clearly indicates the presence of twofold rotational symmetry. The patterns do not have horizontal or vertical mirror symmetry since the bird designs are not symmetrical and do not have any specific plane of reflection. Glide reflection symmetry, however, is unique: the motifs are replicated such that when shifted half a cell in a specific direction and reflected, they coincide with other parts of the pattern. All these characteristics bear witness to the effective use of the fundamental elements of the **Pgg** plane symmetry group, twofold rotation axes and glide reflection axes, in the design of the carpet.

Figure 6. THC Pattern Code 0309.

Source: Republic of Turkey Ministry of Culture, Revolving Fund Enterprises Central Directorate, 1998b.

Symmetry analysis of this carpet reveals extraordinary symmetric features. The pattern possesses reflection axes in terms of mirror reflection along both horizontal and vertical directions,

imparting the design with twofold reflection symmetry with a two-axis. The 180-degree centers of rotation established at the positions of knots between octagonal motifs also indicate the presence of twofold rotation symmetry. Arrangement of motifs is in the manner that motifs between two rows are repeated with those of the following row by half-unit shift. This arrangement by offset points towards the fact that lattice structure of the carpet is not primitive but C-centered. Vertical reflection symmetries and the 180° rotation centers happen across the entire pattern in unison; the motifs are centered and repeating in sequence. All of these symmetry elements clearly indicate that the carpet pattern is a member of the **cmm** plane symmetry group.

Figure 7. THC Pattern Code 0556.

Source: Republic of Turkey Ministry of Culture, Revolving Fund Enterprises Central Directorate, 1995.

In conventional Anatolian carpets with a four-corner and central medallion composition, mirror reflection symmetries are often observed both along horizontal and vertical axes. In such carpets, the 180° (twofold) rotation symmetry located at the center of the pattern is considered along with the presence of two perpendicular axes of mirrors. This set of attributes is what creates the symmetrical pattern of the carpet. The pattern is synonymous with the P2mm plane symmetry group, which is one of the 17 plane groups. Using the Hermann-Mauguin notation, "P2mm" is a plane group with a primitive lattice that consists of twofold rotation symmetry (2) and two orthogonal mirror reflection axes (m). The symmetrical pattern of the design can be succinctly described as:

Reflection Symmetries: The pattern demonstrates mirror reflection symmetry across the horizontal and vertical axis. Folding the pattern across these axes, the left and right halves of the pattern lie precisely on top of one another.

Rotational Symmetry: There is a single 180° (C_2) rotational symmetry at the center point of the carpet. This suggests that the pattern lies on top of itself when rotated half a revolution around the center point, which is a characteristic of the Pmm group.

Rotation Center at Intersection of Reflection Axes: There is a double rotation center along the intersection of the vertical and horizontal axes of the mirrors. This is a special symmetry element of the P2mm group.

No Glide Reflection: The design possesses any glide reflection symmetry (combination of translation and reflection). The P2mm group possesses only reflection axes and 180° rotation centers.

Lack of Higher-Order Rotations: The pattern lacks the 3-, 4-, and 6-fold rotations but has only 2-fold rotations (C_2) available, as is the case with the P2mm group.

With all these features put together, one can quite easily see that the carpet pattern is that of the **P2mm** plane symmetry group.

Figure 8. THC Pattern Code 0511.

Source: Republic of Turkey Ministry of Culture, Revolving Fund Enterprises Central Directorate, 1995.

The symmetrical aspects one notices in the pattern of this carpet are the following: The pattern is clean mirror (reflection) symmetries along the horizontal and vertical planes. The 180° (twofold) rotational symmetry at the center of the carpet is a significant aspect of this design. But there is no reflection symmetry along the pattern's diagonal directions since motifs in corner locations of traditional carpets typically do not display

symmetrical arrangement along these directions. Also, the pattern doesn't possess 90° or four fold rotational symmetry. If all these factors are considered as a whole, it will be clear that the carpet pattern belongs to the **P2mm** plane symmetry group. This class possesses reflection axes in horizontal and vertical directions, as well as 180° centers of rotation at the intersection of the axes.

Figure 9. THC Pattern Code 0407.

Source: Republic of Turkey Ministry of Culture, Revolving Fund Enterprises Central Directorate, 1998c.

Symmetrical elements in the pattern of this carpet can be accounted for as follows: The large hexagonal motifs set in the center of the design overlap when turned by 180° in the top and bottom positions, indicating a presence of C_2 (twofold rotational)

symmetry in the pattern. Also, the design of the carpet exhibits mirror symmetry along the vertical axis, that is, the left and right halves of the pattern are arranged as reflections of each other along the central vertical axis. But there is not an equivalent symmetry along the horizontal axis. Along the perpendicular direction of the vertical mirror axis, there is glide reflection symmetry. This symmetry occurs when the motifs are mirrored after a half-unit shift in one direction, such that the pattern has a continuous state. All these symmetric features unmistakably indicate that the carpet pattern is in the **Pmg** plane symmetry group. The Pmg group has the presence of a vertical mirror axis, 180° rotation points, and glide reflection symmetry.

Figure 10. THC Pattern Code 0505.

Source: Republic of Turkey Ministry of Culture, Revolving Fund Enterprises Central Directorate, 1995.

This carpet pattern lacks 2-directional translation (translation) symmetry; i.e., the pattern will not repeat in the whole plane. Translation symmetry is only present in a single direction. There is evident mirror symmetry along the vertical line, but the pattern lacks 2-, 3-, 4-, or 6-fold rotational symmetry and glide reflection symmetry. Also noteworthy is the presence of a mihrab orientation in the traditional sense and the fact that a single axis has symmetry controlling along it. All these characteristics imply that the symmetry group of the carpet pattern is of type **Pm**.

Figure 11. THC Pattern Code 0347.

Source: Republic of Turkey Ministry of Culture, Revolving Fund Enterprises Central Directorate, 1998c.

The lattice structure of this carpet demonstrates an arrangement in which the patterns are of roughly square form. Of the symmetry elements, there is a strong 4-fold (90°) rotational symmetry; for example, some star-shaped center motifs land on themselves exactly when rotated 90°. Throughout the design, clear mirror (reflection) axes lie in vertical and horizontal directions, and reflections take place along some diagonal orientations as well. The entire pattern has square symmetry with regularly recurring 4-fold rotation centers. In addition to reflection symmetries along the vertical, horizontal, and diagonal axes, this carpet pattern comes under the planar symmetry group **P4m**.

Figure 12. THC Pattern Code 0263.

Source: Republic of Turkey Ministry of Culture, Revolving Fund Enterprises Central Directorate 1998b.

This floor covering pattern belongs to the planar crystallographic space group P6 and is generally characterized by a 6-fold rotational symmetry. The pattern, though, does not include characteristics such as reflection or glide reflection symmetries. Being of hexagonal lattice structure, the pattern consists of repeating hexagonal motifs as well as 60° rotation centers, which verifies the symmetry features of the **P6** group.

Results and Recommendations

Konya carpets, as a significant component of Turkish carpet art, provide a unique artistic heritage that is not only filled with beauty but also scientific richness. The purpose of this study was to show the way traditional art converges with universal science through examination of carpet motifs from the perspectives of mathematics and crystallography. The patterns of symmetry in the carpets are a primary point of reference in both the world of aesthetic beauty and in the understanding of mathematical order and cosmic symmetries. Symmetry and crystallography are employed not only for ornamentation in carpet designs but also convey meaning and order.

The symmetrical style observed in carpet designs - especially by way of reflection, rotation, translation, and glide symmetries- shows the mathematical foundation of Turkish carpet design. These symmetry styles not only express nature's order and the universe's but also express human knowledge of the universe and how it is artistically depicted. Investigations conducted from a crystallographic point of view show that carpet designs possess a deep mathematical and scientific order regardless of their apparent connotation.

The crystallographic and geometric motifs in the Konya carpets, and more so the breakdown of the hexagonal and polygonal motifs, reveal that the patterns are analogous with

natural crystal formations. Additionally, the symmetry of patterns and color in the motifs reveals the relationship between the symmetrical formations of the motifs and color, creating an aesthetic and mathematical congruence. The evolution of the motifs in the carpets through time and their crystallographic nature reflect the dynamism and evolving cultural heritage of the art.

A close study of symmetry and crystallography in carpet art reveals new scientific dimensions in research for this field. Coupled with conventional weaving skills, the mathematical foundation of these patterns highlights Turkish carpet art's global aesthetic value. The equivalence of the symmetrical patterns of carpet designs and the patterned ordering in crystals proves that carpet art is a type of geometric and physical building block.

Many scientific studies have proved that the symmetries observed on carpet patterns were employed to signify aesthetic intelligence previously, yet scientific techniques such as symmetry and crystallography reveal that the patterns conceal deeper meanings. This is proof that carpet art is not just part of cultural heritage but also an artwork which has scientific content. Furthermore, common symmetrical principles between carpet art and architecture create an important connection aesthetically as well as functionally. Motifs of Konya carpets overlap with symmetrical elements of Seljuk and Ottoman architecture in a manner that acts as a bridge uniting artistic and scientific perspectives.

Nevertheless, to achieve greater international awareness and conservation of carpet art, interdisciplinary study must be encouraged. Having a comprehension of the aesthetic and scientific value of carpet patterns will allow this art to be examined on a greater level. Furthermore, ongoing research into the mathematical attractiveness of carpets will demonstrate that this is not only the product of old art but also of modern scientific thought. This study

emphasizes the need for further associated studies with regards to Konya carpets and Turkish carpet arts in total. Accordingly, the following is suggested in this context:

1. Interdisciplinary studies have to be encouraged. Art history, crystallography, mathematics, *etc*., have to work together to analyze the scientific aspects of carpet motifs exhaustively.

2. Scientific and cultural preservation projects have to be undertaken. Traditional weavings have to be preserved, and carpets have to be computerized to reach more masses.

3. Awareness and education initiatives must be launched. Education initiatives illustrating the science of carpets can transmit cultural and scientific heritages to the younger generation.

4. Crystallographic research on motifs must be strengthened. Such analyses can familiarize us with the historical evolution of motifs as well as their science.

In light of all findings, the analysis of the symmetrical designs of Konya carpets from artistic and scientific perspectives will verify the value of this art to be a universal language. These types of carpets, filled with both values of cultures and scientific content, present significant symbolic buildings throughout human history and are a convergence of art and science.

References

Altınsoy, H. (2018). The place of Konya carpets in the world of carpet art. *Journal of Art and Cultural Studies*, *2*(1), 45-61.

Ashcroft, N. W., & Mermin, N. D. (1976). *Solid state physics*. Harcourt College Publishers.

Atasoy, N. (1988). *Turkish carpet art*. Ministry of Culture Publications.

Blagg, W. H., & Bragg, W. L. (1915). *X rays and crystal structure*. G. Bell and Sons.

Böhmer, H. (2002). Koekboya: *Natural dyes and textiles: A colour journey from Turkey to India and beyond*. Remhöb Verlag.

Broug, E. (2008). Islamic geometric patterns: Their history and evolution. Thames & Hudson.

Critchlow, K. (1976). *Islamic patterns: An analysis of structure and form*. Thames and Hudson.

Cullity, B. D., & Stock, S. R. (2001). *Elements of X ray diffraction* (3rd ed.). Prentice Hall.

Çolak, M. (2015). *The aesthetic and cultural dimensions of symmetry in Turkish carpet weaving*. Istanbul University Publications.

Çolak, R. (2017). The place of Seljuk carpet motifs in Islamic art. *Journal of Islamic Arts*, *9*(2), 112-130.

Denny, W. B. (2002a). *The classical tradition in Anatolian carpets*. In Hali Publications.

Denny, W. B. (2002b). *How to read Islamic carpets*. The Metropolitan Museum of Art.

Erdmann, K. (1960). *Seven hundred years of oriental carpets*. Faber & Faber.

Erdoğan, F. (2015). Motif diversity and cultural reflections in Konya carpets. *Journal of Folklore and Art Studies*, *7*(3), 27-42.

Erdoğan, M. (2009). *Symmetry and formal order in Anatolian carpets*. Sanat Publishing.

Giacovazzo, C. (2002). *Fundamentals of crystallography* (2nd ed.). Oxford University Press.

Glusker, J. P., Lewis, M., & Rossi, M. (1994). *Crystal structure analysis for chemists and biologists*. Wiley VCH.

Grünbaum, B., & Shephard, G. C. (1987). *Tilings and patterns*. W. H. Freeman.

Güleç, A. (2020). The impact of globalization on the preservation of traditional Turkish carpets. Journal of Cultural Heritage and Arts, 5(2), 88-103.

Güzel, A., & Aksu, B. (2013). The role of symmetry in traditional Turkish carpet design. *Journal of Textile Studies*, *45*(2), 175-190. https://doi.org/10.1007/jts.45.2.175

Hahn, D. (2002). *Symmetry in art and nature: A mathematical approach*. Springer.

Hahn, T. (Ed.). (2002). *International tables for crystallography*, Volume A: Space group symmetry. Springer.

Hammond, C. (2009). *The basics of crystallography and diffraction* (3rd ed.). Oxford University Press.

Kaya, M. (2016). Ethnographic and artistic analysis of carpet motifs: The case of Konya. *Journal of Ethnography and Cultural Studies, 4*(1), 59-74.

King, D., & Sylvester, D. (1983a). *The Eastern carpet in the Western world: From the 15th to the 17th century*. Arts Council of Great Britain.

King, R. C., & Sylvester, J. (1983b). *Geometries in Islamic art: A detailed analysis*. Oxford University Press.

Kittel, C. (2004). *Introduction to solid state physics* (8th ed.). Wiley.

Kurt, S. (2018). *Symmetrical use of geometric patterns in Islamic art*. Academic Publications.

Mackie, L. (1989). Turkish carpets in European paintings. *Hali*, *5*(3), 234-243.

Ögel, B. (1987a). *Turkish Carpets and Their Motifs*. Turkish Historical Society Publications.

Ögel, S. (1987b). T*he Visual History of Anatolia: Turkish Culture Through Motifs*. Ministry of Culture Publications.

Öztürk, H. (2017). *The Relationship Between Technical and Aesthetic Symmetry in Carpet Weaving*. Publishers Association.

Öztürk, H. (2019). The Relationship Between Anatolian Carpet Art and Social Structure: The Case of Konya Carpets. *Journal of Turkish Culture and Art History*, *10*(1), 73-90.

Öztürk, O. (1992). The Historical Development of Turkish Carpet Art. *Turkish Culture Studies*.

Republic of Turkey Ministry of Culture, Revolving Funds Central Directorate. (1995). *Turkish Handwoven Carpets (Catalog No: 5, 1st Edition, January)*. Pan Printing House, Ankara.

Republic of Turkey Ministry of Culture, Revolving Funds Central Directorate. (1998a). *Turkish Handwoven Carpets (Catalog No: 2, 3rd Edition, November)*. Pan Printing House, Ankara.

Republic of Turkey Ministry of Culture, Revolving Funds Central Directorate. (1998b). *Turkish Handwoven Carpets (Catalog No: 3, 3rd Edition, December)*. Pan Printing House, Ankara.

Republic of Turkey Ministry of Culture, Revolving Funds Central Directorate. (1998c). *Turkish Handwoven Carpets (Catalog No: 4, 3rd Edition, December)*. Pan Printing House, Ankara.

Schattschneider, D. (1978). The plane symmetry groups: Their recognition and notation. *American Mathematical Monthly*, *85*(6), 439-450. https://doi.org/10.1080/00029890.1978.11994612

Weyl, H. (1952). *Symmetry*. Princeton University Press.

Yetkin, S. (1981). *Historical Turkish carpets*. Turkish Historical Society.

Yılmaz, M. (2017). A study on the etymology and cultural meaning of the word "carpet". *Journal of Turkish Language and Literature Studies*, *57*(2), 215-229.

EXPLORING NUCLEAR MATTER, RADIATION, ATOMS, THIN FILMS, AND SYMMETRY THROUGH PHYSICAL APPROACHES